AN INFRASTRUCTURE FOR EFFICIENT REPORTING WORKFLOW IN GRID BASED TELERADIOLOGY APPLICATIONS

A THESIS SUBMITTED TO
THE GRADUATE SCHOOL OF INFORMATICS
OF
MIDDLE EAST TECHNICAL UNIVERSITY

BY

AYHAN OZAN YILMAZ

IN PARTIAL FULFILLMENT OF THE REQUIREMENTS FOR THE DEGREE OF
PHILOSOPHY OF DOCTORATE
IN
THE DEPARTMENT OF HEALTH INFORMATICS

JULY 2015

Approval of the Graduate School of Informatics

Prof. Dr. Nazife Baykal
Director

I certify that this thesis satisfies all the requirements as a thesis for the degree of Philosophy of Doctorate.

Assoc. Prof. Dr. Yeşim Aydın Son
Head of Department

This is to certify that we have read this thesis and that in our opinion it is fully adequate, in scope and quality, as a thesis for the degree of Philosophy of Doctorate.

Prof. Dr. Nazife Baykal
Supervisor

Examining Committee Members

Prof. Dr. Ünal Erkan Mumcuoğlu (METU, HI)

Prof. Dr. Nazife Baykal (METU, IS)

Assist. Prof. Dr. Aybar Can Acar (METU, HI)

Prof. Dr. Kemal Bıçakcı (ETU, CENG)

Assoc. Prof. Dr. Yeşim Aydın Son (METU, HI)

I hereby declare that all information in this document has been obtained and presented in accordance with academic rules and ethical conduct. I also declare that, as required by these rules and conduct, I have fully cited and referenced all material and results that are not original to this work.

Name, Last Name: AYHAN OZAN YILMAZ

Signature :

ABSTRACT

AN INFRASTRUCTURE FOR EFFICIENT REPORTING WORKFLOW IN GRID BASED TELERADIOLOGY APPLICATIONS

Yılmaz, Ayhan Ozan
Ph.D, Department of Health Informatics
Supervisor : Prof. Dr. Nazife Baykal

July 2015, 108 pages

This study proposes an infrastructure with a global workflow management algorithm in order to interconnect facilities, reporting units and radiologists on a single access interface. This infrastructure is enhanced by a reporting workflow optimization algorithm (RWOA) to determine the optimum match between the inspection and radiologist in terms of experience, subspeciality, response time and workload parameters. RWOA increases the efficiency of the reporting process by decreasing access time to medical images and turnaround time of medical reports and increases the quality of medical reports.

In RWOA implementation, inspection and radiologist attributes are modelled using a hierarchical ontology structure based on Digital Imaging and Communications in Medicine (DICOM) Conformance, DICOM Content Mapping Resource and World Health Organization (WHO) definitions. Attribute preferences rated by radiologists and technical experts are formed into reciprocal matrixes and weights for entities are calculated utilizing Analytic Hierarchy Process (AHP). The assignment alternatives are processed by relation-based semantic matching (RBSM) and Integer Linear Programming (ILP) .

The results are evaluated based on both real case applications and simulated process data in terms of subspecialty, response time and workload success rates. Results obtained using simulated data are compared with the outcomes obtained by applying Round Robin, Shortest Queue and Random distribution policies. It was concluded that RBSM gives the highest subspecialty ratings, but integrating ILP with RBSM ratings provides a better response time and workload success rate. RBSM and ILP based image delivery also prevents bandwidth, storage or hardware related stuck and latencies.

When compared with a real case teleradiology application where inspection assignments were performed manually, the proposed solution was found to increase the subspecialty success rate by 13.25 %, increase the workload success rate by 34.92% and increase the response time success rate by 120%. The total response time in the real case application data was improved by 22.39%.

The proposed architecture has been tested in a total of 35 hospitals, 13 primary care clinics, 3 mobile clinics, 1 reporting unit. 3.35 million inspections were archived and 14216 inspections were reported by the reporting unit. However, an organized reporting process was executed only for 6202 reports which were utilized for RWOA evaluation. The proposed architecture with RWOA is piloted to provide reporting service for 8 primary care and 3 cancer screening medical imaging centers. The piloted application is currently available at *http://eradyoloji.saglik.gov.tr* supported by the Governship of Public Health, Ankara, Turkey.

The insfrastructure and techiniques suggested in this study can be used for or applied to teleradiology applications where the reporting service is outsourced by multiple medical centers to multiple radiology groups or individual radiologists. It is considered that the advantage of the infrastructure will be maximized in large scale applications. Financial models can also be integrated with this architecture where shorter turnaround time and high quality reports can be promoted. The cost of the reporting service per inspection is decreased while the quality of service is increased. Performance assessment, quality control and workload distribution statistics modules can be integrated on this architecture for administrative purposes.

Keywords: Teleradiology, workflow, analytical hierarchy process, integer linear programming, semantic match

ÖZ

GRİD TABANLI TELERADYOLOJİ UYGULAMALARI İÇİN VERİMLİ RAPORLAMA İŞ AKIŞI MİMARİSİ

Yılmaz, Ayhan Ozan
Doktora, Sağlık Bilişimi Bölümü
Tez Yöneticisi : Prof. Dr. Nazife Baykal

Temmuz 2015, 108 sayfa

Bu çalışma, raporlama birimleri, radyologlar ve görüntüleme merkezlerini tek erişim arayüzü üzerinde bağlayan, medikal görüntülere erişim hızını arttırıp rapor dönüş zamanlarını düşürerek raporlama verimliliğini arttıran, tetkik ve radyologlar arasında tecrübe ve uzmanlık alanları açısından en uygun eşleşmeyi belirleyerek rapor kalitesini arttıran Raporlama İş Akış Optimizasyon Algoritması (RİAOA) içeren bir bütüncül mimari önermektedir.

RİAOA uygulamasında tetkik ve radyolog nitelikleri, DICOM, DICOM İçerik Haritalama Kaynağı ve Dünya Sağlık Örgütü (DSÖ) tanımlarına uygun bir hiyerarşik ontoloji yapısı kullanılarak modellenmiştir. Bu yapıdaki özellikler ve bağlantılar için radyologlar ve teknik uzmanlar tarafından atanan önem dereceleri karşılıklı matrisler haline getirilmiş öğelere ait ağırlıklar AHP kullanılarak hesaplanmıştır. Atama seçenekleri İlişki-Temelli Anlamsal Eşleme (İTAE) ve Tamsayılı Doğrusal Programlama (TDP) kullanılarak işlenmiştir. Sonuçlar gerçek uygulama verileri ve simüle edilmiş veriler üzerinde uzmanlık, rapor dönüş, iş yükü başarı oranları bazında değerlendirilmiştir. Simüle edilmiş veriler kullanılarak elde edilen sonuçlar, Dönüşümlü, En Kısa Kuyruk ve Rastgele atama yöntemleri ile karşılaştırılmıştır. İTEA yöntemi ile en yüksek uzmanlık başarı oranı elde edilmiş, İTEA ile TDP birleştirildiğinde ise rapor dönüş ve iş yükü başarı oranınında daha da iyi sonuçlar elde edildiği görülmüştür. İTEA ve TDP bazlı görüntü dağıtımı bant genişliği, depolama alanı ve donanımsal tıkanma ve gecikmeleri de engellemiştir.

Tetkik raporlamaları için atamaların elle yapıldığı teleradyoloji uygulaması ile karşılaştırıldığında, önerilen mimarinin uzmanlık başarı oranını % 13,25, iş yükü başarı oranını % 34,92 ve rapor dönüş başarı oranını % 120 arttırdığı görülmüştür. Uygulamadaki toplam dönüş süresinde ise % 22,39 iyileşme sağlanmıştır.

Önerilen mimari uygulaması toplamda 35 hastane, 13 birinci basamak sağlık kurumu, 3 mobil klinik ve 1 raporlama biriminin entegrasyonu ile test edilmiştir. 3.35 milyon tetkik arşivlenmiş, 14216 tetkik raporlama birimi tarafından raporlanmıştır. Organize bir raporlama sürecine dahil olan 6202 adet rapor RİAOA değerlendirmesinde kullanılmıştır. RİAOA entegre edilmiş olan mimari, 8 birinci basamak sağlık kurumu ve 3 kanser tarama birimi entegre edilerek pilotlanmıştır. Pilotlanan uygulama *http://eradyoloji.saglik.gov.tr* adresinde çalışır durumda olup Ankara Halk Sağlığı Müdürlüğü tarafından desteklenmektedir.

Bu çalışmada önerilen mimari ve teknikler radyoloji raporlama hizmetinin, birden fazla görüntüleme merkezi tarafından, birden fazla radyoloji grubu ya da bireysel radyolog tarafından alındığı teleradyoloji uygulamalarında kullanılabilir ya da uygulanabilir. Bu mimarinin sunduğu avantajların büyük ölçekte en üst düzeye ulaşacağı değerlendirilmektedir. Finansal modeller bu mimari ile entegre edilip kısa rapor dönüş süreleri ve yüksek rapor kaliteleri ödüllendirilebilir. Tetkik başına raporlama hizmeti düşürülürken hizmet kalitesi arttırılabilmektedir. Performans değerlendirme, kalite kontrol ve iş yükü dağılım istatistik modülleri yönetimsel amaçlar ile bu mimariye entegre edilebilir.

Anahtar Kelimeler: teleradyoloji,iş akışı, analitik hiyerarşi işlemi, sayısal lineer programlama, semantik eşleşme

dedicated to Eda Derin and Tuna Doruk

ACKNOWLEDGMENTS

I express sincere appreciation to Prof. Dr. Nazife Baykal for her guidance and insight throughout the research. Thanks go to the other faculty members, Assoc. Prof. Dr. Yeşim Aydın Son and Assist. Prof. Dr. Aybar Can Acar, for their suggestions and comments. To my wife, Dilek, I offer sincere thanks for her unshakable faith in me and her willingness to endure with me the vicissitudes of my endeavors. To my children, Eda Derin and Tuna Doruk, I thank them for understanding my frequent absences.

TABLE OF CONTENTS

LIST OF TABLES

LIST OF FIGURES

LIST OF ABBREVIATIONS

AHP	Analytic Hierarchy Process
API	Application Programming Interface
CDA	Clinical Document Architecture
DAG	Directed Acyclic Graph
DICOM	Digital Imaging and Communications in Medicine
EPR	Electronic Patient Record
FIFO	First In - First Out
GB	Gigabyte
HDC	HTTP-DICOM Connector
h	hour
HIS	Hospital Information System
HL7	Health Level Seven International
HTTP	Hyper-Text Transfer Protocol
ILP	Integer Linear Programming
ILP	Integer Linear Programming
Mbit	Megabit

min minute

MP Mega-pixel

OWL Web Ontology Language

PACS Picture Archiving and Communication System

PDF Portable Document Format

RBSM Relation Based Semantic Matching

RBSM Relation Based Semantic Matching

REST Representational State Transfer

RIS Radiology Information System

ROI Region of Interest

RWOA Reporting Workflow Optimization Algorithm

RWOA Reporting Workflow Optimization Algorithm

SOAP Simple Object Access Protocol

SSL Secure Socket Layer

SUT Sağlıkta Uygulama Tebliği

SVM Support Vector Machine

TB Terabyte

TLS Transport Layer Security

u unit

WADO Web Access to DICOM Objects

WHO World Health Organization

WS Workstation

XDS-I Cross Enterprise Document Sharing for Imaging

XDS Cross Enterprise Document Sharing

XML Extensible Markup Language

CHAPTER 1

INTRODUCTION

1.1 Motivation

Teleradiology service and techniques developed to deliver this service more efficiently have evolved together. As the service requirements evolve, technical capabilities are improved which again produces additional evolvement in the teleradiology service delivery requirements. In the United States almost 70 % of all radiology practices reported using teleradiology and it is foreseen that radiology services can completely be outsourced [1]. Therefore, the growth in teleradiology service demands require that a medical site has to outsource the service to multiple service providers while a service provider delivers medical reporting service to multiple sites. The resultant scenario for teleradiology service workflow is a pool of medical institutions demanding reporting service from a pool of radiology groups or radiologists. The motivation of this study is to fulfill an infrastructure to handle the medical image and report delivery required for such circumstances. As the pool of institutions and radiologist scale, the reporting task assignment decision is also a requirement to be fulfilled. At large scales, manual assignment is not possible as the availibility, subspeciality, workload and schedule of each radiologist can not be managed by the service demander. Another motivation of this study is to enhance the provided infrastructure with a workflow optimization algorithm which automatically decides the optimum radiologist to assign the reporting task to. As a result, image delivery, report task assignment process and report delivery is transparent to medical institutions and radiologists which provides an efficient and automated teleradiology reporting system with better quality outcomes.

1.2 Objectives of the Thesis

The objective of this study, is to design and implement an insfrastructure where multiple medical sites can receive teleradiology services from multiple radiology groups or individual radiologists and where radiology groups can access and report the assigned inspections from multiple sites on a single interface. Based on this objective the architecture is designed to fulfill the following requirements:

- Interoperability : Medical images and electronic patient records are the core components of telemedicine. Medical images are created digitally and stored in the radiology department's Picture Archiving and Communication System (PACS) . Reports are usually stored in the electronic patient record (EPR) of other information systems, such

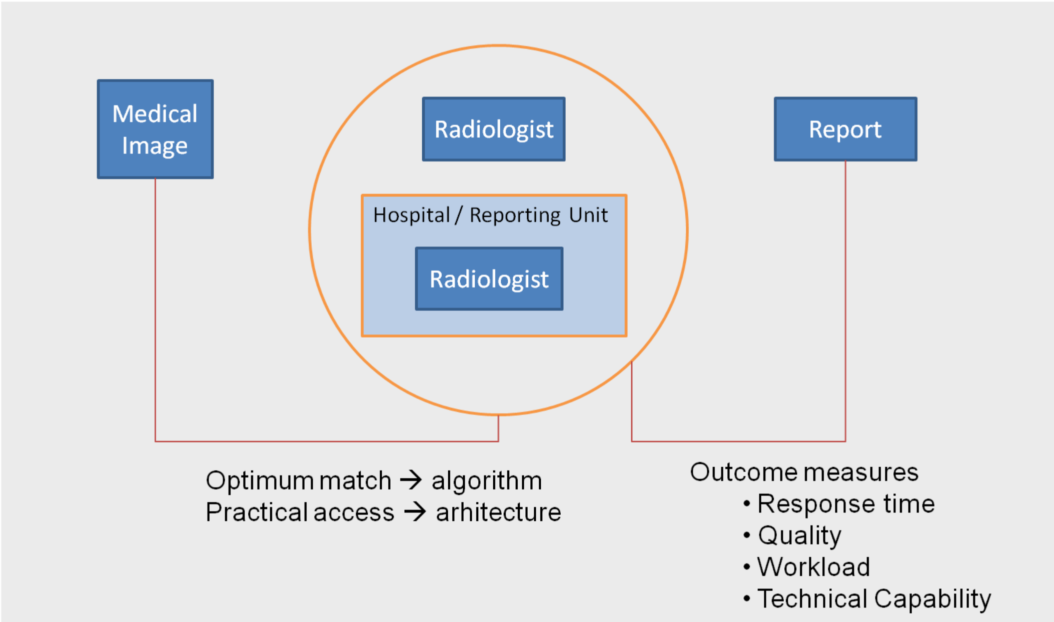

Figure 1.1: Objectives of the Thesis

as the Radiology Information System (RIS) or the Hospital Information System (HIS). However, high-quality service can only be provided if the EPR data is integrated with the PACS digital images so that clinicians can access both systems' data in an integrated and consistent way as part of the regular working environment. The solution should support standardized DICOM, Health Level Seven International (HL7) , Cross Enterprise Document Sharing (XDS), XDS for Imaging (XDS-I) and non-standardized PDF, XML, OWL, HTTP, SOAP medical data and protocols in order to be integrated with PACS, RIS, HIS and EPR. This is provided by introducing a Grid Agent supporting these formats and protocols on the medical site which can interconnect the Grid Manager on the server side with each agent and agents with each other.

- Scalibility : The solution should include data distribution, indexing and caching mechanism to support large scale demands and should be able to scale horizontally. This is provided by designing the server implementation in layers, using Lucene indexing, utilizing Memcached caching mechanisms, distributing database into shards and providing redundancy with Grid Agents.

- Compatibility : The solution should be Vendor Neutral, support each system within a medical site and be compatible with different operating systems or mobile applications. This is provided by developing the software solution with multi-platform compatibility.

The server software is developed with Java and client application is developed using Adobe Air ActionScript technology, which can be exported as Android and iOS applications.

- Accessibility : The system should be accessible anywhere while the technical capabilities on diagnosis and reporting are still provided. This is provided by both Web-Based access and DICOM Viewer compatible access. Web-Based access is provided by the server application while the DICOM Viewer compatible access is provided by the Grid Agent.

In order to automize and optimize this mechanism, another objective is to implement a reasoning component in order to direct the inspection to the optimum reporting unit or radiologist so that the inspection is reported in a short time, with high quality and without exceeding the workload limits of radiologists. In order to implement this component, ontology maps, semantic matching algorithms, analytic hierarchy processing and integer linear programming are integrated together. The inspection and radiologist characteristics are modeled using a hierarchical ontology structure. Based on the studies on radiologist performances, ratings are assigned to the components relevant to their importance on subspecialty, response time, workload and technical factor. These ratings are normalized and formed into reciprocal matrixes utilizing AHP, where weights of contributions are derived. These weights form the coefficients for semantic matching process, where a normalized rating is obtained for each probable assignment alternative between an inspection and radiologist. These assignment alternatives are processed by ILP by defining constraints based on response time, workload and technical requirements. As a result the optimum assignment decisions are obtained for optimum reporting performance.

The algorithm is tested in two simulated and one real case scenarios. The efficiency of the algorithm is compared and investigated with reference to response time, subspecialty, workload and technical success rate parameters.

1.3 Contribution

The proposed software architecture for teleradiology reporting process optimization provides a cloud service where many-to-many connections can be fulfilled between medical institutions and radiologists. This solution is focused on a potential future demand that teleradiology reporting service is also in the form of a cloud service where medical image and report delivery is transparent to the stakeholders. Apart from implementing the software architecture, this study is novel in that the medical image and report delivery is optimized in order to deliver the image to the most appropriate radiologist in terms of subspeciality, response time, workload and technical constraints. As a result, the teleradiology reporting workflow is automized and turnaround time and report quality is improved.

1.4 Outline of the Thesis

Objectives of the study, motivation, contribution and organization is presented in Chapter 1. Background information and literature review on teleradiology architectures and workflow optimization is presented in Chapter 2. The theory and methods on the workflow optimization algorithm integrated with the proposed architecture is presented in Chapter 3. The experiments performed on the architecture implemented for multisite teleradiology service delivery, simulated data and real case data is presented and discussed in Chapter 4. The conclusion based on the provided results are provided in Chapter 5.

CHAPTER 2

BACKGROUND

Telemedicine is the application of clinical medicine where medical information is transferred by telecommunications networks for the purpose of consulting, examination and performing remote medical procedures. Telemedicine based networks have been shown to greatly facilitate bringing patients under a doctor's care, help find problems faster, reduce response time, and decrease number of visits to specialists. Different system architectures have been proposed and implemented as telemedicine solutions. The general purpose of these systems is to transfer patient data to specialists who can access, examine, consult and diagnose the data as fast and as efficiently as possible.

Medical images and electronic patient records are the core components of telemedicine. Medical images are created digitally and stored in the radiology department's PACS. Reports are usually stored in EPR of RIS or HIS. However, high-quality service can only be provided if the EPR data is integrated with the PACS digital images so that clinicians can access both systems' data in an integrated and consistent way as part of the regular working environment. Additionally, this system should allow for teleconferences with other users, e.g., for consultations with a specialist in the radiology department. In order to accomplish this service, studies have been carried out on integration of HL7 and DICOM which are standards for interoperability of health information technology and handling, storing, printing, transmitting information in medical imaging, respectively.

Because there is a variety of clinical workstation software, applications should run on any computer and operating system as a requirement of interoperability. Web-based programs are used for integration with various RIS or HIS and for displaying and processing medical images. Web based programs produce the considerations of bandwidth limitations and security problems. In order to accomplish efficient transmission of data despite bandwidth limitations, compression techniques are utilized. Encryption, authentication and signing processes are executed in order to overcome the security concerns during the transmission and messaging of data.

Storage and retrieval technology for large-scale medical image systems should have cost-effective backup and recovery solutions. Conventional PACS lacks affordable fault-tolerance storage strategies for archive, backup, and disaster recovery. Existing solutions are difficult to administer, and often time consuming for effective recovery after a disaster. Federated or Grid Computing systems have been studied in order to evolve from the familiar realm of parallel, peer-to-peer, and client-server models that can address the problem of fault-tolerant storage for backup and recovery of medical images.

The main characteristics of studies based on teleradiolgy applications can be classified into 4 focus groups:

- Speed
  - Infrastructure and network design
  - Compression Algorithms
- Security and Privacy
  - VPN, SSL, Authentication, Encryption
  - Image encryption algorithms
- Interoperability
  - IHE, XDS
  - DICOM, HL7, XML, OWL
- Quality
  - Structured Reports
  - Workflow Optimization
  - Performance Assessment

When the evolution of PACS and teleradiology is investigated based on these studies and nation-wide case studies are evaluated [2, 3, 4, 5, 6], the improvement steps related to functionality can be illustrated as Figure2.1.

This evolution starts from a simple PACS application where a single client can access the medical images, through Enterprise PACS with several clients querying and retrieving inspections, to Web and Regional PACS solutions. However, it can be concluded that Regional PACS solutions, which are usually utilized in nation-wide studies end up in vendor dependent infrastructures [2] . These solutions are poor in interoperability and produce high migration and integration costs. In financial aspects this also decreases competiton.

Therefore, the trends in teleradiology has been towards quest for standards [7, 8, 9] in order to integrate patient data into a complete electronic health record and towards Virtual PACS solutions interconnecting several vendors and facilities on a cloud platform [10]. The trend in the requirements have also evolved from accessibility to interoperability, compatibility [11] and workflow in the overall process [12]. In order to fulfill this requirement, techinal solutions have evolved from regional VPN-based solutions to Grid-Based solutions [10]. These solutions which are also supported in parallel by the improvements in the content and information centric network solutions [13, 14] propose the employment of a broker [15, 16, 17] or agent [18, 19] .

Zhang *et al* [20] proposed a hospital-integrated PACS architecture where images can be investigated using web browsers. An application server is set up in the hospital which receives http requests from web browsers. On request, it fetches the image in the PACS server using DICOM protocol, converts DICOM file into JPEG and responds with the image. The image processing functions (Window/Level, Zoom/Pan, Rotation, Overlay, and ROI) are executed

	Access	Multi client	Outside Hospital Access	Multi Hospital	Multi vendor integ.	Work flow integ.	Multi System Integ.	Multi platform
PACS	X							
Enterprise PACS	X	X						
Web PACS	X	X	X					
Regional PACS	X	X	X	X				
Virtual PACS	X	X	X	X	X			
Cloud Teleradiology	X	X	X	X	X	X	X	X

Figure 2.1: Evolution of PACS and Teleradiology based on required functionalities

at the server side and each operation results in a DICOM to JPEG conversion. In order to give access to off-site users, a gateway is implemented on the hospital firewall. Each query, retrieve, move operation on DICOM content is translated by the Application Server to the PACS Server and the response from the PACS Server is translated to HTTP message for the response to the browser. This system can only be used to access the hospital PACS images using a browser, but it does not serve as a collective web application where several hospitals can be accessed. Also every operation has to be translated back and forward by the Web Server and the displayed images are always converted to JPEG at each image processing action. This approach gives a heavy load on the server and is not feasible when the number of users scale. Besides, only medical image data is processed and electronic health records are not integrated.

Münch *et al* [21], proposed a web-based solution that integrates the digital images of the PACS, the EPR/HIS/RIS data and a built-in teleconferencing functionality. This solution consists of a Web Server which communicates with the PACS Server and a Java Applet which can be used in a browser, standalone or integrated on the HIS application and which fetches the images by communicating with the Web Server. The image processing operations can be executed within the applet without having to communicate with the Web Server. If the applet is integrated into the HIS application, the images can be viewed with the EPR. Authentication and SSL3/TLS encryption is used for security. This system is feasible in that, the image processing is carried out on the client side without a burden to the server, but for integration with the EPR, and the source code of the HIS application should be edited and the EPR can only be seen by the user only while using the HIS application, which means this system can be used inside and within one hospital only.

Reponena *et al* [22], proposed a system based on a HTTP-DICOM connector (HDC) software. The images are automatically sent to PACS and to the HDC. HDC creates thumbnail images (GIF-format) from the DICOM files and creates an index, which is thereafter stored in the EPR's patient folder. HDC also stores the DICOM images in its cache for 2 weeks to speed up the retrieval of the images. Retrieving of the images is done from the EPR system. In the WWW interface, radiology reports contain a link, which is connected to an on-the-fly generated page containing the thumbnail images. All the thumbnail images are linked to the original DICOM images and by clicking the thumbnail, a DICOM viewer showing the original image is spawned. The images which are no longer in the cache of the HDC are automatically retrieved from the PACS using DICOM protocol. This system is highly dependent on the EPR system structure as it creates an index on the patient folder. It is not feasible in terms of interoperability. The EPR with the images can only be seen using the HIS deployed in the hospital. An interconnection between hospitals is not executed and the system is not secure as all medical images can be accessed by means of a link.

Johannes *et al* [23], implemented a DICOM server in JAVA. Data access is enabled via internet browser technology. Relevant patient and image acquisition information is extracted from the DICOM images and stored into a relational database. Patient information such as radiological findings is transferred from RIS into the database. Image data is accessed either by a fast preview tool or using a JAVA-based DICOM viewer. This implementation is feasible in that, it unifies the radiological findings of patients and medical images in one relational database; therefore all the data can be accessed by a web browser without being dependent to the RIS. However, in order to extract radiology findings, an interface between the PACS Server and the RIS application has to be implemented. The implemented Java PACS Server itself is not an interface application so if the hospital already has a PACS server it should be replaced. Therefore, the proposed system has a dependency on the Java PACS Server.

Cao *et al* [24], developed an Integrated Medical Image Database and Retrieval System (INIS) for easy access by medical staff. The INIS mainly consisted of four parts: specific servers to save medical images from multi-vendor modalities of CT, MRI, CR, ECG and endoscopy; an integrated image database server to save various kinds of images in a DICOM format; a Web application server to connect clients to the integrated image DB and the Web browser terminals connected to an HIS system. The INIS provided a common screen design to retrieve CT, MRI, CR, endoscopic and ECG images, and radiological reports, which would allow doctors to retrieve radiological images and corresponding reports, or ECG images of a patient simultaneously on a screen. This system basically involves the remote access to the HIS through the firewall of the hospital and having access to the medical images through the HIS which are served by Web Servers within the hospital. It has the advantage of accessing the patient records and images from outside the hospital, but the connection between the web browsers and the system is not feasible in terms of scaling the application to several hospitals and users.

Blazona and Koncar [25], aimed to integrate and exchange RIS originated data with HIS based on HL7's CDA (Clinical Document Architecture) standard. They introduced the use of WADO service interconnection to HIS and finally CDA rendering in widely used Internet explorers. The HL7 standard could be adopted radiology data into the integrated healthcare systems. This study is feasible for implementing interconnections to several medical centers and hospital in order to obtain related medical images. Also DCM-CDA application can be implemented in hospitals without affecting the current HIS and PACS processes and giving access to clients through web service requests. However, the medical images are transferred as JPEG or GIF images because of the WADO interface. Therefore, DICOM image processing capabilities are hindered.

Sachpazidis *et al* [26], proposed a medical network based on state-of-the-art medical imaging application for providing health care from a distance. The application consists of a teleconsultation implementation on DICOM images. It has no integration with PACS or HIS and depends on the manual import of images; however, it is innovative in the sense that DICOM images are used as an interactive consultation session where radiology specialist can draw annotations and notes on the images for diagnosis.

Dragan and Iveti [27], proposed a strategy for transmission of scalable JPEG2000 images extracted from a single code stream over DICOM network using the DICOM Private Data Element without sacrificing system interoperability. It employs the request redirection paradigm: DICOM request and response from JPEG2000 server through DICOM server. This system is aimed to be used in stationary and handheld devices. The DICOM2000 server has the role of the Content Manager which redirects medical images from the JPIP server to clients. Clients communicate directly to the DICOM2000 server and they are integrated into PACS. Using JPEG2000 is innovative as JPEG2000 compression besides having good compression performance, supports image streaming. The JPEG2000 streaming services include ROI (region of interest) decoding, progressive transmission, and resolution and quality scalability. In stationary clients DICOM images are transferred directly and in movable and handheld clients JPEG2000 images are used which provides enough quality in required delivery time.

Zhang *et al* [28], developed a web-based system to interactively display EPR, such as DICOM images, graphics, and structure reports and therapy records, for intranet and internet collaborative medical applications. The Web viewer of this system integrates multi-media display modules and remote control module together to provide interactive EPR display and manipulation functions for collaborative applications. This system provides a novel architecture by integrating HIS/RIS/PACS data into an EPR Web server through an EPR gateway. The EPR Web Server in this study is located in the SARS hospital, but there is no obstacle in locating it in a data center where several hospitals' HIS/RIS/PACS data is integrated through EPR Gateways implemented at each hospital. In addition to accomplishing an EPR Web Server, the data in the server is utilized by collaborative teleconsultation applications where images can be manipulated.

Cheung *et al* [29], proposed an image distribution project, ePR, where DICOM images are sent from the mini-PACS systems to the corporate image archive. The central archive caches images at full resolution for one month, from which the images are compressed 10–30 times using lossy compression into the long-term "reference quality" image archive. The RIS at each hospital includes a link to the image as part of the radiology report. When the clinician pulls up the radiology report he/she sees an icon indicating that electronic images are present. Clicking on this icon pulls up the compressed images from the archive. This project is novel in terms of providing a central achieve of medical images. However, the central archive cannot be queried based on DICOM data, but only images can be accessed through links on RIS applications.

Onbay and Kantarcı [30], designed and implemented a distributed PACS system (DIPACS), for small and medium scale medical networks. DIPACS forms a virtual organization by combining the storage of health centers and providing transparent access to images. PACS servers and workstations connected to a DIPACS gateway at a clinical site constitute a DICOM domain. A DIPACS gateway provides transparent connection to the DIPACS environment. Prior to system startup, all PACS servers and display workstations in a DICOM domain are registered to their DIPACS gateway. Similarly, a DIPACS gateway is introduced to the PACS servers and display workstations in its domain. DICOM domains connected over the Internet are introduced each other via a Nameserver. The Nameserver provides a domain with the transparent access to the images stored in other domains. Prior to system startup, a DIPACS gateway is to be configured to the Nameserver. During system operation, a physician in a DICOM domain sends queries to the DIPACS environment over the domain's DIPACS gateway. Queries/Responses received from a DIPACS gateway are sent to the related PACS server(s)/display workstations. Communication among the components of a DICOM domain relies on DICOM standard. Secure communication among DICOM domains is provided with TLS/SSL cryptographic protocols.

Choudhury *et al* [31], proposed hierarchical and semi-centralized telemedicine network architecture has been proposed focusing on the rural underdeveloped areas of Bangladesh. The model utilizes the existing fiber optic backbone and wireless telecommunication infrastructures to connect the remote healthcare centers with the urban specialized hospitals. In this architecture, The entire medical infrastructures will be partitioned into four tiers.

Huang H. K. *et al* [32], proposed a grid computing system which involves the integrated use of geographically distributed computers, networks, and storage systems to create a virtual computing system environment for solving large-scale, fault-tolerant storage for backup and recovery of medical images. This is a novel storage architecture as it accomplishes redundancy and disaster recovery and also reduces the hospital storage expenses as the hospitals can serve images through short term temporary storage areas.

Yang *et al* [18], proposed a PACS based on data grids, and utilize Medical Image File Accessing System (MIFAS) to perform querying and retrieving medical images from the co-allocation data grid. MIFAS can take advantage of the co-allocation modules to reduce the medical image transfer time. Users search the Medical Image Replica Service for the MIFAS catalog service, and requests are reported. The system ranks all replica servers according to replica selection model, and users can then choose the better servers for parallel downloading to fetch and download files from multiple sources. MIFAS co-allocation is then used to transfer the desired files using the algorithms developed [17]. This is one of the first studies to interconnect several facilities on a single interface; however is it mainly focused in parallel download of medical images to improve image delivery time and includes no implementation about interoperability, workflow optimization. It is implemented on an already available interconnected network. The image retrieval operation is initiated by the client and download locations are selected manually.

Benjamin *et al* [33], proposed a teleradiology architecture referred as SuperPACS in order to increase the efficiency of the teleradiology service. The system is proposed for multiple sites and multiple radiology groups. SuperPACS allows a radiology group serving multiple sites to access medical images on a single interface. It also supports HL7, HTTP, XDS and non-standardized data. However, the implementation does not include a workflow optimization. The radiologist retrieves medical images using a global worklist where all tasks are listed.

Also the situation where a medical site employs multiple radiology groups is not considered. This scenario applies for a radiology group serving multiple sites.

Shen *et al* [34], proposed a web-based system for remotely accessing medical images referred as MIAPS. MIAPS includes a novel DICOM indexing and server side caching mechanism in order to provide web based dicom viewer with faster image retrieval and processing capabilities. The techniques utilized for web access show resemblance with this study in being a Java and ActionScript based solution using Lucene Indexing mechanism and server side caching and sliding window approach for Web Dicom Viewer. However, this study does not focus on medical report delivery or interoperability issues.

Valente *et al* [16], proposed a RESTful Image Gateway for multiple image repositories where a mobile access solution is implemented introducing a broker in the image repository site. The broker provides a RESTful API for HTTP GET requests. This implementation resolves the compatibility issues for mobile devices and shows resemblance with this study in that, it utilizes dcm4che Java libraries on the server side and introduces a broker for interoperability with PACS. However, the implementation positions the broker in a single location although it can support several repositories on the internal network. The client directly requests the broker, where an architecture with several brokers is not considered.

In previous research, multiple types of workflow optimization and semantic matching strategies are evaluated such as reinforcement learning [35, 36], machine learning (SVM, Bayes) [37] and relation based negotiation [38]. In this study, an infrastructure for medical image distribution is proposed and a RBSM algorithm enhanced by ILP is utilized to design medical image distribution strategy based on reporting workflow and efficiency.

Among the studies on workflow optimization, only a few have implementations related to radiology process. Huang *et al* have implemented several studies on work distribution [36] and business process management [35, 39]. These studies include mining the task distribution rules in the event log of CT-scan examination process. The common approach is that the rules are learned from the event log regardless of whether they are successful or not[39]. Although reinforcement [35] and adaptive association [36] algorithms are applied the results are only compared with Random, Round Robin, Shortest Queue, FIFO and Retain Familiar distributions with slight improvements rather than testing and comparing with real event log data. Also expertise or subspeciality of the radiologists are not considered. Expertise, subspecialty and quality of report are also critical parameters for teleradiology service delivery workflow. An inspection requiring subspecialty should be assigned to a radiologist with corresponding experience and high quality reports should be promoted in assignment process. In the proposed algorithm, experiences and subspecialties of radiologists are evaluated based on radiologist characteristics [40], [41] and report quality feedback [42] is included in the ontology map for the recalculation of weights by AHP.

There is rarely a study which integrates workflow optimization with teleradiology architecture. However, a partially related example can be given as the telemedicine system called T-TROIE (Telemedicine Tasks and Resources Ontology based system for Inimical Environments) proposed by Nageba *et al* [43]. T-TROIE, takes the previous requirements into account to provide the healthcare professional with efficient decision making support tools. It implements a knowledge framework based on interrelated ontologies, a rule based engine. This system allows a healthcare professional to take a decision for the transfer of the patient into an appropriate hospital that complies with the patient contextual situation.

The attributes that should be considered to fulfill a complete teleradiology architecture with workflow optimization is summarized on Figure 2.2. The studies that can provide these capabilities as closely as possible are compared with the capabilities proposed by RWOA architecture in this thesis study.

	SuperPACS (Benjamin)	MIFAS (Yang)	MIAPS (Shen)	Restful (Valente)	Rein. Learning (Huang)	This Study (Yılmaz)
Accessibility	Radiologist→ Multi Site	Radiologist→ Multi Site Manual retrieval Parallel download	Web based access	Web based and mobile access	X	High Multi site←→Multi Radiologist Web based access Desktop access
Scalability	SuperPACS Agent	Requires VPN and increasing maintenance and operation costs	Modarate Lucene Index Server side Caching	Not considered	X	Grid Agent Lucene Index Server Side Caching Data based Sharding Layered design
Interoperability	HL7, HTTP, XDS and non-standardized data	DICOM	HTTP, DICOM	HTTP, DICOM	X	DICOM, HL7, HTTP, XDS and non-standardized data
Compatibility	Vendor Neutral	X	X	Vendor Neutral , Multi-Platform	X	Vendor Neutral , Multi-Platform
Workflow optimization	Global worklist No optimization	X	X	X	Workload, resource allocation and response time optimization	RBSM and ILP based optimization

Figure 2.2: Comparison between capabilities provided with existing studies and this study

CHAPTER 3

THEORY AND METHODS

3.1 Theory

3.1.1 Ontology-Based Semantic Similarity Measurement

Semantic-similarity measures quantify concept similarities in a given ontology. Potential applications for these measures include search, data mining, and knowledge discovery in database or decision-support systems that utilize ontologies.[44]

Hierarchical Structure of an Ontology Typically, an ontology is represented as a directed acyclic graph (DAG) , in which nodes correspond to terms and edges represent relationships between the terms. In some ontologies, there is only one relationship between nodes, while in more general case, there exist more than one relationship between nodes.[45]

In the DAG corresponding to an ontology, there is a node specified as the root. For every node in the ontology, there exists at least one path pointing from the root to the node. Every node in such a path is called an ancestor of the node, and the ancestor that immediately precedes the node in the path is called the parent of the node. There might be more than one path from the root to a node. Consequently, a node may have several parent nodes, and vice versa. Given two nodes in an ontology, they must share a set of common ancestor nodes, and the one represents the most concrete concept is typically referred to as the lowest common ancestor of the two nodes. Discarding the direction of the edges in an ontology, there exists at least one path between every pair of two nodes. [45]

Comparing Terms There are essentially two types of approaches for comparing terms in a graph-structured ontology: edge-based, which use the edges and their types as the data source; and node based, in which the main data sources are the nodes and their properties. [46]

Edge-based Edge-based approaches are based mainly on counting the number of edges in the graph path between two terms. The most common technique, distance, selects either the shortest path or the average of all paths, when more than one path exists.

Within the edge-based approaches, Pekar and Staab [47] proposed a measure based on the length of the longest path between two terms' lowest common ancestor and the root (maximum common ancestor depth), and on the length of the longest path between each of the terms and that common ancestor, c_a. It is given by the expression

$$sim_{PS}\left(c_1, c_2\right) = \frac{\delta\left(c_a, root\right)}{\delta\left(c_a, root\right) + \ \delta\left(c_1, c_a\right) + \ \delta\left(c_2, c_a\right)}$$

where $\delta\left(c_1, c_2\right)$ is the length in number of edges of the longest distance between term c_1 and term c_2.

Node-based Node-based approaches rely on comparing the properties of the terms involved, which can be related to the terms themselves, their ancestors, or their descendants.

Rasnik [48] measures similarity between two terms as simply the information content (IC) of their most informative common ancestor (MICA):

$$sim_{Res}\left(c_1, c_2\right) = IC\left(c_{MICA}\right)$$

While this measure is effective in determining the information shared by two terms, it does not consider how distant the terms are from their common ancestor. To take that distance into account, Lin's and Jiang and Conrath's measures relate the IC of the MICA to the IC of the terms being compared [49][50]:

$$sim_{Lin}\left(c_1, c_2\right) = \frac{2 \times \ IC\left(c_{MICA}\right)}{IC\left(c_1\right) + IC\left(c_2\right)}$$

$$sim_{JC}\left(c_1, c_2\right) = 1 - IC\left(c_1\right) + IC\left(c_2\right) - 2 \times \ IC\left(c_{MICA}\right)$$

Methods Based on Features of Terms In feature-matching methods, terms are represented as collections of features, and elementary set operations are applied to estimate semantic similarities between terms. A feature-matching model in general consists of three components: distinct features of term A to term B, distinct features of term B to term A, and common features of terms A and B. Using set theory, Tversky defined a similarity measure according to a matching process, which generated a similarity value based on not only common but also distinct features of terms [51]. Unlike the above-mentioned models based on semantic distance, this feature-matching model was not forced to satisfy metric properties. A similarity measure based on the normalization of Tversky's model and the set-theory functions of intersection and difference was given as

$$sim_T\left(c_1, c_2\right) = \frac{\left|D_1 + D_2\right|}{\left|D_1 \cap D_2\right| + \mu\left|D_1 \backslash D_2\right| + \left(\mu - 1\right)\left|D_2 \backslash D_1\right|} for\ 0 \le \mu \le 1$$

where D_1 and D_2 corresponded to description sets of c_1 and c_2, ||, the cardinality of a set, and μ, a function that defines the relative importance of the non-common features. The first term of a comparison (i.e., c_1) was referred to as the target, while the second term (i.e., c_2) was defined as the base.

Methods Based on Hierarchical Structure of an Ontology The strategies that methods employed included lengths of shortest paths, depths of nodes, commonalities between terms, semantic contributions of ancestor terms, and many others. Although the use of these strategies has enabled the successful application of these methods to a variety of problems, the existence of a drawback in these methods is that a term in an ontology has more than one parent node in the corresponding DAG, and thus two terms may have two or more lowest common ancestor (LCA) nodes. However, none of the above methods take such a situation of multiple LCA nodes into consideration in their calculation of semantic similarity.

The semantic similarity between these two terms, was defined by Wang [52] as

$$S_{GO}(A,B) = \frac{\sum_{t \in T_A \cap T_B} (S_A(t) + S_B(t))}{SV(A) + SV(B)}$$

Where

$$S_A(A) = 1,$$

$$SV(A) = \sum_{t \in T_A} S_A(t)$$

$$SV(B) = \sum_{t \in T_B} S_B(t)$$

A similar algorithm proposed by Colucci [53, 54], and Noia [55] is as follows:

Algorithm *rankPotential*(*C,D*);
input Concepts *C*, *D*, in normal form, such that *C*∩*D* is satisfiable
output rank *n ≥0* of *C* w.r.t.*D*, where 0 means that
C∩*D*(best ranking)
begin algorithm
let *n* := 0 **in**
/* add to *n* the number of concept names in *D* */
/* which are not among the concept names of *C* */
    1. *n* := *n* + |*Dnames*+ *Cnames*+|;
    /* add to *n* number restrictions of *D* */
    /* which are not implied by those of *C* */
    2. **for each** concept (*c* ∈(D_-))
    such that there is no concept (*c* ∈(C_-)) with (*y* ≥x)
        n := *n* + 1;
    3. **for each** concept (*c* ∈D_-)
    such that there is no concept (*c* ∈(C_-)) with (*y* ≤x)
        n := *n* + 1;
    /* for each universal role quantification in *D* */
    /* add the result of a recursive call */
    4. **for each** concept for all (*R* ∈D)
        if there does not exist (*R* ∈C)
            then *n* := *n* +
            rankPotential(T,*E*);
        else *n* := *n* +
            rankPotential(*F,E*);
    return *n*;
end algorithm

In this algorithm, the ontology is processed recursively and 1 is added to the result for each mismatch, which means total match is a particular case of potential match, obtained when rankPotential(C,D) = 0. It is easy to modify the algorithm if weights on sub-concepts of D are taken into account instead of adding 1 to n for each D's concept missing in C, one just adds the corresponding weight. Then, a far rank would mean that either many minor characteristic, or a very important one, are left unspecified in C.

3.1.2 Supplier Selection and Optimization

There is a big variety of Multiple Criteria Decision Making (MCDM) methods, but all have the same goal, to estimate the best alternative among several options, based on predefined criteria. In [56] the MCDM methods (deterministic, single decision maker) were classified in a taxonomy given in Figure 3.1.

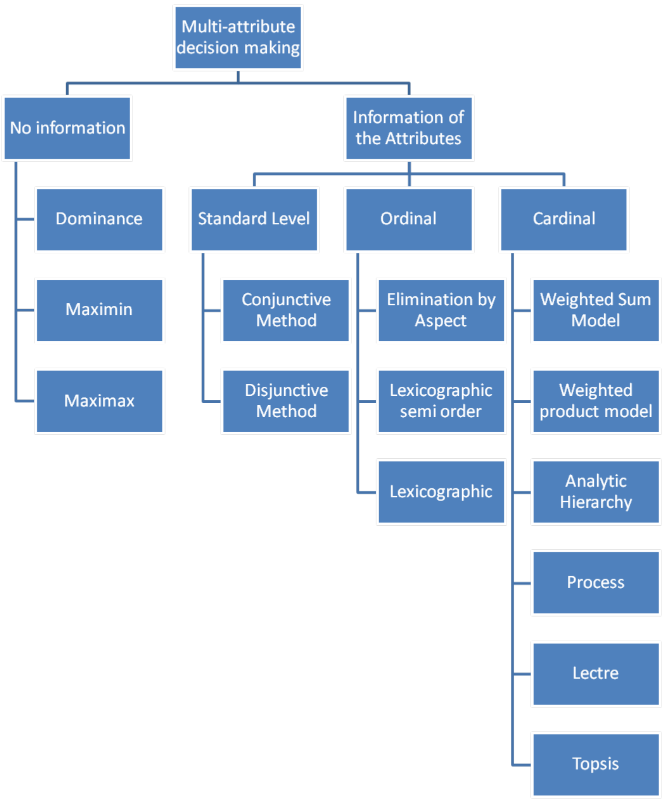

Figure 3.1: Multiple Criteria Decision Making Methods

Analytic Hierarchy Process (AHP) One of possible methods for selection of a supplier is AHP method, which offers a frame of effective tools in complex decision situations, and helps to simplify and speed up natural process of decision making. AHP method is based on breakdown of a complex situation into simple components, where hierarchical system of the problem and pairwise comparisons are made in order to ensure the quantification of qualitative judgments [57]. The components are hierarchically formed into a relational map as seen in

Figure 3.2. Each component represents a criteria that should be provided by the supplier candidates. Each component has sub-components which are qualitative or quantitative relational features. Each supplier candidate can fulfill these demanded features at certain measures which correspond to component scores of suppliers. Each component has certain importance level at the demander side, which is represented by weights, w_{ij} for sub-component j of component i as illustrated in Figure 3.2.

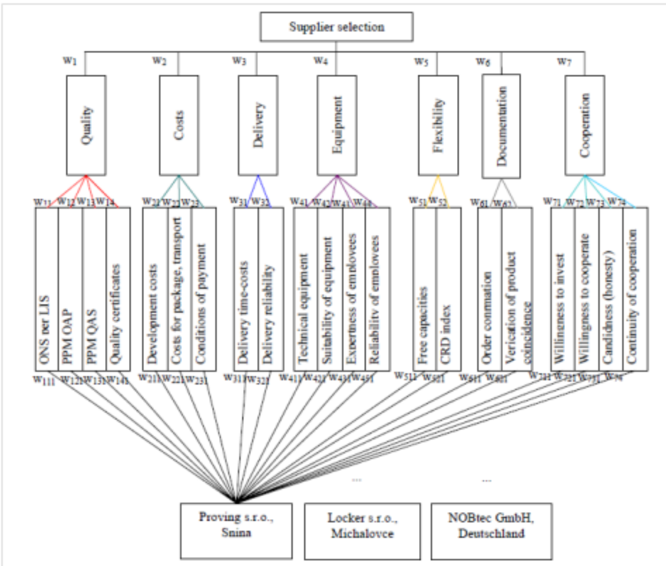

Figure 3.2: Hierarchical system component structure of the selection of supplier problems

In order to calculate the importance weight values, a pairwise reciprocal matrix is created based on importance ratios between reciprocal components at each hierarchical level as illustrated in Figure 3.3.

Based on these statements weights of criteria are determined [58] and principal eigenvector corresponding to a non-consistent matrix is calculated [59] using the following formula:

$$w_i = \lim_{k \to \infty} \frac{\sum_{h=1}^{n} a_{ih}^{(k)}}{\sum_{i=1}^{n} \sum_{h=1}^{n} a_{ih}^{(k)}}, \; i = 1, 2, \ldots, n$$

where w_i are components of the eigenvector and $a_{ih}^{(k)}$ are components of matrix A at level k of the hierarchical map.

In order to make a supplier decision, ratings for each supplier is calculated by executing a multiplicative addition of importance weights and supplier scores for each hierarchical map component.

$$A = \left|\begin{array}{ccccccc} Qty. & Cos. & Del. & E & F & Doc. & Coop. \\ 1 & 2 & 3 & 4 & 4 & 5 & 6 \\ 1/2 & 1 & 2 & 3 & 3 & 4 & 5 \\ 1/3 & 1/2 & 1 & 2 & 2 & 3 & 4 \\ 1/4 & 1/3 & 1/2 & 1 & 1 & 2 & 3 \\ 1/4 & 1/3 & 1/2 & 1 & 1 & 3 & 4 \\ 1/5 & 1/4 & 1/3 & 1/2 & 1/3 & 1 & 4 \\ 1/6 & 1/5 & 1/4 & 1/3 & 1/4 & 1/4 & 1 \end{array}\right| \begin{array}{c} \\ Quality \\ Cost \\ Delivery \\ Equipment \\ Flexibility \\ Documentation \\ Cooperation \end{array}$$

Figure 3.3: Pairwise comparison and reciprocal matrix formation

Elimination Method

Conjunctive elimination For this method, in each level of the ontology map, suppliers that do not satisfy a specific rule are eliminated. The remaining suppliers are chosen or subjected to an additional matching algorithm. [57]

Lexicographic elimination On the first level, the most significant criterion is selected and suppliers are compared with respect to this criterion. If a supplier satisfies this criterion much better than the other suppliers, this supplier is chosen, if not, the suppliers are compared with respect to a second criterion and so on. [57]

Integer Linear Programming (ILP) ILP is a linear programming model in which there a particular function to be maximized is or minimized subject to several constraints. As the unknown variables are all required to be integers, then the problem is called an integer programming (IP) or integer linear programming (ILP) problem. 0-1 integer programming or binary integer programming (BIP) is the special case of integer programming where variables are required to be 0 or 1 (rather than arbitrary integers). In ILP problem constraints forces the variables to take on binary values only. Much of the modeling flexibility provided by integer linear programming is due to the use of 0-1 variables [60].

The main elements of linear programming are:

1. Variables
2. Objective function
3. Constraints

4. Variable Bounds

The objective function is in the form of:

$$Z = \sum_{i=1}^{T} \sum_{j=1}^{M} W_{ij} X_{ij},\ i = 1, 2, \ldots, T \ and\ j = 1, 2, \ldots, M$$

i : Supplier index, j : Demand index, T : Number of suppliers in a set M : Number of demands in a set The objective function represents the maximization of the preference weighting $W_{ij}$and variables X_{ij} subject to constraints:

$$\sum_{j=1}^{M} X_{ij} \geq O_i,\ i = 1, 2, \ldots, T$$

$$\sum_{i=1}^{T} X_{ij} \geq N_j,\ j = 1, 2, \ldots, M$$

$$\sum_{i=1}^{T} \sum_{j=1}^{M} X_{ij} \leq A$$

N_j - Minimum requirement of suppliers for demand j

O_i - Maximum number of demands allocated to supplier i

A - Total number of supplier assignments needed for M number of demands. [61]

3.2 Problem Statement

A typical data integration and communication scenario example covering most of the requirements is as follows:

1. A non-local family doctor requests an MR inspection using the web interface.
2. The imaging request is delivered to the corresponding medical center.
3. HIS is informed and the Modality Work List request is delivered to RIS.
4. When the incoming patient is registered in HIS, the patient's previous medical information is pre-fetched and synchronized to PACS and HIS so that the radiologists can access the history of the patient no matter at which hospital, with which vendor's software the data is acquired.
5. The radiologist investigating the radiology examination makes a consultation or reporting request.
6. The most suitable radiologist and reporting unit is calculated based on the response time, subspecialty, techical capability and workload parameters.
7. the patient's data including previous examination is synchronized to PACS and/or RIS in the unit.

8. The radiologist at the reporting unit retrieves medical images to be reported from several medical centers on a single interface and generates corresponding reports in RIS or using the web interface.

9. The report is first delivered to the regarding medical center and finally to HIS.

The main purpose of this thesis work episode is to develop an algorithm in order to assign radiology inspections to the "most suitable" or "optimum" radiologist to be reported. In order to claim that a radiologist is the optimum choice as a reporter for certain inspections, we have to define measure parameters such as:

1. Subspecialty of the radiologist
2. Response time
3. Workload quota of the radiologist
4. Technical adequacy of the reporting unit that the radiologist is located

In order to optimize reporting workflow for short response time and high quality reports, the inspection demand should be assigned to a radiologist who has subspeciality and experience in the modality, disease, body system features of the inspection and who can respond as fast as possible. In urgent cases, response time is more of concern than profession area.

3.2.1 Subspecialty and Experience of the Radiologist

Based on the subspecialty of the radiologists and experience on practice, radiologists may be better equipped in certain modalities, diseases or body systems. Several studies have been carried out on the association between radiologist characteristics and interpretive performance of diagnostic radiology. [40, 62]

Diana et al illustrated that radiologists who spent 20% or more of their time in breast imaging had a statistically significantly higher sensitivity than those spending less than 20% of their time in breast imaging with a smaller and not statistically significant increase in false-positive rate and a non – statistically significant increased accuracy. Radiologists with a primary appointment at an academic medical center were statistically significantly more likely to detect breast cancer when it was present than other radiologists, with a smaller but statistically significantly increased false-positive rate and a borderline statistically significant improvement in accuracy. Radiologists who performed breast biopsy examinations had a lower threshold for recalling patients than those who did not perform breast biopsy examinations, which resulted in a statistically significantly higher sensitivity, a statistically significantly higher false-positive rate and no difference in accuracy. Neither annual interpretive volume nor the percentage of mammograms that were diagnostic was statistically significantly associated with sensitivity or false-positive rate. Radiologists who worked at least 20% of their time in breast imaging showed less variability than those who spent less time in breast imaging in their false-positive rates.

Therefore, if we generalize the ontology of the radiologist's subspecialty and experience, the hierarchical structure can be defined as:

1. Radiologist
    (a) Subspecialty
        i. Modality (Appendix C. Modality Index)
        ii. Body System
            A. Body Part (Appendix A. Body Part Index)
            B. Anatomy (Appendix B. Anatomy Index)
        iii. Disease (ICD-10-CM - ((WHO), 2013))

The ontology index of the leaf nodes Modality, Body Part, Anatomy (Association, Part 2: Conformance, 2004) (Association, Part 16: Content Mapping Resource, 2004) and Disease can be accessed in the Appendix section. In order to evaluate the experience on these nodes, ”Experience Indicators” node is inserted into each leaf node, which is expressed as Miglioretti and Barlow [40, 62]:

1. Experience Indicators
    (a) Years of interpretation
        i. <10
        ii. 10-19
        iii. >20
        iv. None
    (b) % of time spent working in area
        i. <20
        ii. 20-39
        iii. >40
        iv. None
    (c) % of images interpreted in area in the past year
        i. <25
        ii. 25-50
        iii. >50
        iv. None
    (d) Primary affiliation with an academic medical center on area
        i. Yes
        ii. No
    (e) Performed biopsies on area in the past year
        i. Yes
        ii. No
    (f) Quality of Report
        i. Includes enough technical information (1 to 5)
        ii. Lesion properties explained (1 to 5)
        iii. Secondary issues included (1 to 5)
        iv. Result / Diagnosis / Distinguishing diagnosis included (1 to 5)

3.2.2 Response Time

Response time is another important parameter that should be taken into account while estimating the most suitable radiologist for the inspection. A radiology inspection demand for diagnostic reporting should be conventionally reported within 48 hours while an urgent inspection should be reported in at most 4 hours. The factors effecting the response time are:

1. Response time
   (a) Inspection file delivery time (t_d)
      i. Inspection file size
      ii. Reporting unit bandwidth
   (b) Radiologist availability time (t_a) based on schedule
   (c) Radiologist reporting time (t_r)

3.2.3 Workload Quota of the Radiologist

In order to provide efficient reporting conditions and to balance financial gains, each radiologist should be assigned a certain amount of inspections to be reported. However, every reporting process is not equal in effort. The work load and payments of reporting processes are determined according to the ”Performance Point Documentation (SUT)” announced by the Turkish Ministry of Health in Turkey. ”Performance Point Extension Proposal” proposed by the Turkish Society of Radiology can also be used to strengthen the estimations on the average reporting time (Appendix D. Workload Index).

In urgent cases, response time is much more important than the workload capacity and subspecialty; therefore, subspecialty and workload quota may be evaluated as secondary importance in emergency situations.

3.2.4 Technical Adequacy of the Reporting Unit

Based on the inspection distribution scenario within this thesis study, it is assumed that the radiologists are located in reporting units, where the assigned inspections are synchronized for access. Therefore, the technical infrastructure of the reporting unit effects the response time and the capacity of reporting service. Bandwidth of the reporting unit determines the inspection file delivery time and consequently effects the response time. Storage capacity and performance of the workstations determine the technical adequacy of the reporting unit. In order to measure the technical adequacy, the following ontology can be utilized:

1. Technical adequacy
   (a) Bandwidth
   (b) Storage capacity
   (c) Server performance
      i. RAM capacity

ii. Processor capacity
iii. Capacity of ethernet card(s)

(d) Workstation performance
i. Number of workstations
ii. RAM capacity in workstations
iii. Processor capacity
iv. Avg. capacity of Ethernet cards
v. Medical monitor capacity

3.3 Method

3.3.1 Medical Image Delivery Optimization

In the development of reporting workflow optimization algorithm, RWOA, to assign an inspection to the radiologist, the following steps should be carried out:

1. Render entities (inspection and reporters) into ontology maps
2. Calculate weights of reporter features based on importance using AHP
3. Execute a semantic matching process between each radiologist and inspection
4. Define constraints for the assignment process
5. Execute assignment process using ILP.

3.3.1.1 Rendering Entities into Ontology Maps

The inspection and radiologist attributes are modelled using a hierarchical ontology structure based on DICOM Conformance and DICOM Content Mapping Resource and WHO definitions. Ontology maps include the main nodes of Subspeciality, Response Time, Workload and Technical. Subspeciality is evaluated by the assessment of subquantities for each subnode Modality, Body Part, Anatomy and Disease. Similarly each node is connected hierarchically to subnodes having a weighted relation based on AHP. The input for the assessment process is provided by the inspection DICOM file. *dcm4che* library is used to render inspections in DICOM format. Modality, body part and anatomy examined, protocol requested, file size, series and slice numbers, resolution data are rendered into XML for RWOA. Requested protocol id, which is determined using the web interface by a physician's request for a radiology inspection, is mapped to SUT codes which determine the required effort and time for the reporting process. Pre-diagnosis is entered using the web interface by the report requester as 10^{th} revision of International Classification of Diseases (ICD-10) code. The attributes rendered in the inspection files of DICOM format are used to derive the demand criterias for the radiologist. It is assumed that the pre-diagnosis is either embedded into the inspection or entered manually by the report requester as ICD-10 code. As a result data structure illustrated in Figure 3.4 is obtained.

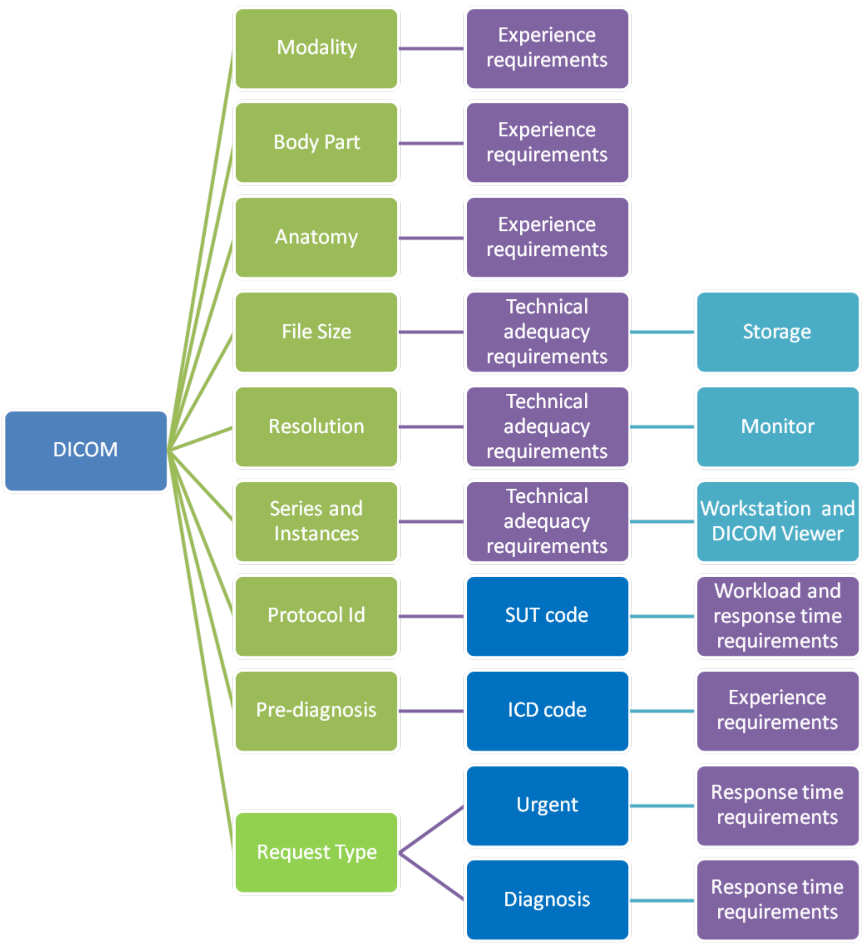

Figure 3.4: DICOM file structure. The file structure is rendered to obtain components and these components are used to form the ontology map of the inspection which the DICOM file belongs.

Table 3.1: SUT Performance Code Structure. Each SUT code defines a certain inspection demand which has standardized values of effort points based on risk factors, technology requirements, urgency, frequency, alternative cure presence and estimated time of the inspection.

Code	Name	Points	Risk	Tech. Req.	Staff Req.	Urgency	Freq.	Alt.	Est. time
803910	CT, brain	92,75	3	4	3	4	3	4	15

The attributes rendered in the DICOM formatted inspection files are used to derive the demands for the radiologist. Table 3.1 illustrates SUT performance information for a sample ”CT”, ”Brain” inspection for the ”Spine” which is requested with a pre-diagnosis of ICD-10 code ”D33.4 : Spinal cord benign neoplasm”. Figure 3.5 also illustrates the sample inspection attributes on the ontology map highlighted in green. Therefore, the radiologist assigned for this inspection should be specialized in Brain CT for spine cord benign neoplasms and have time and effort quota of 15 minutes and 5.51 units respectively. As this inspection is not an urgent inspection, the experience characteristics of the radiologist can be rated higher than the response time, workload and technical requirements. Each inspection is a reporting demand with certain subspeciality, response time, workload and technical requirements. The detailed ontology map of each demand is illustrated in Figure 3.5. The modality, anatomy, body system and pre-diagnosis parameters of the inspection form sub-nodes of required subspecialities. SUT code determine the workload and required effort parameters. Inspection file size and modality determine the required storage, bandwidth and monitor resolution parameters.

The radiologist which is the supplier in the AHP problem has corresponding attributes in the form of an ontology map illustrated in Figure 3.6. The subspeciality of the radiologist is based on modality, body system, anatomy and disease sub-groups. Each subspecialty sub-group has experience indicators stating the number of interpretation years, percentage of time spent, percentage of images interpreted, academic study performed and report quality feedback. Each indicator has a score at the supplier side and an importance weight determined at the demander side.

Figure 3.5: Ontology Map of the demand or requirement for the reporting process based on the inspection ontology.

Figure 3.6: Ontology Map of the radiologist based on experience, response time, workload and technical components.

Table 3.2: Reciprocal matrix to calculate weights between subspecialty, response time, workload and technical components for diagnostic reporting processes. For diagnostic inspection reporting demands, subspecialty is evaluated to be the most important attribute compared to response time, workload and technical components. It can be seen that subspecialty importance ratios with reference to response time, workload and technical components are 2, 1.33 and 4 respectively. Therefore, workload is evaluated to be the second important component, which has a close importance ratio of 1.5 to response time. Technical adequecy is evaluated to be the least important component for diagnostic reporting.

DIAGNOSTIC	Subspecialty	Response Time	Workload	Technical	Geometric Mean	Weight
Subspecialty	1	2	1,33	4	1,81	0,40
Response Time	0,5	1	0,67	2	0,90	0,20
Workload	0,75	1,5	1	3	1,36	0,30
Technical	0,25	0,5	0,33	1	0,45	0,10
				SUM	4,52	1,00

3.3.1.2 Calculate weights using AHP

The pairwise comparison is carried out at each level of the ontology map. For each level, components of the node is represented by a pairwise comparison matrix. If there are n items that need to be compared for a given node, then a total of n(n-1)/2 judgments have to be made. These judgements were executed by surveying expert radiologists to compare the importance of the components in pairs at each level of the ontology map. The weight w_l for each entity l at hierarchical level k of the ontology map including n entities is calculated using pair-wise comparison matrix element a_{lm} by the following equation:

$$w_l = \frac{\sqrt[n]{\prod_{m=1}^{n} a_{lm}^{(k)}}}{\sum_{l=1}^{n} \sqrt[n]{\prod_{m=1}^{n} a_{lm}^{(k)}}}, \quad l, m = 1, 2, \ldots, n \tag{3.1}$$

The pairwise matrix calculations for each level in the ontology map starting from first level to the leaf are illustrated in the following Tables 3.2, 3.3, 3.4, 3.5, 3.6, 3.7, 3.8, 3.9, 3.10 and 3.11. The resultant ontology map with calculated weight vectors is illustrated in Figure 3.7.

In order to evaluate the subspecialty of a radiologist on a modality, body system, anatomy or disease, the possible characteristics of radiologists are investigated in literature. Most typical research to find a correlation between radiologist characteristics and diagnosis accuracy is mammography scan application where the gold standard is determined by biopsies. Based on the studies of Diana L. Miglioretti, 2007 [40] and William E. Barlow, 2004 [62] there is a correlation between certain characteristics of radiologists and diagnosis accuracy, which is illustrated in Main Property (A, B, C, D, E), Sub Property and Accuracy columns in Table 3.5. In order to enhance the subspeciality rating of radiologists "Quality of Report" (F) attribute is introduced which is updated based on feedbacks within the proposed architecture. As this component is a sub-node to modality, body part, anatomy and disease; any feedback on an inspection report applies to the correspond subspecialty score. The accuracy values are taken as references to determine rating scores for sub-properties. Normalized ratings are calculated

Table 3.3: Reciprocal matrix to calculate weights between subspecialty, response time, workload and technical components for urgent reporting processes. Response time is evaluated to be the most important attribute compared to subspecialty, workload and technical components. Subspecialty is evaluated to have an importance ratio of 0.4 to response time. Resultant normalized importance weights are 0.56, 0.22, 0.11, 0.11 for response time, subspecialty, workload and technical components respectively.

URGENT	Subspecialty	Response Time	Workload	Technical	Geometric Mean	Weight
Subspecialty	1	0,4	2	2	1,12	0,22
Response Time	2,5	1	5	5	2,81	0,56
Workload	0,5	0,2	1	1	0,56	0,11
Technical	0,5	0,2	1	1	0,56	0,11
				SUM	5,06	1,00

Table 3.4: Reciprocal matrix to calculate weights for subspecialty sub components : modality, body part, anatomy and disease. In order to determine subspecialty of a radiologist, modality is evaluated to be the most significant attribute. The resultant normalized importance weights are 0.37, 0.27, 0.18, 0.18 for modality, body part, anatomy and disease respectively, which means subspecialty of a radiologist in a certain modality or body system is more powerful in the inspection assignment process compared to prediagnosis and anatomy attributes of the inspection.

SUBSPECIALTY	Modality	Body Part	Anatomy	Disease	Geometric Mean	Weight
Modality	1	1,5	2	2	1,57	0,37
Body Part	0,67	1	1,33	2	1,16	0,27
Anatomy	0,5	0,75	1	1	0,78	0,18
Disease	0,5	0,75	1	1	0,78	0,18
				SUM	4,29	1,00

by normalizing the accuracy values and mapping to 100 scale. It can be seen that accuracy values for some sub-properties are very close to each other, which means that the parent property is not very deterministic for accuracy outcomes. This fact is utilized to determine the importance weight of the main properties. Variance to mean ratios of the accuracy values for each sub-property group is calculated and determined to be the importance weight for the corresponding main group.

Although workload distribution is mainly handled by the ILP process, inspection assignment to radiologists with high workload quota is also promoted at AHP level. The measure for weight evaluation is determined to be the ratio of available workload quota of the radiologist, Q and the required workload effort, RWE to execute the reporting for the inspection demand according to SUT standard. The schedule of the radiologist is also taken into account such that assignment process is promoted for radiologists that have large time slots in their schedule. The measure for schedule weight evaluation is determined to be the ratio of the remaining time in the working slot of the radiologist, $t_{r,remaining}$ and the time required to execute the reporting process for the inspection demand, $t_{r,req}$, according to SUT standard. Schedule and Quota subnodes of Workload component are equally weighted and the Q/RWE, $t_{r,remaining}/t_{r,req}$ parameter evaluation is illustrated in Tables 3.9 and 3.10.

Technical parameters such as monitor resolution, bandwidth, available free storage, and number of available workstations effect the quality of the reporting process and response time. MG inspections require 5 MP monitor resolution for medical assessment while DX, CR, DR modalities require 2 MP monitor resolution. Therefore, reporting units or radiologists that fulfill the corresponding monitor resolution for modality of inspection demand are promoted in the assignment process. Bandwidth effects the image delivery time, which also has to be taken into account while evaluating the response time. Available storage size is another parameter that is evaluated to prevent technical stucks during the assignment process.

Table 3.5: Ratings and weight calculations based on sub properties of subspecialty and variance of corresponding performance outcomes.

Experience on matching Modality / Body Part / Anatomy / Disease				
Main Property	weight	Sub property	Accuracy	Normalized Rating
Years of interpretation (A)	0.14	<10	1.00	100
		10-19	0.81	81
		>20	0.66	66
		None	0	0
% of time spent working in area (B)	0.14	<20	1.00	77
		20-40	1.30	100
		>40	0.92	71
		None	0	0
% of images interpreted in area in the past year (C)	0.08	<25	1.00	97
		25-50	1.03	100
		>50	0.85	83
		None	0	0
Primary affiliation with an academic medical center on area (D)	2.01	Yes	3.01	100
		No	1.0(referent)	0
Performed biopsies on area in the past year (E)	0.16	Yes	1.16	100
		No	1.0(referent)	0
Quality of report (F)	2	Includes enough technical information (1-5)	-	25 x (rate/5)
		Lesion properties explained (1-5)	-	25 x (rate/5)
		Secondary issues included (1-5)	-	25 x (rate/5
		Result / Diagnosis / Distinguishing diagnosis included (1-5)	-	25 x (rate/5)

Table 3.6: Reciprocal matrix to obtain normalized weights of subspecialty and experience factors: A, B, C, D, E and F. The ratio values are calculated based on the Normalized Score values in Table 3.5. Academic affiliation (D) and Quality of Report (F) feedback is evaluated to be the most important attributes to determine the subspecialy rating of a radiologist on a certain modality, body system, disease or anatomy.

	A	B	C	D	E	F	Geometric Mean	Weight
A	1,00	1,00	1,75	0,07	0,88	0,07	0,44	0,03
B	1,00	1,00	1,75	0,07	0,88	0,07	0,44	0,03
C	0,57	0,57	1,00	0,04	0,50	0,04	0,25	0,02
D	14,36	14,36	25,13	1,00	12,56	1,01	6,35	0,45
E	1,14	1,14	1,14	0,08	1,00	0,08	0,46	0,03
F	14,29	14,29	25,00	1,00	12,50	1,00	6,32	0,44
						SUM	14,26	1,00

Table 3.7: Reciprocal matrix for response time weights in diagnostic reporting processes. The response time is evaluated in 6 time slots. For diagnostic processes the optimal response time is within 24 hours. Therefore, response time longer than 24 hours is not promoted while shorter response times are promoted up to an importance ratio of 2.5 (<4/<24).

RESPONSE TIME (diagnostic)	<4	<8	<12	<24	<48	>48	Geometric Mean	Weight
<4	1	1,25	1,67	2,5	5	10	2,53	0,32
<8	0,8	1	1,33	2	4	8	2,02	0,26
<12	0,6	0,75	1	1,5	3	6	1,52	0,19
<24	0,4	0,5	0,67	1	2	4	1,01	0,13
<48	0,2	0,25	0,33	0,5	1	2	0,50	0,06
>48	0,1	0,125	0,17	0,25	0,5	1	0,25	0,03
				SUM			7,83	1,00

Table 3.8: Reciprocal matrix for response time weights in urgent reporting processes. The response time is evaluated in 6 time slots. For urgent demands the optimal response time is within 4 hours. Therefore, response time longer than 8 hours is strictly not promoted.

RESPONSE TIME (Urgent)	<4	<8	<12	<24	<48	>48	Geometric Mean	Weight
<4	1	10	10	10	10	10	6,81	0,59
<8	0,5	1	5	5	5	5	2,61	0,23
<12	0,1	0,2	1	1	1	1	0,52	0,05
<24	0,1	0,2	1	1	1	1	0,52	0,05
<48	0,1	0,2	1	1	1	1	0,52	0,05
>48	0,1	0,2	1	1	1	1	0,52	0,05
				SUM			11,50	1,00

Table 3.9: Reciprocal matrix for quota factors based on workload ratings

QUOTA	Q/RWE >10	Q/RWE <10	Geometric Mean	Weight
Q/RWE >10	1	2	1,41	0,67
Q/RWE <10	0,5	1	0,71	0,33
		SUM	2,12	

Table 3.10: Reciprocal matrix for schedule factors based on workload ratings

SCHEDULE	$t_{r,rem}/t_{r,req}$ >10	$t_{r,rem}/t_{r,req}$ <10	Geometric Mean	Weight
$t_{r,rem}/t_{r,req}$ >10	1	2	1,41	0,67
$t_{r,rem}/t_{r,req}$ <10	0,5	1	0,71	0,33
		SUM	2,12	

Table 3.11: Reciprocal matrix for technical factors. Monitor resolution, which effects the quality of medical assessment, is evaluated to be the most important attribute compared to bandwidth, storage and workstation sub-components of the Technical component. Bandwidth and storage are equally weighted as second place importance in technical adequacy contribution for radiologist rating score calculation.

TECHNICAL	Monitor	Bandwidth	Storage	Workstation	Geometric Mean	Weight
Monitor	1	1,5	1,5	3	1,61	0,37
Bandwidth	0,67	1	1	2	1,08	0,25
Storage	0,67	1	1	2	1,08	0,25
Workstation	0,33	0,5	0,5	1	0,54	0,12
				SUM	4,30	1,00

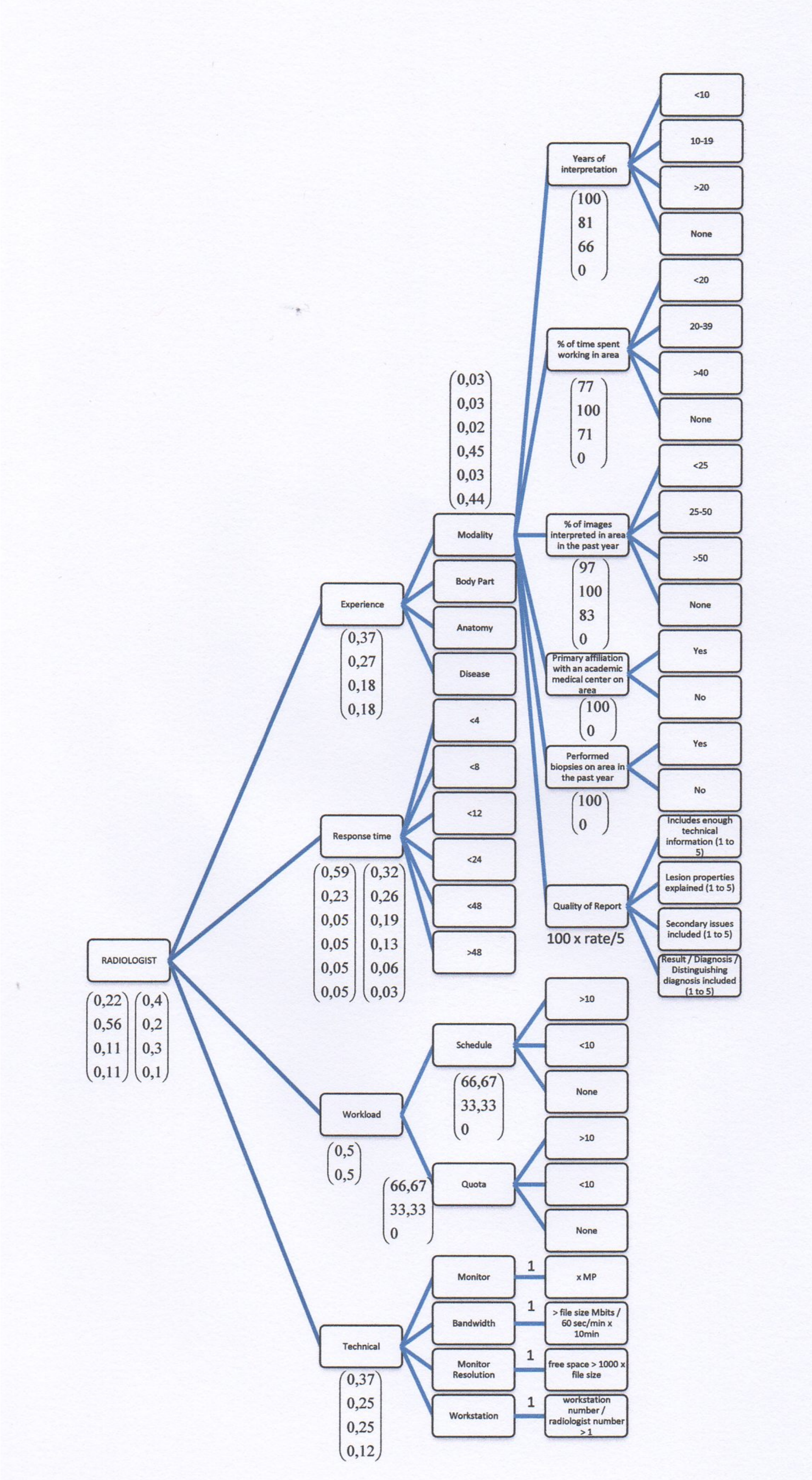

Figure 3.7: Ontology map for radiologist requirements and importance weights to calculate total ratings subspeciality, response time, workload and technical requirements for each potential match or assignment. Leaf nodes are indicators for each entity which are rated based on a qualitative property or quantitive value condition. In urgent cases, response time is much more important than the workload capacity and subspeciality; therefore, subspeciality and workload quota are evaluated as secondary importance in emergency situations and consequently there are two different weight matrixes on the response time node

3.3.1.3 Semantic matching process

In semantic matching process, the ontology map and calculated weights are taken into account. A similar algorithm proposed by Colucci and Di Noia [53, 54, 55] is used to calculate the ratings of each reporter. However, in the algorithm proposed in this study, weights are used rather than adding 1 for mismatch and addition of multiplicative weights implies similarity rather than mismatch.

Ratings are evaluated with a recursive relation based semantic matching process [53] by normalizing the sum of multiplicative weights with the following equation:

$$r_l^{(k-1)} = \frac{\sum_{m=1}^{M} w_m^{(k)} r_m^{(k)} q_m c_{lm}}{\sum_{l=1}^{L} \sum_{m=1}^{M} w_m^{(k)} r_m^{(k)} q_m c_{lm}}, \tag{3.2}$$

l=1, 2,. . . ,L, m=1, 2,. . . ,M where L and M are the number of entities at levels $k-1$ and k of the ontology map respectively. q_m is equal to 1 if the qualitative or quantitative condition is satisfied by the potential assignee on entity m and 0 otherwise. c_{lm} is the binary value representing the presence of the connection between entities l and m in the ontology map.

3.3.2 Definition of constraints

Constraint 1: Assignment Constraint As an assumption, an inspection is assigned only to one radiologist.

$$x_{ij} = \begin{cases} 1, & i \text{ is assigned to } j \\ 0, & i \text{ is not assigned to } j \end{cases}$$

where

i - Inspection index, i = 1, 2, ... T, T = Number of inspections to be assigned j – Radiologist index, j = 1, 2, ... M, M = Number of radiologists available.
Therefore, the constraint can be defined as; For each inspection i,

$$\sum_{j=1}^{M} x_{ij} = 1$$

Constraint 2: Workload Constraint Each inspection has an estimated effort which is derived from the workload index.(Appendix D. Workload Index) Also each reporter has a daily workload that should not be exceeded except urgency cases.

$$\sum_{i=1}^{T} e_i x_{ij} \leq l_j$$

where,

$$\begin{aligned} l_j &: \ workload\ of\ radiologist\ j \\ e_i &: \ effort\ required\ for\ inspection\ i \end{aligned}$$

Constraint 3: Response Time Constraint It is defined that for the response time for reporting differs for urgent and diagnostic demands. For urgent cases, the response time should be typically less than 4 hours, while for diagnostic cases; it is typically determined to be less than 48 hours.

The constraint for diagnostic cases can be defined as follows:

For each inspection i;

$$\begin{aligned} urgent: &\quad \textstyle\sum_{j=1}^{T} t_{resp,ij} x_{ij} \leq C_1 \\ diagnostic: &\quad \textstyle\sum_{j=1}^{T} t_{resp,ij} x_{ij} \leq C_2 \end{aligned}$$

where,

$$\begin{aligned} t_{d,ij}&: \ file\ i\ delivery\ time\ to\ j\ in\ s \\ f_i&: \ inspection\ file\ size\ in\ MB \\ b_j&: \ reporting\ unit\ bandwidth\ for\ j\ in\ Mbits/s \\ t_{a,j}&: \ availability\ time\ of\ j\ in\ s \\ t_{r,ij}&: \ reporting\ time\ of\ j\ for\ i\ in\ s \end{aligned}$$

and

$$\begin{aligned} t_{resp,ij} &= t_{d,ij} + t_{a,j} + t_{r,ij} \\ t_{resp,ij} &= \tfrac{8 \times f_i}{b_j} + t_{a,j} + t_{r,ij} \end{aligned}$$

where $t_{a,j}$ is based on the schedule of the radiologist and queue of inspections waiting to be reported and $t_{a,j}$ is evaluated based on the workload index (Appendix D. Workload Index). C_1 and C_2 are conventionally taken as 4 hours and 48 hours respectively.

Constraint 4: Storage Constraint It is stated as a rule that the free space in the server at the reporting unit should be at least C_3 times that of the incoming inspection file size so that big files should be directed to big storages and disk volume problems are prevented. Constraint 4 can be defined as:

$$\sum_{j=1}^{T} \frac{s_j}{f_i} x_{ij} \leq C_3$$

where,

$$s_j: \ storage\ capacity\ at\ j\ in\ MB$$

This constraint also provides that the disk volume is filled by the assigned inspections. C_3 is taken as 1000 in calculations.

Constraint 5: Bandwidth Constraint It is stated as a rule that the transfer of an inspection to a reporting unit should not take more than C_4 minutes. In other words, if an inspection file size is large then it should be directed to a reporting unit that has high bandwidth capacity so that network traffic is not stuck and inspection is transferred in shorter time. Constraint 5 can be defined as:

$$\begin{aligned} &\textstyle\sum_{j=1}^{T} \frac{8 \frac{Mbits}{MB} \times f_i}{b_j} x_{ij} \leq C_4 \min \times 60 \frac{\sec}{\min} \\ &\textstyle\sum_{j=1}^{T} \frac{8 \times f_i}{b_j} x_{ij} \leq 60 C_4 \end{aligned}$$

C_4 is taken as 10 minutes in calculations.

3.3.2.1 ILP process

As a result of problem statement, weight calculations and constraint definitions, the ILP problem becomes:

$$
\begin{aligned}
&Max\left(\sum_{i=1}^{M}\sum_{j=1}^{T} w_{ij}x_{ij}\right)\\
&w.r.t\\
&\sum_{j=1}^{M} x_{ij} = 1\\
&\sum_{i=1}^{T} e_i x_{ij} \leq l_j\\
&\sum_{j=1}^{T}\left(\frac{8\times f_i}{b_j} + t_{a,j} + t_{r,ij}\right)x_{ij} \leq C_1 \quad or \quad \sum_{j=1}^{T}\left(\frac{8\times f_i}{b_j} + t_{a,j} + t_{r,ij}\right)x_{ij} \leq C_2\\
&\sum_{j=1}^{T}\frac{s_j}{f_i}x_{ij} \leq C_3\\
&\sum_{j=1}^{T}\frac{8\times f_i}{b_j}x_{ij} \leq 60C_4
\end{aligned}
$$

where w_{ij} is calculated using the semantic matching and AHP for each inspection i and radiologist j. In order to carry out ILP process, Eclipse development environment and Java programming language is used. The program for ILP is developed utilizing the open source *lp_solve* library *OptimJ*.

CHAPTER 4

RESULTS AND DISCUSSION

In order to evaluate the solution, architecture and RWOA have been tested in 3 different stages as illustrated in Figure 4.1. In Stage 1, the architecture is piloted in a reporting unit where 10 radiologists were employed and 2 reporting periods, RP-1 and RP-2, were investigated.

In RP-1, 4738 medical inspections which involved 4481 CT, 116 MR, 106 CR and 35 MG, were archived and reported. Inspections were imported from an archive to test the functionality of the reporting unit and user interface. At this stage, the radiologists were obliged to finish the overall reporting process within one month; therefore the chief radiologist had to make the reporting assignment considering the parameters of subspeciality, response time and workload limits.

In RP-2 22 hospitals were integrated to the system and generated inspections were synchronized to the Reporting Unit with the help of Grid Manager and Grid Agent architecture. 1464 medical inspections, which involved 1445 CT, 18 MR, and 1 CR, were archived and reported. The assignment was done by the chief radiologist to 9 radiologists.

In Stage 2, Stage 1/RP-1 event logs and archive data are utilized to extract radiologists' reporting time, assigned workload, frequency of reporting, which are indicators of response time, workload limit and subspeciality respectively. The extraction is also executed with reference to body part and imported into the ontology map. Stage 1/RP-2 data and assignment decisions are utilized to make a comparison with RWOA assignment decisions. The ontology map of radiologists formed using Stage 1/RP-1 data is used in RWOA. The assignment results are compared between manual assignment and reporting workflow optimization applied assignment based on subspeciality, response time and workload success rates.

During the period Stage 1 and Stage 2, the architecture has been tested in a total of 35 hospitals, 13 primary care clinics, 3 mobile clinics, 1 reporting unit. 3.35 million inspections were archived and 14216 inspections were reported by the reporting unit. However, an organized reporting process was executed only in Stage 1; therefore, 6202 reports which were archived during Stage 1 were utilized for RWOA evaluation.

In Stage 3, 8 primary care medical imaging centers, 3 cancer screening centers and one reporting unit are integrated to the system. Grid Agents are deployed on each site controlled by Grid Manager on the server side.

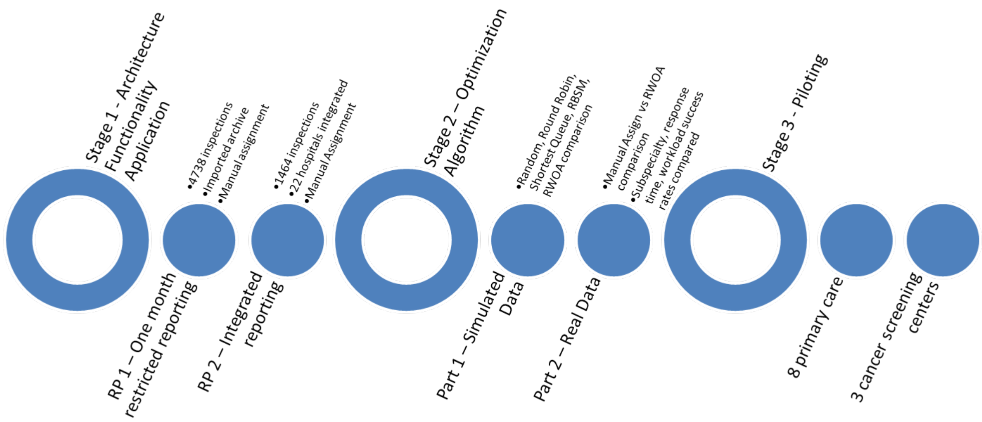

Figure 4.1: Implementation stages to evaluate architecture and RWOA. In Stage 1, both the architecture has been tested in terms of functionality and the process data has been archived for future use in the RWOA evaluation phase. In Stage 2, RWOA is evaluated using simulated data and the data obtained in Stage 1. In Stage 3, 8 primary care medical imaging centers, 3 cancer screening centers and one reporting unit are integrated to the system. Grid Agents are deployed on each site controlled by Grid Manager on the server side.

4.1 Stage 1

At this stage RWOA is not activated and the inspections generated are syncronized to the reporting unit Grid Agent. The inspections are assigned manually by the chief radiologist to an expert among 9 radiologists. Two reporting periods are defined as RP-1 and RP-2. In RP-1, 4738 medical inspections were archived and reported. The distribution with reference to modality and body part is illustrated in Figure 4.2 and Figure 4.3. In RP-2 1464 medical inspections were archived and reported. The distribution with reference to modality and body part is illustrated in Figure 4.4 and Figure 4.5.

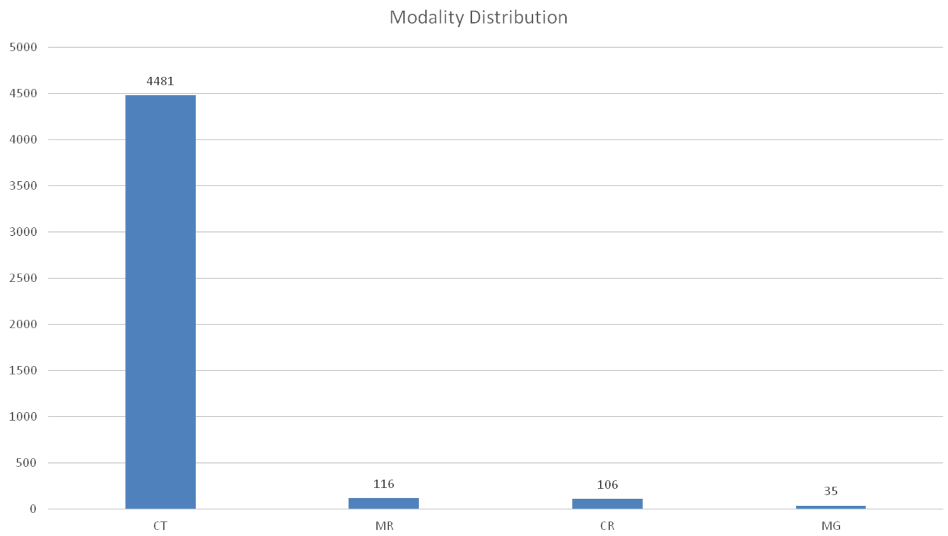

Figure 4.2: Distribution of radiology inspections in RP-1 with reference to modalities; CT, MR, CR, MG. In this period 4481 CT, 116 MR, 106 CR and 35 MG inspections are archived and reported.

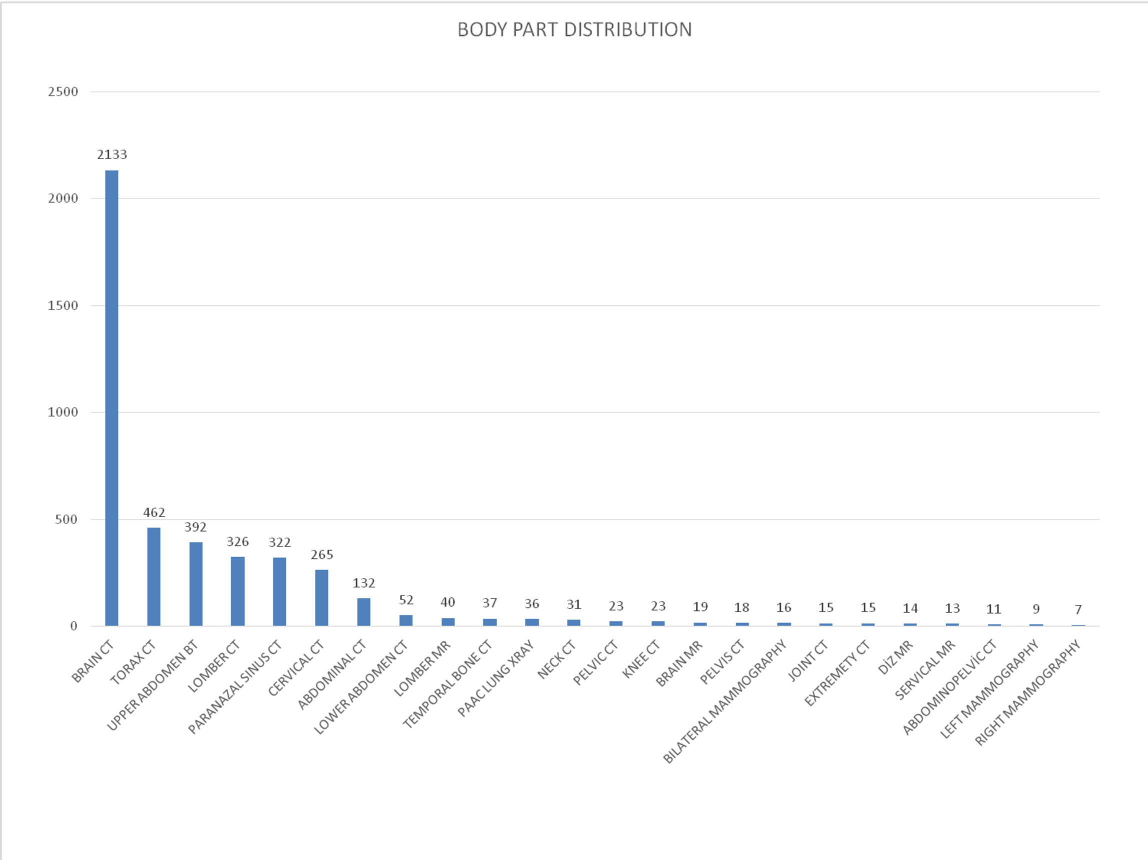

Figure 4.3: Distribution of radiology inspections in RP-1 with reference to bodypart.

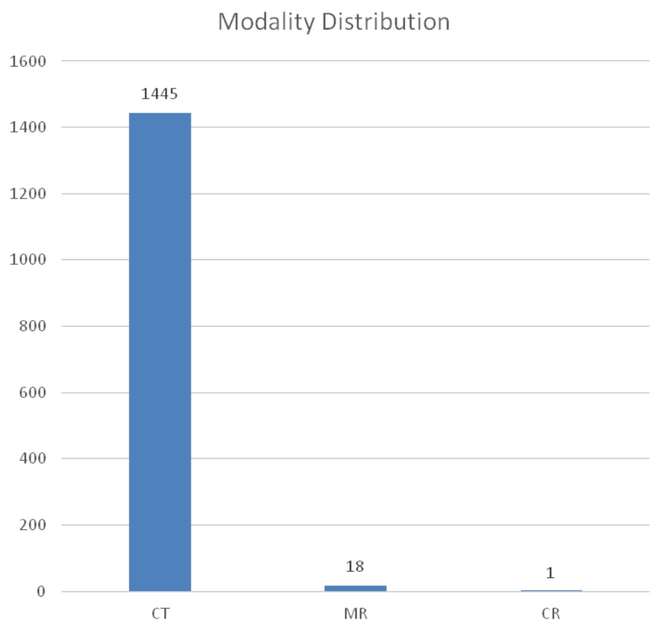

Figure 4.4: Distribution of radiology inspections in RP-2 with reference to modalities; CT, MR, CR. In this period 1445 CT, 18 MR and 1 CR inspections are archived and reported.

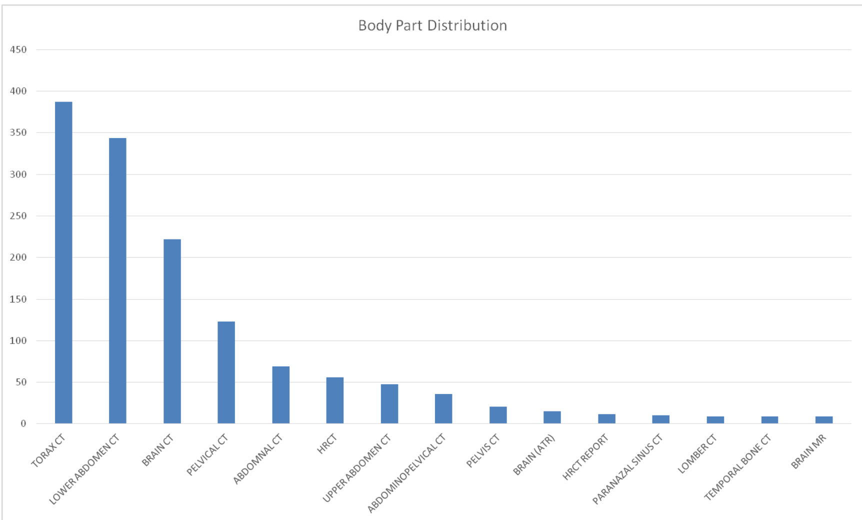

Figure 4.5: Distribution of radiology inspections in RP-2 with reference to body part.

4.1.1 The Architecture

Workflow centric network architecture with an enhanced caching, querying and retrieving mechanism is implemented by seamlessly integrating *Grid Agent* and *Grid Manager* to conventional digital radiology systems as illustrated in Figure 4.6. Grid Agent is deployed on each site and is responsible for rendering medical data and incoming messages or transferring radiology data between PACS, RIS, HIS, Workstations, non-local clients, Grid Manager and other Grid Agents. Grid Manager is responsible for the flow management of images between sites and reporting units or distribution of reports generated by radiologists. It communicates with Grid Agents and performs database, indexing and file operations at the center.

A typical data integration, communication and medical image delivery scenario starts with a non-local physician's request for a radiology inspection using the web interface. When the request is received, Grid Manager delivers the imaging request as an Extensible Markup Language (XML) message to the Grid Agent at the regarding medical center. Grid Agent informs the HIS and delivers the Modality Work List (MWL) request to the RIS. When the incoming patient is registered in HIS, Grid Agent is informed which afterwards gets the index of Grid Agents that have patient's data regarding previous examinations from the Grid Manager. Grid Agent pre-fetches the patient's previous medical information and synchronizes PACS and HIS in case a local radiologist examines the inspection. In parallel, Grid Manager automatically assigns the inspection to a remote radiologist after evaluating the subspecialty, experience, report quality, response time and technical adequecy parameters of registered radiologists and corresponding reporting units. Grid Agent at the reporting unit of the assignee receives the updated request list from the Grid Manager and fetches the patient's data including previous examination with the Grid Agent Index and synchronizes the data to PACS in the unit. The non-local radiologist can access the history of the patient independent from the vendor's software and the hospital where the data is acquired. The radiologist at the reporting unit retrieves medical images to be reported from several medical centers on a single interface and generates corresponding reports in RIS or using the web interface. The report is first delivered to the Grid Manager, then to the Grid Agent at the regarding medical center and finally to HIS.

The architecture is designed to fulfill the requirements of *Interoperability*, *Scalibility*, *Compatibility*, *Accessibility* and *Workflow Optimization* with four main components: *Grid Agent*, *Grid Manager*, *Data Management Platform* and *Front-End*.

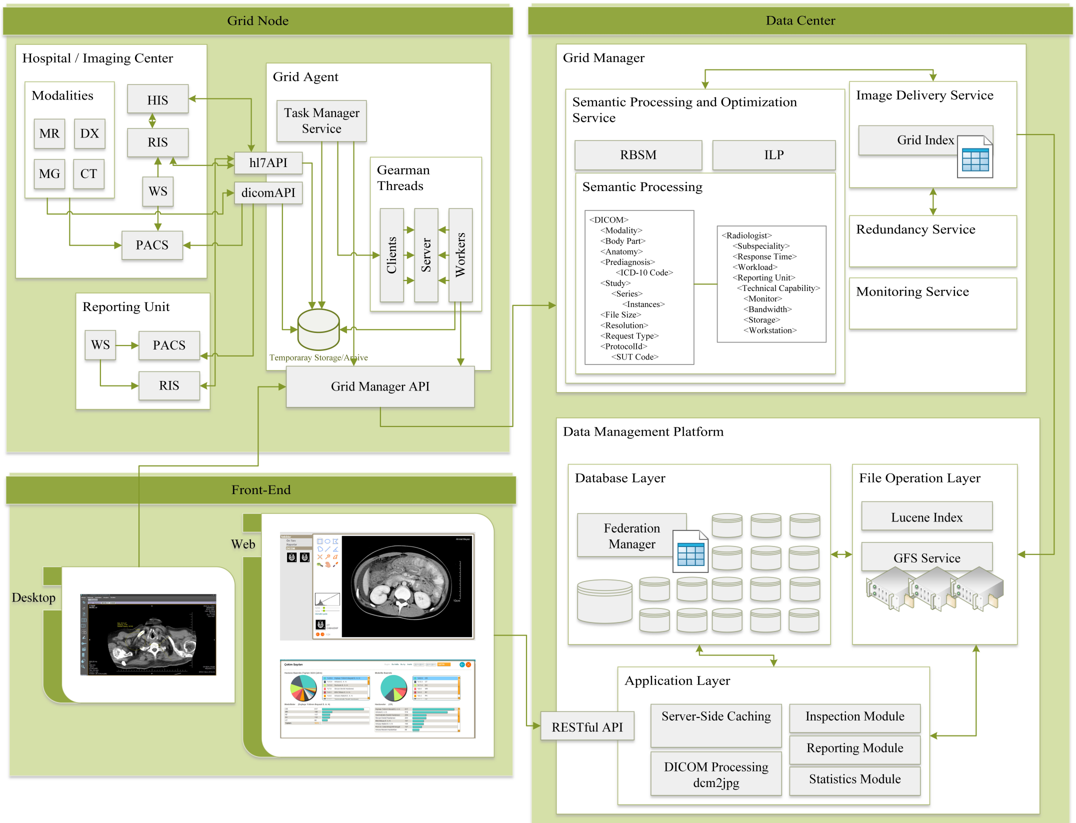

Figure 4.6: Workflow centric framework with an integrated caching, querying and retrieving mechanism. Grid Agent and Grid Manager are seamlessly integrated to conventional digital radiology systems. Grid Agent can be deployed in hospitals, medical centers and reporting units. A service based version of Grid Agent can be used for individual use by radiologists in order to synchronize assigned medical inspections for desktop access. Grid Agent is responsible for rendering and transferring radiology data to local PACS, RIS, Workstations, Grid Manager and clients. Grid Manager is responsible for the flow management of images between sites and reporting units or distribution of reports based on the RWOA.

4.1.1.1 The Grid Agent

Grid Agent communicates with PACS, RIS, HIS and workstations using DICOM and HL7 protocols. The communication between Grid Agents and Grid Manager is accomplished using encrypted XML messages using HTTP and Real Time Messaging Protocol (RTMP) protocols.

Grid Agent software is developed to run on open source Red5 media server which supports streaming and shared object communication over RTMP. DICOM and HL7 messages are handled by asynchronous Java threads using dcm4che and HAPI Java libraries. Grid Agent is composed of two main components:

Interface Layer DICOM, HL7 and Grid Manager interfaces are implemented in order to interconnect Grid Manager with local PACS, RIS, HIS and imaging facilities. *dicomAPI* handles DICOM Send requests from modalities using DcmRcvScp. The received data is archived in a temporary storage and the reference is saved in Postgresql database. Medical images imported by the Grid Manager API can also be transfered to local PACS. *hl7API* is implemented to handle HL7 message communication with RIS and HIS. Modality Worklist requests and medical report updates are handled with the help of hl7API functions. *Grid Manager API* is responsible for delivering workflow management requests between local site and Grid Manager with encrypted XML messages using HTTP and RTMP protocols or sychronizing medical image and report data between local site and Grid Manager using HTTP Post or DICOM requests implemented by open source Apache Http Client or dcm4che libraries respectively.

Task Manager Worker threads are implemented using open source Gearman java library for transfer, import and deletion tasks. Gearman workers utilize Interface Layer functions in order to fulfill tasks registered by Gearman clients. Gearman client requests are generated by *Task Manager Service* which listens to state changes in the local archive and Grid Manager. Transfer workers, synchronize the archived DICOM studies or medical reports to the Grid Manager using *Grid Manager API*. Import workers are responsible for synchronizing DICOM studies of a patient's previous studies that are archived by different image acquisition sites to local PACS. Import workers can also synchronize imaging worklist requests or medical report updates to local RIS or HIS. Delete workers are responsible for deleting the archived studies on the temporary storage based on the permission by the Grid Manager. Grid Manager can decide to delete the study considering the storage capacity of site and the redundancy of the study in other sites.

4.1.1.2 Grid Manager

Grid Manager is developed to run on Red5 and is specialized to send and receive encrypted XML and SOAP messages or DICOM files utilizing DICOM, HTTP or RTMP protocols. It communicates with Grid Agents and performs database, indexing and file operations at the center.

Grid Index Grid Manager has the Grid Index which includes the patient examination map archived by Grid Agents. The index is in shared object form so that a change in the index is pushed to all agents with the help of RTMP protocol.

Image Delivery Service DICOM images received by the Grid Manager are rendered into semantic data objects and semantic attributes involving modality, body part, anatomy, reporting effort estimate, prediagnosis values are extracted utilizing SUT and ICD-10 lookup tables. Grid Index is updated and DICOM objects linked with semantic data objects are forwarded to Data Management Platform. Image Delivery Service delivers inspection assignments decisions by *Reporting Workflow Optimization Service* to corresponding Grid Agents with the help of Task Manager Service at sites.

Reporting Workflow Optimization Service Based on the reporting requests from imaging sites, RWOA implemented with Java are applied to semantic data objects of inspections and registered reporting units or radiologists. Open source *OptimJ* library *lpsolve* solver is utilized for the ILP process. Based on the assignment results, the inspections are synchronized to corresponding Grid Agents via Image Delivery Service.

Monitoring Service Task Manager Service of the Grid Agents periodically posts worker thread activities and recent storage capacity and bandwidth values to the Grid Manager using Grid Manager API at each site. Statistics about transfer, import, deletion processes and storage and bandwidth capacities are archived with reference to time and are utilized for RWOA for technical capability requirement parameters.

Redundancy Service The temporary storage mechanism at the agents provides the redundancy of the medical data so that the data achieve is distributed and web server maintenance costs are prevented. Based on the Grid Index and Monitoring Service storage capacity or transfer activity statistics, Grid Manager can decide to delete or move medical image data to different Grid Agents with the help of Task Manager Service at sites.

4.1.1.3 Data Management Platform

File Operation Layer File Operation layer is implemented with Tomcat Servlet Container. DICOM images rendered by Grid Manager are indexed using *Lucene Indexing* to improve image query response time for web access. File Operation Layer involves a Global File System (GFS) cluster where medical image files are archived in a hierarchical structure (year/month/day/patientId/studyId/seriesId/instanceId). DICOM objects are directed to the *Federation Manager* with the url reference for database operations.

Database Layer Database Layer is implemented with open source Postgresql software. The database instances are implemented in 1 master and 16 slave shards to deliver large scale loads. The master instance store the patient, inspection and report related information while shard instances store the study, series and instance information for patient inspections. *Federation Manager* performs a mapping between the 32-hexadecimal-digit unique identifier (UID) formed patientId and corresponding shard; therefore, a patient's image data is stored on a single shard and the overall data is distributed among 16 shards.

Application Layer Application layer is implemented with Red5 media server. A RESTful interface is provided for web access using HTTP or web service SOAP requests. Web service interface is considered for external system integrations. XML is utilized for client-server communication and open source *memcached* software is used as *Server-Side Caching* mechanism in order to cache recently accessed inspection objects or frequent query results. *JPEG Streaming* mechanism is implemented using open source dcm4che-toolkit library in order to process DICOM files with window level, window width or preset parameters and stream JPEG files as an output for mobile access.

4.1.1.4 Front-End

Front-End application is developed using Adobe Air ActionScript technology, which can be exported as Web, Android and iOS applications. For web clients, Java based open source DICOM viewer software, as seen in Figure 4.7 , *ImageJ* is embedded in the application as an Applet. *ImageJ* is customized to pre-fetch 3-neighbour slices in study series image instances and to cache the stack of downloaded slices so that the client can view images before all image instances are downloaded and investigate slices faster. For mobile clients *JPEG Streaming* implemented on the server Application Layer is utilized and annotations can be saved on the image instances.

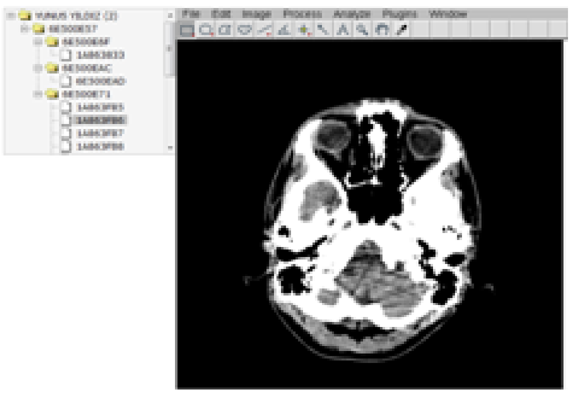

Figure 4.7: Web based DICOM Viewer

4.2 Stage 2

4.2.1 Simulated Data

Two experiments are designed for simulation; one is a simplistic case to illustrate the calculations and the process; and second is a complex case which is designed as close as possible to a real possible case.

4.2.1.1 Experimental Setup

Experiment 1 : Simplistic Case In this case, there are 10 inspections to be assigned to 3 radiologists in 2 reporting units. The characteristics of the sample inspections are given in Table 4.1. The inspections are generated using the modality, body part, anatomy and disease index in Table 4.2. It can be seen that there are 4 CT, 3 MR, 2 DX and 1 MG inspections. 1 CT and 1 DX inspection is demanded as urgent, so these inspections should be assigned to a radiologist that can respond within 4 hours. Also some of the inspections are very large in file size, so these inspections should be assigned to a radiologist that is working in a reporting unit with high storage and bandwidth capacity. The workloads for each inspection are defined based on the related SUT code.

Table 4.1: Characteristics of the inspections based on subspecialty, response time, workload and technical requirements. Subspecialty requirements are represented by the inspection DICOM file attributes of Modality, Body Part, Anatomy and pre-diagnosis info in ICD-10 formation. These attributes also form subnodes of Subspecialty node in the ontology map. Response time requirement is categorized as "Urgent" or "Diagnostic" which map to requirement constraints of $< 4h$ and $< 24h$ respectively. Workload is represented by the SUT code that is mapped by the requested inspection protocol. SUT standardization provide the estimated effort, e_i in units and estimated time t_{ei} in minutes for each inspection, I_i. Technical requirements are represented as attributes of File Size, f_i, Monitor Resolution, Bandwidth and Storage Capacity. These attributes also form subnodes of Technical node in the ontology map.

Inspection	Subspecialty Requirement	Response time req.	Workload	Technical
I_1	CT, Head, Skull, S02	Urgent	803900 e_i = 6.51 u, t_{ei} = 15 min	f_i=30 MB, 1 MP, >0,4 Mbit/s, >30 GB
I_2	DX, Leg, Leg, S82	Urgent	801790 e_i = 1.19 u, t_{ei} = 4 min	f_i=20 MB, 2 MP, >0,27 Mbit/s, >20 GB
I_3	CT, Thorax, Upper Abdomen, C39	Diagnostic	804090 e_i = 5.51 u, t_{ei} = 20 min	f_i=80 MB, 1 MP, >1,07 Mbit/s, >80 GB
I_4	CT, Brain, Spine, D43	Diagnostic	803910 e_i = 6.51 u, t_{ei} = 15 min	f_i=20 MB, 1 MP, >0,37 Mbit/s, >20 GB
I_5	CT, Thorax, Lower Abdomen, C76	Diagnostic	803890 e_i = 5.51 u, t_{ei} = 15 min	f_i=40 MB, 1 MP, >0,53 Mbit/s, >20 GB
I_6	MR, Brain, Skull, C71	Diagnostic	804190 e_i = 6.51 u, t_{ei} = 25 min	f_i=50 MB, 1 MP, >0,67 Mbit/s, >50 GB
I_7	MR, Thorax, Lower Abdomen, C78	Diagnostic	804180 e_i = 5.51 u, t_{ei} = 20 min	f_i=320 MB, 1 MP, >4,27 Mbit/s, >320 GB
I_8	MR, Knee, Knee, S83	Diagnostic	804240 e_i = 5.51 u, t_{ei} = 25 min	f_i=150 MB, 1 MP, >2 Mbit/s, >150 GB
I_9	DX, Shoulder, Shoulder, S42	Diagnostic	801790 e_i = 1.19 u, t_{ei} = 4 min	f_i=20 MB, 2 MP, >0,37 Mbit/s, >20 GB
I_{10}	MG, Breast, Breast, C50	Diagnostic	801590 e_i = 1.70 u, t_{ei} = 10 min	f_i=65 MB, 5 MP, >0,87 Mbit/s, >65 GB

The characteristics of the generated radiologists are given in Table 4.4. While assigning the inspections to these radiologists, the workload of each radiologist should be taken into account. It can be seen that R_1 is very experienced in CT and MR and highly available for quick response; however, he/she has lower workload limit than other radiologists. R_2 is experienced in MG and has moderate response time. R_3 is experienced in DX; however, due to his/her schedule and technical limitations of the reporting unit U_2, is not adequate for large file and urgent inspections assignments. Reporting unit simulated characteristics is illustrated in (Table 4.3). It can be seen that U_1 is a well-equipped reporting unit with 3 workstations and 3 medical monitors including a high resolution 5 MP monitor, moderate bandwidth and high storage capacity, while U_2 has limited bandwidth and storage capacity. Therefore, in technical parameter evaluation, U_1 should be promoted for large files and MG inspections.

Table 4.2: Modality, body part, anatomy and disease index that is utilized for simulations

Modality	MR, CT, DX, MG
Body Part	Head, Leg, Thorax, Brain, Knee, Shoulder
Anatomy	Skull, Leg, Upper Abdomen, Lower Abdomen, Shoulder, Spine
Disease	C39 : Malign neoplasm of inspiration system and inner thorax organs, C50 : Malign neoplasm of breast, C71 : Malign neoplasm of brain, C76 : Malign neoplasm of thorax, C78 : Malign neoplasm of rectum, D43: Neoplasm of brain and central neural system S02 : Skull and face bone fracture S42 : Shoulder and fore arm fracture S82 : Calf and knee fracture S83 : Dislocation, sprain or strain of knee and ligaments

Table 4.3: Reporting unit characteristics for U_1 and U_2 based on staff and technical capabilities such as number of workstations, monitor resolutions, bandwidth and storage capacity.

Reporting Unit	Staff	Technical
U_1	R_1, R_2	3 WS 1 MP, 2 MP, 5 MP 20 Mbit/s, 5 TB
U_2	R_3	1 WS 2 MP 1 Mbit/s, 60 GB

Table 4.4: Characteristics of 3 radiologists, R_1, R_2, R_3 generated for Experiment 1 based on modality, body part, anatomy and disease subspecialties; response time capability, workload capacity and reporting unit categorization. Radiologists R_1 and R_2 reside at reporting unit U_1, while radiologist R_3 reside at reporting unit U_2. Workload of each radiologist, R_j, is represented with l_j in units determined by SUT standardization. Average reporting time of each radiologist, R_j, is represented with $t_{a,j}$ in hours. Subspecialty column is divided into 2 columns. First column represents the Modality, Body Part, Anatomy and Disease (ICD-10 Code) subspecialty group and the second column represent the experience attributes represented at the ontology map; Years of Interpretation, % of time spent, % of images interpreted, primary academic affiliation, performed biopsies and quality report scores out of 100. Points values are the weighted sums of this subgroup based on calculated weights on the ontology map.

Rad.	Subspecialty		Points	Response time	Workload	Reporting Unit
R_1	CT	81 77 83 100 100 100	98,40	$t_{a,j}$=2h	l_j = 15 u	U_1
	DX	66 0 97 0 0 60	30,32			
	MR	100 77 100 100 100 75	88,31			
	Brain	66 0 83 0 100 80	41,84			
	Head	81 77 100 100 100 60	81,14			
	Spine	66 71 0 100 0 70	79,91			
	Skull	66 100 97 100 100 80	90,12			
	S02	66 0 100 100 100 90	91,58			
	D43	81 100 97 100 0 95	94,17			
	C71	100 77 0 0 0 60	31,71			
R_2	MG	100 71 83 100 100 100	98,79	$t_{a,j}$=10h	l_j = 20 u	U_1
	MR	81 77 83 0 0 60	32,80			
	Thorax	66 0 97 100 100 75	84,92			
	Breast	66 100 97 100 100 95	96,72			
	Abdomen	81 77 100 0 0 55	30,94			
	Breast	100 100 97 100 100 65	84,54			
	C39	81 71 0 0 0 80	39,76			
	C50	100 100 100 100 100 95	97,80			
	C76	66 71 97 0 0 95	47,85			
	C78	100 77 83 0 100 60	36,37			
R_3	CT	66 0 83 0 0 100	47,64	$t_{a,j}$=24h	l_j = 20 u	U_2
	DX	100 100 97 100 100 100	99,94			
	Thorax	100 77 100 100 100 75	88,31			
	Brain	66 0 83 0 100 80	41,84			
	Shoulder	81 77 100 100 100 60	81,14			
	Abdomen	81 71 0 0 0 70	35,36			
	Spine	100 100 97 100 100 80	91,14			
	S42	66 0 100 100 100 90	91,58			
	S82	81 100 97 100 0 95	94,17			
	S83	100 77 0 100 0 60	76,71			

4.2.1.2 Results for Experiment 1

When semantic matching algorithm is executed based on the ontology map and weights derived by AHP process, the ratings for each inspection-radiologist assignment is obtained as illustrated in Figure 4.8. These ratings are utilized by the ILP algorithm to decide which assignment alternatives are optimum with reference to workload, response time and technical constraints.Based on these ratings ILP algorithm is run with the defined objective function and constraints,

	I9	I4	I10	I2	I8	I3	I5	I1	I7	I6
Radiologist R2	,34	,24	,72	,21	,28	,38	,38	,17	,42	,28
Radiologist R1	,41	,58	,26	,54	,39	,41	,41	,65	,39	,53
Radiologist R3	,63	,35	,25	,29	,18	,31	,36	,20	,24	,22

Figure 4.8: Overall ratings of alternatives calculated by semantic matching and weights derived by AHP Method. Each cell value is the evaluation for the assignment possibility of one inspection to a radiologist. These ratings are utilized by the ILP process to decide which assignment alternatives are optimum with reference to workload, response time and technical constraints.

In Figure 4.8, it seen that R_1 has the best ratings for matching alternatives: I_4, I_2, I_8, I_3, I_5, I_1 and I_6. However, RWOA execution assigns only inspections I_1, I_2 and I_6 to R_1 as seen in Figure 4.9. When investigated it is seen that I_1 and I_2 are urgent inspections which can only be responded by R_1 with response time 2-3 hours. The highest difference between his/her rivals for the remaining inspections is for I_6; however, when I_6 is assigned to R_1, his/her workload limit is reached. Therefore, it is seen that I_3 and I_8, which are large files are passed to R_2 rather than R_3, who has technical limitations. I_7 is also assigned to R_2 due to high file size and the MG inspection I_{10} is also assigned to R_2 due to both experience and technical factors. And R_3 is assigned diagnostic purpose DX and CT images with small size, as his/her reporting unit has technical limitations (small storage and bandwidth, monitor with 1 MP resolution) and response time is not suitable for urgent demands.

In Figure 4.10, it is more clearly seen that two inspections (I_1 and I_2) have urgent reporting demands and this requirement has been fulfilled by assigning the inspections to R_1, who has responded with report within 4 hours.

In Figure 4.11, it can be seen that the inspections are distributed such that the workload limitations of radiologists are not exceeded and the radiologists are utilized as efficient as possible.

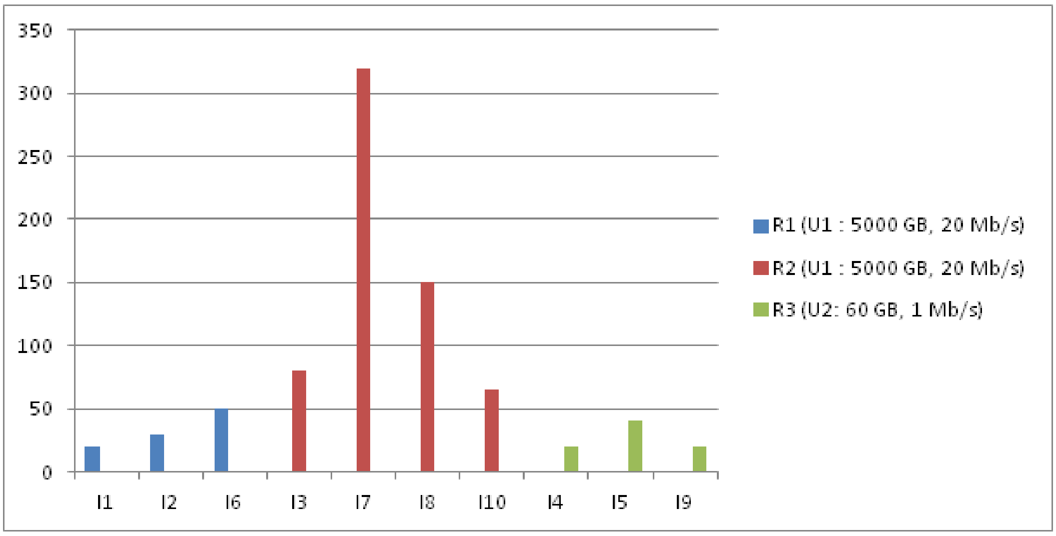

Figure 4.9: RWOA Assignment of inspections to radiologists. I_1, I_2, I_6 are assigned to R_1; I_3, I_7, I_8 and I_{10} are assigned to R_2; I_4, I_5, I_9 are assigned to R_3. y-axis shows the file size of the inspections in MB. R_1 and R_2 reside at reporting unit U_1 with 5000 GB of storage capacity and 20 Mbit/s of bandwidth. R_3 resides at reporting unit U_3 with 60 GB of storage capacity and 1 Mbit/s of bandwidth.

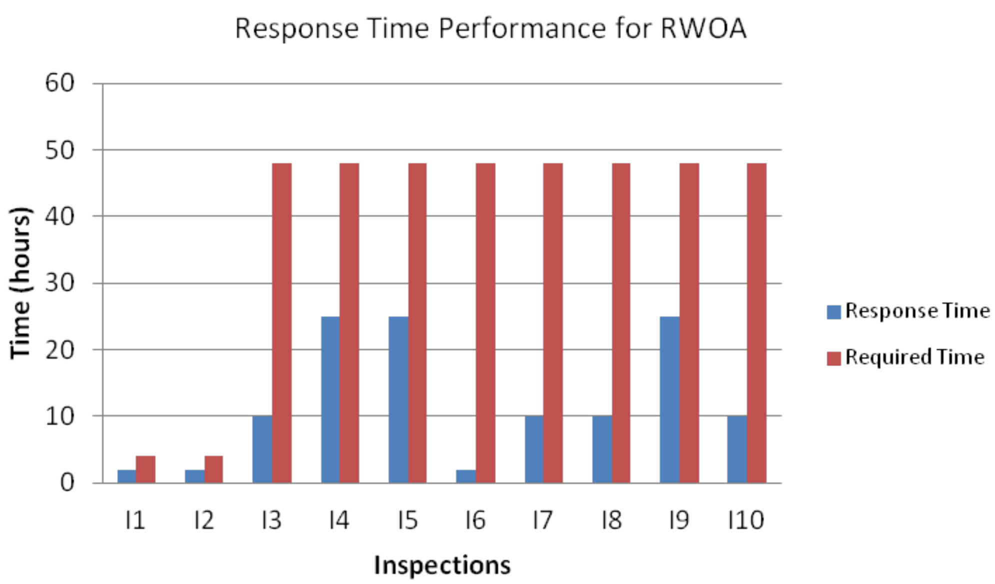

Figure 4.10: Requested response time requirements (in red bars) and resultant response time responses after the RWOA assignment process.

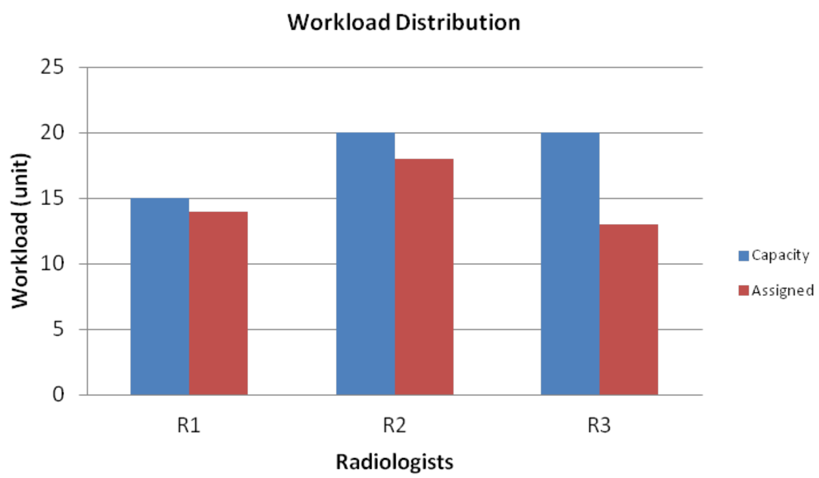

Figure 4.11: Present allowed workload capacity of radiologists (in blue bars) and the resultant workload after the RWOA assignment of inspections (in red bars) for radiologists R_1, R_2, R_3.

Experiment 2 : Complex Case The performance of the proposed algorithm is tested using 100 sample radiology inspections. A simulation is adopted with 4 imaging facilities and 3 reporting units, 1 data center and 2 non-local clients as virtual machines on different subnets. 6 radiologists working in 3 reporting units are registered and their experience, reporting unit technical capabilities are defined using the web interface. Round robin, random, shortest queue distribution policies are compared to RBSM and RWOA distribution algorithms. Sample inspections are generated based on the index data in Table 4.2. Modalities include MR, CT, DX and MG data sets. When DICOM data is rendered the body part attributes consist of Brain, Leg, Thorax, Upper Abdomen, Lower Abdomen, Knee, Shoulder values. The attributes for prediagnosis data is generated based on a list of 10 ICD-10 codes (C39, C50, C71,C76, C78, D43, S02, S42, S82, S83). The results are evaluated based on subspeciality, response time and workload success rates.

4.2.1.3 Results for Experiment 2

Subspeciality success rate is the normalized value of RBSM calculated rating between 0 and 1 where higher subspeciality success rate is required for better reporting quality.

Response time success rate for policy p is defined as

$$sr_p = \frac{1}{S} \sum_{j=1}^{R} \sum_{i=1}^{S} s_{ij,p} x_{ij,p} \tag{4.1}$$

where $s_{ij,p} = \left\{ \begin{array}{ll} 1, & t_{ij,rep} \leq t_{i,req} \\ 0, & otherwise \end{array} \right\}$

for reporting time of inspection i by radiologist j, $t_{ij,rep}$ and required reporting time for inspection i, $t_{i,req}$. The maximum possible value for sr_p is 1 where higher response time success rate is required for better distribution policy performance.

Workload success rate for policy p, ld_p, is a measure of how efficient the radiologist resources

Table 4.5: Subspeciality, response time and workload success rate values for the applied distribution policies: Round Robin, Random, Shortest Queue, RBSM and RWOA. RBSM gives the highest subspeciality success rate and integrating ILP with RBSM as RWOA provides a better response time and workload success rate.

	Round Robin	**Random**	**Shortest Queue**	**RBSM**	**RWOA**
Subspeciality Success Rate	0.34	0.37	0.40	0.75	0.71
Response Time Success Rate	0.74	0.72	1.00	0.93	0.99
Workload Success Rate	0.37	0.28	0.52	2.04	3.57

are utilized indicating reciprocal of the distance from load limit.

$$ld_p = \frac{R}{\sum_{j=1}^{R} \frac{|\sum_{i=1}^{S} e_i x_{ij,p} - l_j|}{l_j}} \tag{4.2}$$

where e_i is the estimated time to report the assigned inspection i and l_j is the workload of radiologist j. The minimum possible value for the denomitor expression in ld_p equation is 0, which means that all assignment workloads are equal to the defined workload limits for each radiologist. Therefore, distribution policy can be evaluated as more successful in terms of workload efficiency when ld_p is high. The results for applied distribution policies are displayed in Table 4.5.

4.2.2 Real Case Data

The data arhieved in Stage 1 is utilized in order to evaluate the workflow optimization algorithm on real data.

4.2.2.1 Experimental Setup

Stage 1 event logs and archive data are used where workflow optimization was not implemented. Inspections are assigned manually by the chief radiologist to an expert among 9 radiologists. In Stage 1/RP-1, 4738 medical inspections which involved 4481 CT, 116 MR, 106 CR and 35 MG, were archived and reported. In Stage 1/RP-2, 1464 medical inspections, which involved 1445 CT, 18 MR, and 1 CR, were archived and reported. The body parts involved Brain, Thorax, Lower/Upper Abdomen, Pelvis, Temporal Bone and Paranasal Sinuses.

In Stage 1/RP-1 the inspections were imported from an archive to test the functionality of the reporting unit and user interface. At this stage, the radiologists were obliged to finish the overall reporting process within one month; therefore the chief radiologist had to make the reporting assignment considering the parameters of subspeciality, response time and workload limits. The reporting time, assigned workload, frequency of reporting, which are indicators of response time, workload limit and subspeciality respectively, are extracted for each radiologist using the resultant event logs and archive data based on modality as illustrated in Figure 4.12. The extraction is also executed with reference to body part and imported into the ontology map.

In Stage 1/RP-2 the inspections from 22 hospitals were synchronized to the Reporting Unit with the help of Grid Manager and Grid Agent architecture. The assignment was done by the chief radiologist to 9 radiologists. RWOA is applied to RP-2 data and the resultant assignment decisions are saved.

4.2.2.2 Results

The ontology map of radiologists formed and evaluated extracted from RP-1 data is used in RWOA. The frequency that the chief assigns a certain modality, body system or pre-diagnosis inspection is assumed to be an indicator to the assignee radiologist's subspecialty and experience on that modality, body system or disease. The subspecialty scores and average response time values with reference to modality is illustrated in Figure 4.12. It can be seen that MG inspections are always assigned to R_4 and R_9. R_8 has highest subspeciality rating, but worst reporting time for CR. A similar extraction operation is also executed for body system attributes of the inspections. As the inspections involved no pre-diagnosis information, data extration for disease attribute could not be performed.

The assignment results are compared between manual assignment and RWOA assignment based on subspeciality, response time and workload success rates as seen in Figure 4.13.

(a)

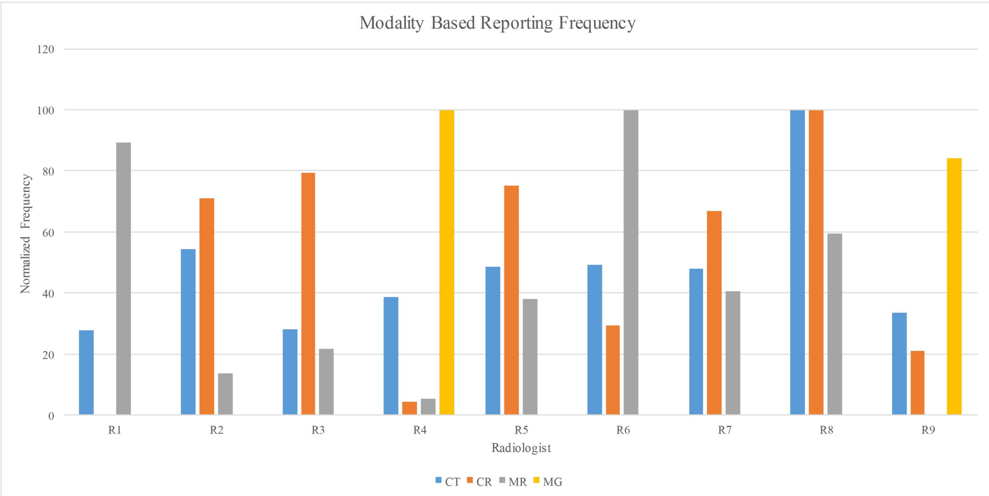

(b)

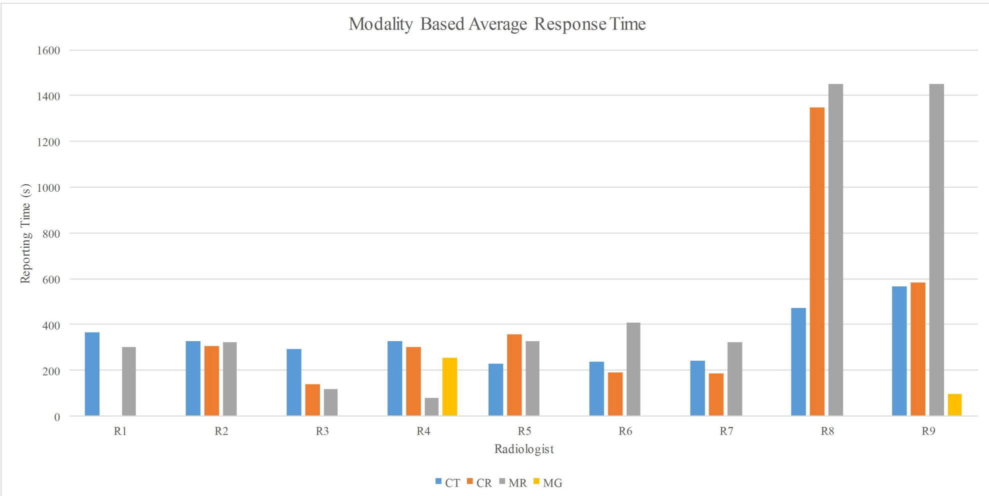

Figure 4.12: (a)Radiologist expertise rates with reference to modality. (b)Radiologist response time values with reference to modality.

(a)

(b)

(c)

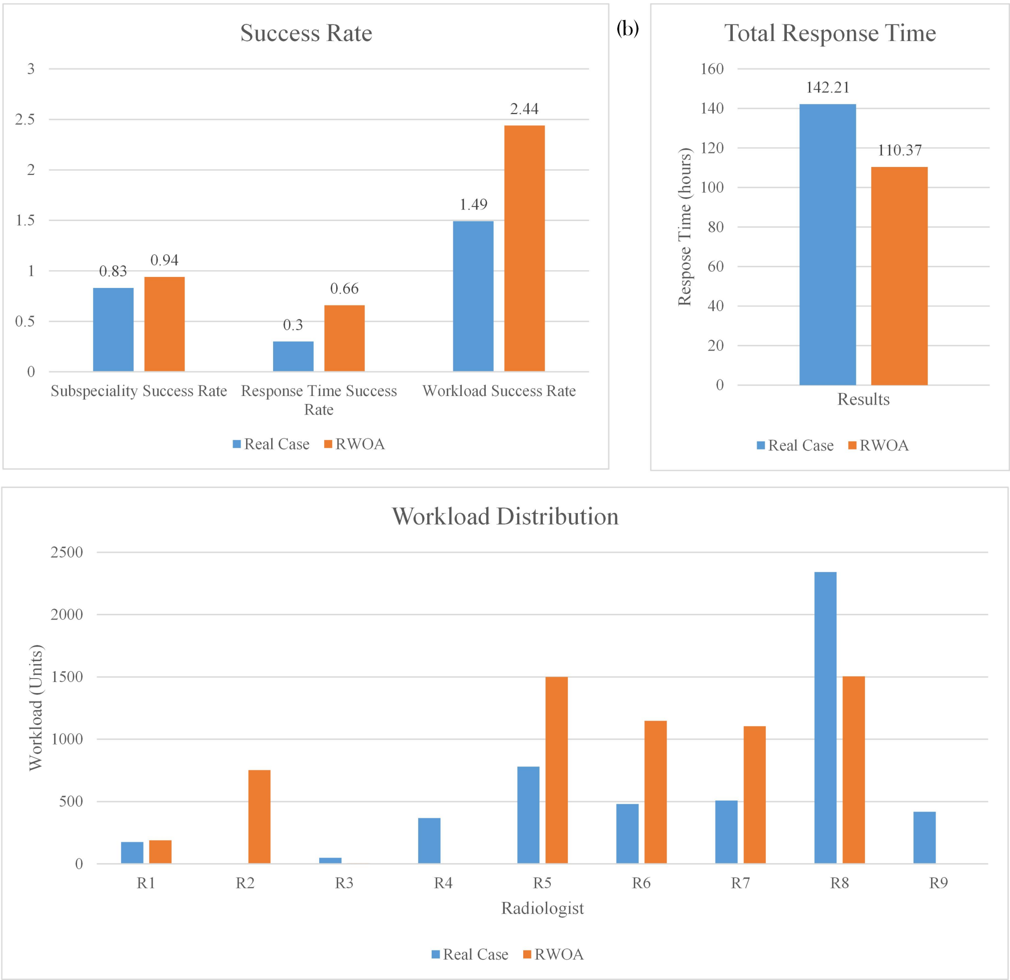

Figure 4.13: (a)Real case test period results compared by the RWOA assignment results in terms of subspeciality, response time and workload success rates. (b) Total response time for Real Case test period compared with the workflow optimization algoritm. (c)Workload distribution values for real case test period compared with the resultant workload distribution by RWOA. RWOA increases the subspeciality success rate by 13.25 %, workload success rate by 63.76% and response time success rate by 120%. Total response time in the real case application data is improved by 22.39%.

When compared with the real case test period process where inspection assignments were performed manually, RWOA increases the subspecialty success rate by 13.25 %, increases the workload success rate by 63.76% and increases the response time success rate by 120% as seen in Figure 4.13 The total response time in the real case application data was improved by 22.39%. Workload distribution is also optimized and distributed among resources. As there are no MG inspections in the RP-2 data, assignments to R_4 and R_9 are not promoted. The workload of the overloaded radiologist R_8 is distributed among other radiologists increasing the utilization efficiency. R_2, which is unutilized at the manual assignment process, is utilized with RWOA. In manual assignment process, 8 radiologists were allocated, while in RWOA process, 6 radiologists were allocated, still distributing the workload evenly and keeping the response time and subspecialty success rates higher.

In order to check the correctness of the average response time values, presence of outliers and standard deviation percentages of response times with reference to modalities for each radiologist are investigated. It is seen that response time standard deviation percentages for CT inspections among all radiologists; while the percentage is generally high for MR inspections. This can be interpreted as an indicator to the variety of complexity in MR inspections compared to CT inspections. It is also seen that R_8 has highest response time standard deviation percentage values for CR and MR inspections. This can be indicating that R_8 does additional research and spends extra time related to the complexity of the inspections; especially for CR and MR.

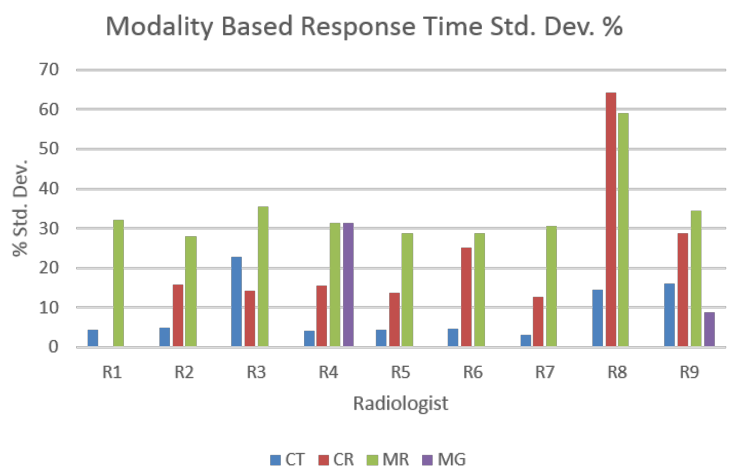

Figure 4.14: Standard deviation percentages for the response time of radiologists based on inpection assignment modalities.

The data set size and solution time relation is illustrated in Figure 4.15. It is seen that the solution time increases exponentially as the data set size increases.

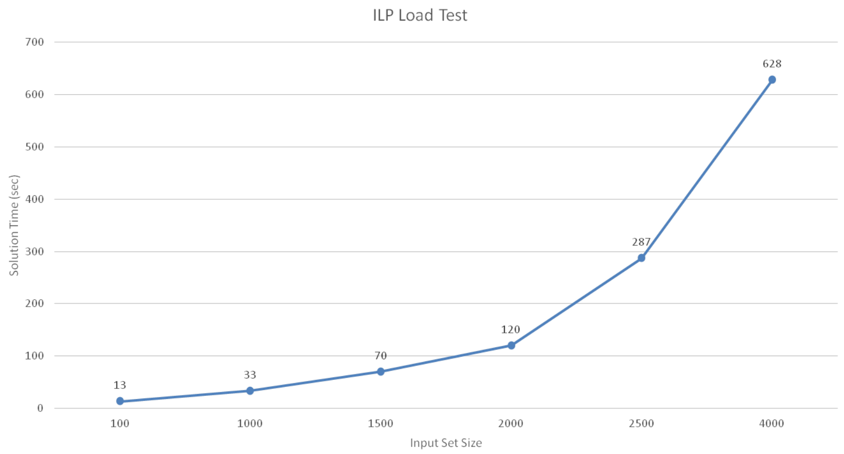

Figure 4.15: Relation between solution time and data set size for the ILP Phase of RWOA.

4.3 Stage 3

4.3.1 Piloting

The proposed architecture with the evaluated RWOA is piloted to provide reporting service for 8 primary care and 3 cancer screening medical imaging centers. For the time being, one radiologist at a single reporting unit delivers the reporting service. The number of medical centers is foreseen to increase to 19 and more radiologists are foreseen to be integrated into the architecture. The workflow optimization is meaningful where there are several reporting units and radiologist to deliver medical reporting service to multiple medical imaging centers. The advantage provided by the proposed architecture is maximized at large-scale applications. The piloted application is currently available at *http://eradyoloji.saglik.gov.tr* supported by the Governship of Public Health, Ankara, Turkey.

4.4 Discussion

ILP solution process can take long or stucks can occur in large data sets or strict boundary constraints. As a workaround solution to this situation, the boundary conditions are relaxed in real time or the data set is divided into smaller chunks.

The reporting frequency which is the only available indicator of subspeciality in the experimental setup can be misleading for overloaded radiologists. Therefore, this data is cross-checked with manually rated subspeciality evaluations by the chief radiologist. The ratings were found to be compliant except CT subspeciality rating for R_8 which was rated to be lower by the chief radiologist. No correction was done based on this cross-check which was actually a disadvantage for the algorithm as it should still accomplish high speciality success rate while decreasing the workload of R_8. The subspeciality rating node is foreseen to be evaluated more precisely with the inclusion of report quality feedback indicator. This process can be carried out by a chief radiologists scoring the quality of reports in an assessment interface which randomly displays inspection and corresponding reports with random sampling.

In manual assignment process, 8 radiologists were allocated, while in RWOA process, 6 radiologists were allocated, but still distributing the workload evenly and keeping the response time and subspecialty success rates higher. This is interpreted as a success as RWOA tries to maximize the response time and subspecialty success rates as long as the workload limits of radiologists are not reached. However, if allocating each radiologist evenly is a concern or if there exists minimum salaries for each radiologist, an additional workload lower limit contraint can be introduces which has to keep every radiologist in the system pool at a minimal allocation level.

Implemented infrastructure can be utilized to develop a teleradiology portal where radiologists and medical institutions sign-up to give or receive reporting services. Radiologist can be initially accredited to be a member of the system and subspecialty and response time attributes can be updated dynamically within the system. This system can also be used to manage the schedule, resource management and salary management processes. All these processes can have performance assessments to improve the efficiency of RWOA.

CHAPTER 5

CONCLUSION

5.1 Conclusion

The proposed architecture increases the efficiency of reporting process for teleradiology applications and provides a process centric network structure with an enhanced caching, querying and retrieving mechanism. The Grid Agent and Grid Manager solutions provide integration of several standard compliant medical systems regardless of the developer or manufacturer vendor and accomplishes medical data redundancy without the maintenance cost of a single central web solution.

The architecture is better in several aspects such as interoperability, scalibility, compatibility and workflow optimization than the previous research studies. It is novel in that, it integrates an arhitecture implementation with a workflow optimization algorithm for a complete solution to teleradiology service delivery on the cloud. This arhitecture can still be enhanced by other studies that focus on security, faster file delivery algorithms, information centric distribution networks.

The proposed infrastructure decreases the storage costs, reporting costs, turnaround times and increases report quality and effectiveness of resultant treatments. The adaptation of medical sites and reporting groups to the architecture only requires the integration of Grid Agent into the present systems deployed on these sites which decreases integration costs and provides high interoperability.

Based on the results obtained from simulation data in reporting assignment workflows, Shortest Queue policy has the highest response time performance; however it is inefficient in experience rating and workload distribution. Applying only RBSM gives the highest experience ratings, but integrating ILP with RBSM ratings provides a better response time success rate and the best performance for workload distribution with a small optimization trade off in experience rating. ILP can take long time to solve or can get stuck in large data sets, but heuristics solutions can be applied at this situation.

When real test case comparison results are evaluated, the workflow optimization algorithm increases the experience success rate by 13.25 %, increases the workload success rate by 34.92% and increases the response time success rate by 120% and the total response time is improved by 22%. It can be concluded that the integration of the workflow optimization algoritm into the architecture automizes the delivery of medical inspections to optimum radiologists. This process has been proven to surpass the manual assignment process of the head radiologist who has the knowledge about the expertise and subspeciality areas of the radiologists. The results are predicted to be better and more helpful when large-scale applications are considered. In such a condition there will be a large number of inspections to be reported by a large pool of radiologists where no one has any idea about each other's expertise, subspeciality or reporting performance. Also when technical and schedule constraints are introduced, the improvement ratios are also predicted to increase. RBSM and ILP based image delivery also prevents bandwidth, storage or hardware related locks and latencies.

The proposed architecture has been tested in a total of 35 hospitals, 13 primary care clinics, 3 mobile clinics, 1 reporting unit. 3.35 million inspections were archived and 14216 inspections were reported by the reporting unit. However, an organized reporting process was executed only for 6202 reports which were utilized for RWOA evaluation. The proposed architecture with RWOA is piloted to provide reporting service for 8 primary care and 3 cancer screening medical imaging centers. The piloted application is currently available at *http://eradyoloji.saglik.gov.tr* supported by the Governship of Public Health, Ankara, Turkey.

The response time and report quality statistics for each radiologist are updated in real time. Therefore, it is considered that the proposed solution can be even more efficient and accurate in real case scenarios. Also the recalculation of performance values based on the satisfaction level feedback for response time, report quality and workload distribution enhences the algorithm to make more accurate decisions.

The integration procedure of medical institutions and reporting units to the proposed architecture is quite simple where only the Grid Agent is required to be deployed at sites. The deployment is possible with a moderate workstation capability and does not require high performance server or storage cluster capabilities. Also the deployment procedure does not effect available systems such as PACS, RIS and HIS. Instead, it also integrates these systems to the architecture for grid-based synchronization operations. The data archive is cached temporarily at sites and managed by the Redundancy Service at the Data Center. Therefore, redundancy and content distribution network is accomplished without additional storage or data center costs at sites. As a result, integration with the architecture at sites is low-cost, fast and practical. Therefore, the adaptation of this solution decreases the hardware and maintenance costs at sites.

The operations at sites executed by Grid Agents can be monitored and controlled remotely with the help of Monitoring Service at the Data Center, which decreases the maintanence, technical staff allocation and training costs.

This solution can be applied in order to outsource radiology services to multiple groups, decrease radiologist payment costs, increase report quality and decrease turnaround time, manage workload and payment distribution based on performance evaluations. Nation-wide teleradiology solution can be accomplished with the integration on hospitals, medical centers and radiologists with the proposed solution. This architecture can also be used to deliver a qualified international reporting service to countries that have radiologist deficiency and subspecialty or consultation requirements. Global accredited reporting units can be accomplished for delivering a standardized, interoperable cloud-based radiology service to subscripted institutions. As a result, employment, financial management and performance assessment of radiologists processes are practically possible, image and report delivery mechanism is automized and optimized, quality and statistics assessment is accomplished and an innovative teleradiology service workflow is fulfilled.

5.2 Future Work

The workflow optimization is meaningful where there are several reporting units and radiologists to deliver medical reporting service to multiple medical imaging centers. The advantage provided by the proposed architecture is maximized at large-scale applications. Therefore, it is planned to apply the architecture to a nation-wide solution.

In order to provide an international teleradiology service architecture, structured reporting and multilanguage support is planned to be integrated with the proposed solution.

Image compression, encryption and transmission methods are planned to be developed in order to decrease the image delivery time and security concerns.

It is also planned to deploy the application as a cloud-based service where teleradiology service providers and demanders subscribe to deliver and receive reporting service with a per report pricing structure. Financial optimization methods are planned to be implemented where performance evaluation, promotion and payments are related to the quality and turnaround time of reporting service. Adaptation of this architecture into an outsourcing model is planned which will decrease the reporting per inspection cost and increase service quality.

Due to the interoperability and compatibility capabilities of the architecture, teleconsultation and case-based medical education modules can be integrated with the system. In order to serve data to extension modules and accomplish ontology mapping to a variety of medical concepts, it is planned to develop additional metadata tagging by image and text processing algorithms for categorization and clustering of inspections and reports.

Bibliography

[1] F. H. Barneveld Binkhuysen and E. R. Ranschaert. Teleradiology: Evolution and concepts. *European Journal of Radiology*, 78:205–209, 2011.

[2] L. N. Sutton. PACS and diagnostic imaging service delivery–a UK perspective. *European journal of radiology*, 78:243–249, 2011.

[3] H. K. Huang. Short history of PACS. Part I: USA, 2011.

[4] H. U. Lemke. Short history of PACS (Part II: Europe). *European Journal of Radiology*, 78:177–183, 2011.

[5] K. Inamura and J. H. Kim. History of PACS in Asia. *European Journal of Radiology*, 78:184–189, 2011.

[6] N. Lundberg, M. Wintell, and L. Lindsköld. The future progress of teleradiology-An empirical study in Sweden. *European Journal of Radiology*, 73:10–19, 2010.

[7] B. Gibaud. The quest for standards in medical imaging. *European Journal of Radiology*, 78:190–198, 2011.

[8] M. S. Marshall, R. Boyce, H. F. Deus, J. Zhao, E. L. Willighagen, M. Samwald, E. Pichler, J. Hajagos, E. Prud'Hommeaux, and S. Stephens. Emerging practices for mapping and linking life sciences data using RDF - A case series. *Journal of Web Semantics*, 14:2–13, 2012.

[9] J. Fernandez-Bayó. IHE profiles applied to regional PACS. *European Journal of Radiology*, 78:250–252, 2011.

[10] L. Faggioni, E. Neri, C. Castellana, D. Caramella, and C. Bartolozzi. The future of PACS in healthcare enterprises. *European Journal of Radiology*, 78:253–258, 2011.

[11] T. C. M. Pechet, G. Girard, and B. Walsh. The value teleradiology represents for Europe: A study of lessons learned in the U.S. *European Journal of Radiology*, 73:36–39, 2010.

[12] E. Bellon, M. Feron, T. Deprez, R. Reynders, and B. Van Den Bosch. Trends in PACS architecture. *European Journal of Radiology*, 78:199–204, 2011.

[13] Y. Kim and I. Yeom. Performance analysis of in-network caching for content-centric networking. *Computer Networks*, 57:2465–2482, 2013.

[14] G. Carofiglio, G. Morabito, L. Muscariello, I. Solis, and M. Varvello. From content delivery today to information centric networking. *Computer Networks*, 57:3116–3127, 2013.

[15] V. Sourlas, P. Flegkas, G. S. Paschos, D. Katsaros, and L. Tassiulas. Storage planning and replica assignment in content-centric publish/subscribe networks. *Computer Networks*, 55:4021–4032, 2011.

[16] F. Valente, C. Viana-Ferreira, C. Costa, and J. Oliveira. A RESTful image gateway for multiple medical image repositories. *IEEE Transactions on Information Technology in Biomedicine*, 16:356–364, 2012.

[17] C. T. Yang, M. F. Yang, and W. C. Chiang. Enhancement of anticipative recursively adjusting mechanism for redundant parallel file transfer in data grids. *Journal of Network and Computer Applications*, 32:834–845, 2009.

[18] C. T. Yang, L. T. Chen, W. L. Chou, and K. C. Wang. Implementation of a Medical Image File Accessing System on cloud computing. In *Proceedings - 2010 13th IEEE International Conference on Computational Science and Engineering, CSE 2010*, pages 321–326, 2010.

[19] Luís A. Bastião Silva, Carlos Costa, and José Luís Oliveira. A common API for delivering services over multi-vendor cloud resources. *Journal of Systems and Software*, 86:2309–2317, 2013.

[20] J. Zhang, J. Sun, and J. N. Stahl. PACS and Web-based image distribution and display, 2003.

[21] H. Munch, U. Engelmanna, A. Schroeter, and H.P. Meinzer. Web-based distribution of radiological images from PACS to EPR. In *International Congress Series 1256*, pages 801–804, 2003.

[22] J. Reponena, J. Niinimakia, T. Leinonenb, J. Korpelainenc, J. Oikarinena, and E. Vierimaad. Linking a web based electronic patient record with a DICOM PACS. In *International Congress Series 1230*, pages 801–804, 2001.

[23] J. Bernarding, A. Thiel, and A. Grzesik. A JAVA-based DICOM server with integration of clinical findings and DICOM-conform data encryption. In *International Journal of Medical Informatics*, volume 64, pages 429–438, 2001.

[24] P. Cao, M. Hashiba, K. Akazawa, T. Yamakawa, and T. Matsuto. An integrated medical image database and retrieval system using a web application server. *International Journal of Medical Informatics*, 71:51–55, 2003.

[25] B. Blazona and M. Koncar. HL7 and DICOM based integration of radiology departments with healthcare enterprise information systems. *International Journal of Medical Informatics*, 76, 2007.

[26] I. Sachpazidis, R. Ohl, A. P. D. Binottoc, M. S. Torres, L. A. Messina, A. Sales, R. Gomes, and G. Sakas. Ehealth applications applied to underserved areas in Latin America. *Nuclear Instruments and Methods in Physics Research*, A 569:635–639, 2006.

[27] D. Dragan and D. Ivetić. Request redirection paradigm in medical image archive implementation. *Computer Methods and Programs in Biomedicine*, 107:111–121, 2012.

[28] J. Zhang, J. Sun, Y. Yang, X. Chen, L. Meng, and P. Lian. Web-based electronic patient records for collaborative medical applications, 2005.

[29] N. T. Cheung, A. Lam, W. Chan, and J. H. B. Kong. Integrating images into the electronic patient record of the hospital authority of Hong Kong, 2005.

[30] T. U. Onbay and A. Kantarci. Design and implementation of a distributed teleradiography system: DIPACS. *Computer Methods and Programs in Biomedicine*, 104:235–242, 2011.

[31] S. H. Choudhury, C. B. Peterson, S. Kyriazakos, and N. R. Prasad. A novel hierarchical semi-centralized telemedicine network architecture proposition for Bangladesh. In *IFMBE Proceedings*, volume 34 IFMBE, pages 176–179, 2011.

[32] H.K. Huang, A. Zhang, B. Liu, Z. Zhou, J. Documet, N. King, and L. W. C. Chan. Data Grid for Large-Scale Medical Image Archive and Analysis, 2005.

[33] M. Benjamin, Y. Aradi, and R. Shreiber. From shared data to sharing workflow: Merging PACS and teleradiology. *European Journal of Radiology*, 73:3–9, 2010.

[34] Hualei Shen, Dianfu Ma, Yongwang Zhao, Hailong Sun, Sujun Sun, Rongwei Ye, Lei Huang, Bo Lang, and Yan Sun. MIAPS: A web-based system for remotely accessing and presenting medical images. *Computer Methods and Programs in Biomedicine*, 113:266–283, 2014.

[35] Z. Huang, W.M.P. van der Aalst, X. Lu, and H. Duan. Reinforcement learning based resource allocation in business process management, 2011.

[36] Z. Huang, W. M. P. Van Der Aalst, Xudong Lu, and Huilong Duan. An adaptive work distribution mechanism based on reinforcement learning. *Expert Systems with Applications*, 37:7533–7541, 2010.

[37] Y. Liu, J. Wang, Y. Yang, and J. Sun. A semi-automatic approach for workflow staff assignment. *Computers in Industry*, 59:463–476, 2008.

[38] W. K. Cheng, B. Y. Ooi, and H. Y. Chan. Resource federation in grid using automated intelligent agent negotiation. *Future Generation Computer Systems*, 26:1116–1126, 2010.

[39] Z. Huang, X. Lu, and H. Duan. Mining association rules to support resource allocation in business process management. *Expert Systems with Applications*, 38:9483–9490, 2011.

[40] D. L. Miglioretti, R. Smith-Bindman, L. Abraham, R. J. Brenner, P. A. Carney, E. J. A. Bowles, D. S. M. Buist, and J. G. Elmore. Radiologist characteristics associated with interpretive performance of diagnostic mammography. *Journal of the National Cancer Institute*, 99:1854–1863, 2007.

[41] E. Molins, F. Macià, F. Ferrer, M. T. Maristany, and X. Castells. Association between radiologists' experience and accuracy in interpreting screening mammograms. *BMC health services research*, 8:91, 2008.

[42] J. Hohmann, P. De Villiers, C. Urigo, D. Sarpi, C. Newerla, and J. Brookes. Quality assessment of out sourced after-hours computed tomography teleradiology reports in a Central London University Hospital. *European Journal of Radiology*, 81, 2012.

[43] E. Nageba, J. Fayn, and P. Rubel. A Telemedicine System for Hostile Environments, 2011.

[44] W. N. Lee, N. Shah, K. Sundlass, and M. Musen. Comparison of ontology-based semantic-similarity measures. *AMIA Annual Symposium proceedings / AMIA Symposium. AMIA Symposium*, pages 384–388, 2008.

[45] X. D. Mingxin Gan. From Ontology to Semantic Similarity: Calculation of Ontology-Based Semantic Similarity. *The ScientificWorld Journal*, pages 1–11, 2013.

[46] C. Pesquita, C. Pesquita, D. Faria, D. Faria, André O. Falcão, André O. Falcão, P. Lord, , F. M Couto, and F. M. Couto. Semantic similarity in biomedical ontologies. *PLoS computational biology*, 5:e1000443, 2009.

[47] V. Pekar and S. Staab. Taxonomy learning: factoring the structure of a taxonomy into a semantic classification decision, 2002.

[48] P. Resnik. Using information content to evaluate seantic similarity in a taxonomy. In *Proceedings of the 14th International Joint Conference on Artificial Intelligence (IJ-CAI)*, 1995.

[49] D. Lin. An Information-Theoretic Definition of Similarity. In *Proceedings of ICML*, pages 296–304, 1998.

[50] J. J. Conrath. Semantic similarity based on corpus statistics and lexical taxonomy. In *Proceedings of the IInternational Conference on Research in Computational Linguistics*, pages 19–33, 1997.

[51] A. Tversky. Features of similarity., 1977.

[52] J. Z. Wang, Z. Du, R. Payattakool, P. S. Yu, and C. F. Chen. A new method to measure the semantic similarity of GO terms. *Bioinformatics (Oxford, England)*, 23:1274–1281, 2007.

[53] S. Colucci, T. D. Noia, E. D. Sciascio, F. M. Donini, M. Mongiello, and M. Mottola. A formal approach to ontology-based semantic match of skills descriptions. *Journal of Universal Computer Science*, 9:1437–1454, 2003.

[54] S. Colucci. Finding Skills through Ranked Semantic Match of Descriptions. In *IKNOW03: 3rd International Conference on Knowledge Management, Skills Management, Graz*, 2003.

[55] T. Di Noia, E. Di Sciascio, F. M. Donini, and M. Mongiello. A System for Principled Matchmaking in an Electronic Marketplace. In *Proceedings of the 12th International Conference on World Wide Web*, pages 321–330, 2003.

[56] S. J. Chen and C. L. Hwang. *Fuzzy multiple attribute decision making: methods and applications*, volume 375. Springer, 1992.

[57] H. D. Lyes Benyoucef. *Supplier Selection Problem: selection criteria and methods*. Indria Lorraine, 2008.

[58] M. Hudymacova. *Supplier selection based on multi-criterial AHP method*. Acta Montanistica Slovaca Rocnik, 2010.

[59] T. L. Saaty. Axiomatic Foundation of the Analytic Hierarchy Process, 1986.

[60] A. J. Rajan. Application of Integer Linear Programming Model for Vendor Selection in a Two Stage Supply Chain. In *Proceedings of the 2010 International Conference on Industrial Engineering and Operations Management*, pages 1–6, 2010.

[61] S. Cokelez. An Optimization Methodology for Selecting Suppliers in Purchasing Management for Improved Customer Service. *Journal of Customer Service in Marketing and Management*, 3:7–17, 1997.

[62] W. E. Barlow, C. Chi, P. A. Carney, S. H. Taplin, C. D'Orsi, G. Cutter, R. E. Hendrick, and J. G. Elmore. Accuracy of screening mammography interpretation by characteristics of radiologists. *Journal of the National Cancer Institute*, 96:1840–1850, 2004.

APPENDIX A

Body Part Index

1	ABDOMEN
2	ANKLE
3	ARM
4	BREAST
5	CHEST
6	CLAVICLE
7	COCCYX
8	CSPINE
9	ELBOW
10	EXTREMETY
11	FOOT
12	HAND
13	HEAD
14	HEART
15	HIP
16	JAW
17	KNEE
18	LEG
19	LSPINE
20	NECK
21	PELVIS
22	SHOULDER
23	SKULL
24	SSPINE
25	TSPINE

APPENDIX B

Anatomy Index

ID	CODE SCHEMA	CODE	NAME
1	SNM3	T-42501	Abdominal aorta
2	SNM3	T-42303	Aortic arch
3	SNM3	T-45011	Carotid
4	SNM3	T-A600A	Cerebellum
5	SNM3	T-45526	Circle of Willis
6	SNM3	T-A0193	Cranial venous system
7	SNM3	T-41040	Iliac arterial system
8	SNM3	T-62002	Liver
9	SNM3	T-D4034	Pancreas
10	SNM3	T-D4909	Kidney
11	SNM3	T-D4035	Spleen
12	SNM3	T-9400F	Testis
13	SNM3	T-4600A	Thoracic aorta
14	SNM3	T-C8001	Thymus
15	SNM3	T-83009	Uterus
16	SNM3	T-D4000	Abdomen
17	SNM3	T-15420	Acromioclavicular joint
18	SNM3	T-15750	Ankle joint
19	SNM3	T-280A0	Apex of Lung
20	SNM3	T-D8200	Arm
21	SNM3	T-60610	Bile duct
22	SNM3	T-74000	Bladder
23	SNM3	T-04000	Breast
24	SNM3	T-26000	Bronchus
25	SNM3	T-12770	Calcaneus
26	SNM3	T-11501	Cervical spine
27	SNM3	T-D3000	Chest
28	SNM3	T-12310	Clavicle
29	SNM3	T-11BF0	Coccyx
30	SNM3	T-58200	Duodenum

ID	CODE SCHEMA	CODE	NAME
31	SNM3	T-D8300	Elbow
32	SNM3	T-56000	Esophagus
33	SNM3	T-D0300	Extremity
34	SNM3	T-11196	Facial bones PS 3.16 - 2004
35	SNM3	T-12710	Femur
36	SNM3	T-D8800	Finger
37	SNM3	T-D9700	Foot
38	SNM3	T-12402	Forearm bone
39	SNM3	T-63000	Gall bladder
40	SNM3	T-D8700	Hand
41	SNM3	T-D1100	Head
42	SNM3	T-32000	Heart
43	SNM3	T-15710	Hip joint
44	SNM3	T-12410	Humerus
45	SNM3	T-D9200	Knee
46	SNM3	T-59000	Large intestine
47	SNM3	T-24100	Larynx
48	SNM3	T-D9400	Leg
49	SNM3	T-11503	Lumbar spine
50	SNM3	T-11180	Mandible
51	SNM3	T-11133	Mastoid bone
52	SNM3	T-11170	Maxilla
53	SNM3	T-D1213	Jaw region
54	SNM3	T-D3300	Mediastinum
55	SNM3	T-11149	Nasal bone
56	SNM3	T-D1600	Neck
57	SNM3	T-11102	Optic canal
58	SNM3	T-D0801	Orbital region
59	SNM3	T-22000	Paranasal sinus
60	SNM3	T-61100	Parotid gland
61	SNM3	T-12730	Patella
62	SNM3	T-D6000	Pelvis
63	SNM3	T-59600	Rectum
64	SNM3	T-11300	Rib
65	SNM3	T-15680	Sacroiliac joint
66	SNM3	T-11AD0	Sacrum
67	SNM3	T-12280	Scapula
68	SNM3	T-D1460	Sella turcica
69	SNM3	T-12980	Sesamoid bones of foot
70	SNM3	T-D2220	Shoulder
71	SNM3	T-11100	Skull
72	SNM3	T-58000	Small intestine
73	SNM3	T-11500	Spine
74	SNM3	T-15610	Sternoclavicular joint
75	SNM3	T-11210	Sternum PS 3.16 - 2004

ID	CODE SCHEMA	CODE	NAME
76	SNM3	T-57000	Stomach
77	SNM3	T-61300	Submandibular gland
78	SNM3	T-15770	Tarsal joint
79	SNM3	T-15290	Temporomandibular joint
80	SNM3	T-11502	Thoracic spine
81	SNM3	T-D8810	Thumb
82	SNM3	T-D9800	Toe
83	SNM3	T-25000	Trachea
84	SNM3	T-70010	Upper urinary tract
85	SNM3	T-75000	Urethra
86	SNM3	T-88920	Uterus and fallopian tubes
87	SNM3	T-D8600	Wrist
88	SNM3	T-11167	Zygomatic arch
89	SRT	T-28770	Lobe of lung
90	DCM	112085	Midlung window
91	DCM	112054	Secondary pulmonary lobule
92	SRT	T-280D0	Segment of lung
93	SRT	T-20001	Airway structure
94	SRT	T-26000	Bronchus
95	SRT	T-25201	Carina
96	DCM	112086	Carina angle
97	DCM	112087	Centrilobular structures
98	SRT	T-28080	Hilum of lung
99	DCM	112088	Anterior junction line
100	SRT	T-D051D	Fissure of lung
101	DCM	112089	Posterior junction line
102	DCM	112090	Azygoesophageal recess interface
103	DCM	112091	Paraspinal line
104	DCM	112092	Posterior tracheal stripe
105	DCM	112093	Right tracheal stripe
106	DCM	112094	Stripe
107	SRT	T-25000	Trachea
108	SRT	T-56000	Esophagus
109	SRT	T-B6000	Thyroid
110	SRT	T-26100	Right main bronchus
111	SRT	T-26500	Left main bronchus
112	SRT	T-25201	Carina
113	SRT	T-D3412	Esophageal Hiatus
114	SRT	T-14171	Trapezius muscle
115	SRT	T-15420	Acromioclavicular Joint
116	SRT	T-D0634	Fascial layer
117	SRT	T-18774	Axillary Fascia
118	SRT	T-11240	Costal Cartilage
119	SRT	T-B4000	Carotid Body
120	SRT	T-42370	Ligamentum arteriosum

ID	CODE SCHEMA	CODE	NAME
121	SRT	T-C6510	Thoracic Duct
122	DCM	112095	Hiatus
123	SRT	T-C8000	Thymus Gland
124	SRT	T-C4000	Lymph node
125	SRT	T-32000	Heart
126	SRT	T-32400	Ventricle
127	SRT	T-32100	Atrium PS 3.16 - 2004
128	SRT	D4-31220	Atrial Septal Defect
129	SRT	T-35300	Mitral Valve
130	SRT	T-35400	Aortic Valve
131	SRT	T-35100	Tricuspid Valve
132	SRT	T-11300	Rib
133	SRT	T-12310	Clavicle
134	SRT	T-11500	Spine
135	SRT	T-11210	Sternum
136	SRT	T-12280	Scapula
137	SRT	T-12410	Humerus
138	SRT	T-11510	Vertebra
139	SRT	T-11301	Head of rib
140	SRT	T-11303	Neck of rib
141	SRT	T-11304	Tubercle of rib
142	SRT	T-11309	Shaft of rib
143	SRT	T-11307	Angle of rib
144	SRT	T-11308	Costal groove
145	DCM	112096	Rib Scalene Tubercle
146	SRT	T-11211	Manubrium of sternum
147	SRT	T-11218	Suprasternal notch
148	SRT	T-11219	Clavicular notch of sternum PS 3.16 - 2004
149	SRT	T-11221	Sternal angle
150	SRT	T-11220	Body of sternum
151	SRT	T-11227	Xiphoid process of sternum
152	SRT	T-11511	Arch of vertebra
153	SRT	T-11515	Pedicle of vertebra
154	SRT	T-11513	Transverse process or vertebra
155	SRT	T-11514	Lamina of vertebra
156	SRT	T-1153F	Inferior articular process of vertebra
157	SRT	T-1153E	Superior articular process of vertebra
158	DCM	112097	Vertebral Intervertebral Notch
159	SRT	T-11531	Vertebral foramen
160	SRT	T-1151F	Vertebral canal

ID	CODE SCHEMA	CODE	NAME
161	SRT	T-11512	Spinous process of vertebra
162	SRT	T-116EF	Inferior articular facet of axis
163	SRT	T-116EE	Superior articular facet of axis
164	SRT	T-12281	Acromion process of scapula
165	SRT	T-1228A	Glenoid cavity of scapula
166	DCM	112098	Subscapular Fossa
167	SRT	T-12287	Dorsal aspect of scapula
168	DCM	112099	Scapular Spine
169	DCM	112100	Scapular Supraspinatus Fossa
170	DCM	112101	Scapular Infraspinatus Fossa
171	SRT	T-12282	Coracoid process of scapula
172	SRT	T-D2236	Pectoral girdle
173	SRT	T-14110	Pectoralis major muscle
174	SRT	T-14120	Pectoralis minor muscle
175	SRT	T-D3400	Diaphragm
176	SRT	T-1416B	External intercostal muscle
177	SRT	T-14165	Innermost intercostal muscles
178	SRT	T-14183	Internal intercostal muscle PS 3.16 - 2004
179	SRT	T-14150	Levatores costarum muscles
180	SRT	T-14166	Subcostal muscle
181	SRT	T-141A5	Transversus thoracis
182	SRT	T-14171	Trapezius muscle
183	SRT	T-13650	Subscapularis muscle
184	SRT	T-13610	Supraspinatus muscle
185	SRT	T-13620	Infraspinatus muscle
186	SRT	T-13630	Teres minor muscle
187	SRT	T-14140	Serratus anterior muscle
188	SRT	T-13660	Deltoid muscle
189	SRT	T-14172	Latissimus dorsi muscle
190	SRT	T-14020	Erector spinae muscle
191	SRT	T-14030	Iliocostalis muscle
192	SRT	T-14040	Longissimus muscle
193	SRT	T-14050	Spinalis muscle
194	SRT	T-13450	Scalenous anterior muscle
195	SRT	T-13310	Sternocleidomastoid muscle
196	SRT	T-13640	Teres major muscle
197	SRT	T-35020	Chordae tendineae cordis
198	SRT	T-32410	Interventricular septum
199	SRT	T-32423	Trabeculae carnae
200	SRT	T-46100	Subclavian artery

ID	CODE SCHEMA	CODE	NAME
201	SRT	T-42100	Ascending aorta
202	SRT	T-46010	Brachiocephalic trunk
203	SRT	T-45100	Common carotid artery
204	SRT	T-46200	Internal thoracic artery
205	SRT	T-45700	Vertebral artery
206	SRT	T-46130	Thyrocervical trunk PS 3.16 - 2004
207	SRT	T-46180	Costocervical trunk
208	SRT	T-461A0	Dorsal scapular artery
209	SRT	T-47100	Axillary Artery
210	SRT	T-47160	Brachial artery
211	SRT	T-42300	Aortic arch
212	SRT	T-48170	Internal jugular vein
213	SRT	T-48330	Subclavian vein
214	SRT	T-48620	Brachiocephalic vein
215	SRT	T-48610	Superior vena cava
216	SRT	T-A9090	Brachial plexus
217	SRT	T-D0765	Descending aorta
218	DCM	112102	Aortic knob
219	SRT	T-42310	Aortic isthmus
220	SRT	T-48340	Azygos vein
221	SRT	T-D305A	Intercostal artery
222	SRT	T-4630D	Esophageal artery
223	SRT	T-46210	Pericardiophrenic Artery
224	SRT	T-46350	Superior phrenic artery
225	SRT	T-46940	Inferior phrenic artery
226	SRT	T-46310	Bronchial artery
227	DCM	112103	Arch of the Azygos vein
228	SRT	T-49110	Axillary vein
229	SRT	T-48710	Inferior vena cava
230	SRT	T-44100	Pulmonary trunk
231	SRT	T-44000	Pulmonary artery
232	SRT	T-48500	Pulmonary vein
233	SRT	T-AA050	Anterior chamber of eye
234	SRT	T-AA180	Both eyes
235	SRT	T-AA310	Choroid of eye
236	SRT	T-AA400	Ciliary body
237	SRT	T-AA860	Conjunctiva
238	SRT	T-AA200	Cornea
239	SRT	T-AA000	Eye
240	SRT	T-AA810	Eyelid

ID	CODE SCHEMA	CODE	NAME
241	SRT	T-AA621	Fovea centralis
242	SRT	T-AA500	Iris
243	SRT	T-AA862	Lacrimal caruncle
244	SRT	T-AA910	Lacrimal gland
245	SRT	T-AA940	Lacrimal sac
246	SRT	T-AA700	Lens
247	SRT	T-AA830	Lower Eyelid
248	SRT	T-45400	Ophthalmic artery
249	SRT	T-AA630	Optic nerve head
250	SRT	T-AA610	Retina
251	SRT	T-AA110	Sclera
252	SRT	T-AA820	Upper Eyelid

APPENDIX C

Modality Index

ID	CODE	NAME
1	AU	Audio
2	BI	Biomagnetic Imaging
3	CD	Color flow Doppler
4	CR	Computed radiography
5	CT	Computed tomography
6	DD	Duplex Doppler
7	DG	Diaphanography
8	DSA	Digital Subtraction Angiography
9	DX	Digital Radiography
10	ECG	Electrocardiography
11	EPS	Cardiac Electrophysiology
12	ES	Endoscopy
13	GM	General Microscopy
14	HC	Hard Copy
15	HD	Hemodynamic Waveform
16	IO	Intra-Oral Radiography
17	IVUS	Intravascular Ultrasound
18	LS	Laser surface scan
19	MG	Mammography
20	MR	Magnetic Resonance

ID	CODE	NAME
21	NM	Nuclear Medicine
22	OCT	Optical Coherence Tomography
23	OP	Ophthalmic Photography
24	OPM	Ophthalmic Mapping
25	OPR	Ophthalmic Refraction
26	OPV	Ophthalmic Visual Field
27	OT	Other
28	PR	Presentation State
29	PET	Positron Emission Tomography - PET
30	PX	Panoramic X-Ray
31	REG	Registration
32	RF	Radio Fluoroscopy
33	RG	Radiographic imaging (conventional film/screen)
34	SEG	Segmentation
35	SM	Slide Microscopy
36	SMR	Stereometric Relationship
37	SR	SR Document
38	ST	Single-photon emission computed tomography (SPECT)
39	TG	Thermography
40	US	Ultrasound
41	XA	X-Ray Angiography
42	XC	External-camera photography
43	RTDOSE	Radiotherapy Dose
44	RTIMAGE	Radiotherapy Image
45	RTPLAN	Radiotherapy Plan
46	RTRECORD	RT Treatment Record
47	RTSTRUCT	Radiotherapy Structure Set

APPENDIX D

Workload Index

SUT is a standardization for evaluation of medical processes published by Turkish Ministry of Health for performance assessment and payment measurements. The entries for radiology processes is listed below and utilized in order to take effort and time estimations as a reference for workload calculations in RWOA. Each process has a unique code and process attribute values determined by Ministry of Health experts. ”Point” is an indicator for resource and effort usage and used to estimate the payment for the corresponding operations as a function of ”Risk”, ”Technical Requirement”, ”Work Required”, ”Urgency”, ”Presence of Alternative” and ”Required Time”. RWOA utilizes normalized values of ”Point” and ”Required Time” in SUT standardization for Radiology.

Id	Code	Name	Point	Risk	Tech. Req.	Work. Req.	Urg.	Freq.	Alter.	Time
2		A-Direkt Grafiler								
3	801560	El-bilek grafisi (tek film)	10,12	2	2	2	2	2	4	3
4	801570	Floroskopi	17,20	2	2	4	2	2	4	10
5	801580	Kemik survey	125,80	2	2	2	2	2	4	10
6	801590	Mammografi (tek meme)	28,67	5	5	4	3	5	5	10
7	801600	Mandibula (tek yön)	10,12	2	2	2	2	2	4	3
8	801610	Schuller grafisi (mukayeseli)	25,80	2	2	2	2	2	4	3
9	801620	Sella spot grafisi	10,12	2	2	2	2	2	4	3
10	801630	Sinüs (Waters) grafisi (tek yön)	10,12	2	2	2	2	2	4	3
11	801640	Skolyoz tetkiki	64,42	2	2	2	2	2	4	6
12	801650	Stenvers grafisi (mukayeseli)	18,72	2	2	2	2	2	4	3
13	801660	Temporamandibular eklem	25,80	2	2	2	2	2	4	3
14	801670	Uzun kemikler (tek film) (tek yön)	12,98	2	2	2	2	2	4	3
15	801680	Kopya film (her bir film için)	10,12	2	2	2	1	2	4	3
16		Akciğer grafileri								
17	801690	Akciğer grafisi (iki yön)	21,59	2	2	2	3	2	4	4
18	801700	Akciğer grafisi (üç yön) baryumlu	34,40	2	2	2	3	2	4	5
19	801710	Akciğer grafisi (üç yön)	24,45	2	2	2	3	2	4	4
20	801720	Akciğer grafisi P.A. (tek yön)	11,47	2	2	2	3	2	4	3
21		Bacak uzunluk grafileri								
22	801730	Bacak uzunluk grafisi	20,07	2	3	2	2	3	4	3
23		Düz karın grafisi								
24	801740	Düz karın grafisi	12,98	2	2	2	3	2	3	3
25		Eklemler								
26	801750	Eklem grafisi (iki yön) mukayeseli	24,45	2	2	2	3	3	4	4
27	801760	Eklem grafisi (tek yön) mukayeseli	12,98	2	2	2	3	3	4	3
28	801770	Eklem grafisi (tek yön) tek eklem	10,12	2	2	2	3	3	4	3
29	801780	Eklem grafisi(iki yön)tek eklem	12,98	2	2	2	3	3	4	4
30	801790	Eklem grafisi(üç yön)	20,07	2	2	2	3	3	4	4

Id	Code	Name	Point	Risk	Tech. Req.	Work. Req.	Urg.	Freq.	Alter.	Time
31		Kafa grafileri								
32	801800	Kafa grafisi (dört yön)	27,32	2	2	2	3	3	3	4
33	801810	Kafa grafisi (iki yön)	18,72	2	2	2	3	3	3	3
34	801820	Kafa grafisi (tek yön)	10,12	2	2	2	3	3	3	3
35		Kalp telekardiogram-lar								
36	801830	Kalp teleradyogram-lar (iki yön)	22,93	3	2	2	3	2	4	4
37	801840	Kalp teleradyogram-lar (tek yön)	12,98	3	2	2	3	2	4	4
38	801850	Kalp teleradyogram-lar (üç yön) baryumlu	34,40	3	2	2	3	2	4	5
39	801860	Kalp teleradyogram-lar (üç yön)	24,45	3	2	2	3	2	4	4
40		Pelvis grafileri								
41	801870	Pelvis gr.(tek yön)	12,98	2	2	2	3	3	4	3
42	801880	Pelvis gr.(üç yön)	24,45	2	2	2	3	3	4	4
43	801890	Pelvimetri (iki yön)	18,72	2	2	2	3	3	4	4
44		Vertebra grafileri								
45	801900	Vertebra grafileri, servikal (dört yön)	27,32	2	2	2	2	3	3	5

Id	Code	Name	Point	Risk	Tech. Req.	Work. Req.	Urg.	Freq.	Alter.	Time
46	801910	Vertebra grafileri, servikal (iki yön)	17,20	2	2	2	2	3	3	4
47	801920	Vertebra grafileri, servikal (tek yön)	10,12	2	2	2	2	3	3	3
48	801930	Vertebra grafileri, servikal (üç yön)	25,80	2	2	2	2	3	3	4
49	801940	Vertebra grafileri, dorsal veya lomber (dört yön)	43,00	2	2	2	2	3	3	5
50	801950	Vertebra grafileri, dorsal veya lomber (iki yön)	20,07	2	2	2	2	3	3	4
51	801960	Vertebra grafileri, dorsal veya lomber (tek yön)	12,98	2	2	2	2	3	3	3
52	801970	Vertebra grafileri, dorsal veya lomber (üç yön)	27,32	2	2	2	2	3	3	4
53	801980	L5-S1 spot grafisi	11,47	2	2	2	2	3	3	3
54		B-Kontrastlı tetkikler								
55	801990	Anterograd pyelografi, var olan kateterden	25,80	2	3	4	2	4	3	15
56	802000	Anterograd pyelografi, ince iğne ile, işlemin tümü	350,25	5	3	5	3	4	3	30
57	802010	Artrografi	64,42	4	3	5	2	4	4	30
58	802020	Bronkografı	50,08	5	3	5	2	4	2	30
59	802030	Çift kontrast kolon tetkiki	157,34	3	3	4	2	3	3	30
60	802040	Çift kontrast mide tetkiki	107,25	2	3	4	2	3	3	30

Id	Code	Name	Point	Risk	Tech. Req.	Work. Req.	Urg.	Freq.	Alter.	Time
61	802050	Dakriosistografi	50,08	3	3	5	2	4	4	20
62	802060	Defekografi	107,25	3	3	4	2	4	5	30
63	802070	Distal kolon grafisi	64,42	3	3	4	2	4	3	20
64	802080	Duktografi-galaktografi	64,42	4	3	4	2	4	4	20
65	802090	Enteroklizis	157,34	4	3	5	2	4	5	60
66	802100	Faringografi	27,32	3	3	4	2	4	4	15
67	802110	Faringo-ozefagografi	32,88	3	3	4	2	4	4	15
68	802120	Fistülografi	48,74	3	3	4	2	4	5	15
69	802130	HSG	43,00	4	3	4	2	4	5	30
70	802140	I.V.P.	54,47	3	3	4	2	3	3	30
71	802150	I.V.P.(dakikalık)	65,77	3	3	4	2	3	3	30
72	802160	İnce barsak tetkiki	57,17	2	3	4	2	3	3	45
73	802170	Kolon tetkiki	120,07	3	3	4	2	3	3	30
74	802180	Laringografi	64,42	3	3	4	2	4	3	15
75	802190	Lenfanjiografi	278,75	5	3	5	2	4	4	120
76	802200	Mide duedonum tetkiki	70,15	3	3	4	2	3	3	30
77	802210	Miyelografi	214,50	4	3	4	2	4	2	30
78	802220	Oral kolesistografi	27,32	2	3	4	2	4	1	15
79	802230	Özefagografi	27,32	3	3	4	2	3	4	15
80	802240	Peroperatuar kolanjiografi	34,40	3	3	4	2	4	4	15
81	802250	Poş grafisi	34,40	3	3	4	2	4	3	15
82	802260	Retrograd pyelografi	25,80	3	3	4	2	4	3	30
83	802270	Retrograd üretrografi	50,08	3	3	4	2	4	3	20
84	802280	Sialografi (iki taraf)	43,00	4	3	4	2	4	4	40
85	802290	Sialografi (tek taraf)	25,80	4	3	4	2	4	4	30
86	802300	Sine özefagografi	117,20	3	3	4	2	4	5	20
87	802310	Sistogram (üç film)	27,32	3	3	4	2	4	3	20
88	802320	T tüp kolanjiografi	34,40	3	3	3	2	4	3	15
89	802330	Velofaringeal sine-floroskopi	71,50	3	3	4	2	4	5	20
90	802340	Voiding sistoüretrografi	107,25	3	3	4	2	3	5	30

Id	Code	Name	Point	Risk	Tech. Req.	Work. Req.	Urg.	Freq.	Alter.	Time
91		C-Anjiografik tetkikler								
92		Normal anjiografik tetkikler								
93	802350	Aorto-femoro-popliteal arteriografi	228,67	4	5	5	4	4	3	40
94	802360	Aortografi, torakal	228,67	4	5	5	4	4	3	40
95	802370	Aortografi, abdominal	228,67	4	5	5	4	4	3	40
96	802380	Coliak anjiografi ve arteriel portografi	271,67	4	5	5	4	4	3	50
97	802390	İki taraflı selektif renal anjiografi	271,67	4	5	5	4	4	3	50
98	802400	İnferior mesenterik anjiografi	228,67	4	5	5	4	4	3	50
99	802430	Pelvik arteriografi	228,67	4	5	5	4	4	3	40
100	802440	Pulmoner Anjiografi	143,00	4	5	5	4	4	3	40
101	802450	Superior mesenterik angiografi	228,67	4	5	5	4	4	3	50
102	802460	Tek taraflı üst ekstremite arteriografi	228,67	4	5	5	4	4	3	40
103	802470	Tek taraflı femoro-popliteal arteriografi	228,67	4	5	5	4	4	3	30
104	802480	Tek taraflı selektif renal anjiografi	228,67	4	5	5	4	4	3	40
105	802490	Translomber aorto-femoro-popliteal arteriografi	228,67	4	5	5	4	5	3	40

Id	Code	Name	Point	Risk	Tech. Req.	Work. Req.	Urg.	Freq.	Alter.	Time
106	802500	Transplant renal anjiografi	228,67	4	5	5	4	4	3	50
107		Nöroradyolojik anjiografik tetkikler								
108	802510	Amytal Testi (VADA)	228,67	5	5	5	4	5	5	90
109	802520	Arkus aortografi	228,67	4	5	5	4	4	3	40
110	802530	Çift taraflı selektif karotid anjiografi	350,25	5	5	5	4	4	3	50
111	802540	4 sistem selektif serebral anjio	450,25	5	5	5	4	4	3	60
112	802550	Orbital flebografi	157,34	4	5	5	4	5	5	50
113	802560	Petrozal sinüs kan örneklemesi	271,67	4	5	5	4	5	5	60
114	802570	Çift taraflı selektif vertebral anjiografi	350,25	5	5	5	4	4	3	50
115	802580	Spinal anjiografik tarama	450,25	5	5	5	4	5	5	90
116	802590	Tek taraflı selektif karotid anjiografi	228,67	5	5	5	4	4	3	40
117		Venografik tetkikler								
118	802600	Dializ fistülogram	85,83	4	5	5	4	4	3	40
119	802610	Hepatik venografi ve wedge venografi	150,08	3	5	5	4	5	5	40
120	802620	İki taraflı surrenal venografi	150,08	3	5	5	4	5	3	60

Id	Code	Name	Point	Risk	Tech. Req.	Work. Req.	Urg.	Freq.	Alter.	Time
121	802630	İki taraflı gonadal venografi	150,08	3	5	5	4	5	3	45
122	802640	İnferior/superior vena kavagrafi	105,90	3	5	5	4	5	3	30
123	802650	Portal venöz kan örneklemesi	350,25	5	5	5	4	5	5	60
124	802660	Renal venografi ve renal ven kan örnekleri alın.	107,25	3	5	5	4	5	5	40
125	802670	Santral venöz kateter patensi kontrastlı değerlendirmesi	85,83	3	5	5	4	3	5	25
126	802680	Splenoportografi	150,08	5	5	5	4	5	3	40
127	802690	Tek taraflı surrenal venografi	107,25	3	5	5	4	5	3	40
128	802700	Tek taraflı gonadal venografi	107,25	3	5	5	4	5	3	40
129	802710	Venografi, alt ekstremite, tek taraf	65,77	3	5	5	4	4	3	30
130	802720	Venografisi, üst ekstremite, tek taraf	65,77	3	5	5	4	4	3	30
131		Vasküler girişimsel radyolojik tedavi işlemleri								
132	802730	Aortik stent-greft uygulaması	1429,17	5	5	5	5	5	4	210
133	802740	Beyin AVM embolizasyonu / AV Fistül Tedavileri	1683,58	5	5	5	5	5	5	210
134	802750	Diğer organ ve Tümör Embolizasyon	841,79	5	5	5	5	5	4	120
135	802760	Endovasküler Serebral Anevrizma Tedavisi	1683,58	5	5	5	5	5	4	210

Id	Code	Name	Point	Risk	Tech. Req.	Work. Req.	Urg.	Freq.	Alter.	Time
136	802770	Geçici Kateter Yerleştirilmesi	100,17	4	5	5	5	5	5	35
137	802780	Perkütan Translüminal Anjiyoplasti işlemleri	414,50	5	5	5	5	5	4	120
138	802790	Pseudoanevrizma tedavisi, renkli Doppler	100,17	3	5	5	4	5	4	40
139	802800	Selektif Trombolitik Tedavi İşlemleri	643,17	5	5	5	5	5	5	120
140	802810	Subkütan Port Çıkarılması	85,83	3	5	5	3	5	5	30
141	802820	Subkütan Port Yerleştirilmesi	353,00	4	5	5	4	5	5	45
142	802830	Supraaortik / Visseral İntravasküler Stent Yerleştirilmesi	841,79	5	5	5	4	5	4	120
143	802840	Transarteriyel Kemo-Embolizasyon	643,17	5	5	5	4	5	4	120
144	802850	Transjuguler Intrahepatik Porto-Sistemik Şant	1071,84	5	5	5	4	5	4	120
145	802860	Tünelli Kateter Çıkarılması	85,83	3	5	5	3	5	5	30
146	802870	Tünelli Kateter Yerleştirilmesi	300,17	4	5	5	5	5	5	45
147	802880	Vena Kavaya Filtre / Stent Yerleştirilmesi	714,67	4	5	5	4	5	5	45
148	802890	Periferik aterektomi, trombektomi veya lazer, tek lezyon	714,67	5	5	5	5	5	4	120
149		D-Kemik dansitometresi								
150	802900	Kemik dansitometresi (Lokal)	30,02	1	3	2	1	2	3	15

Id	Code	Name	Point	Risk	Tech. Req.	Work. Req.	Urg.	Freq.	Alter.	Time
151	802910	Kemik dansitometresi, tüm vucut	40,13	1	3	2	1	2	3	20
152		E-Nonvasküler girişimsel radyolojik tedaviler								
153	802920	Dakriosistoplasti, balon ile	428,84	4	5	5	2	5	4	60
154	802930	Görüntüleme eşliğinde biopsi (kalın ya da ince iğne)	90,52	4	3	4	3	2	5	30
155	802940	Gastrointestinal stent yerleştirilmesi	714,67	5	5	5	3	5	4	60
156	802950	İnvajinasyon, baryumlu kolon ile redüksiyon	347,57	3	4	4	5	5	4	50
157	802960	İnvajinasyon, ultrason eşliğinde redüksiyon	347,57	3	4	4	5	5	4	50
158	802970	Nazolakrimal kanala stent yerleştirilmesi	428,84	4	5	5	3	5	4	60
159	802971	Nazojejunal beslenme tüpü yerleştirilmesi, floroskopi eşliğinde	214,50	3	4	5	4	5	4	40
160	802980	Özefagus dilatasyonu.	214,50	5	5	5	4	5	4	45
161	802990	Perkütan akciğer absesi drenajı	714,67	5	5	5	5	5	4	50
162	803000	Perkütan alkol ablasyon tedavisi	643,17	4	5	5	4	4	4	50
163	803010	Perkütan ampiyem drenajı	428,84	5	5	5	5	4	4	50
164	803020	Perkütan apse drenajı	428,84	5	5	5	5	4	4	50
165	803030	Perkütan asit, plevral effüzyon drenajı	428,84	4	5	5	4	4	4	30

Id	Code	Name	Point	Risk	Tech. Req.	Work. Req.	Urg.	Freq.	Alter.	Time
166	803040	Perkütan bilier drenaj	714,67	5	5	5	5	4	4	120
167	803050	Perkütan bilier stent konması	714,67	4	5	5	4	5	4	90
168	803060	Perkütan bilier taş çıkarılması	714,67	5	5	5	5	5	4	120
169	803070	Perkütan çölyak ganglion blokajı	571,67	4	5	5	4	5	4	50
170	803080	Perkütan enterik fistül tedavisi	428,84	4	5	5	4	5	4	60
171	803090	Perkütan gastrojejunostomi	857,50	4	5	5	4	5	4	60
172	803100	Perkütan gastrostomi	714,67	4	5	5	4	5	4	45
173	803110	Perkütan kist hidatik tedavisi	857,50	5	5	5	4	4	4	90
174	803120	Perkütan koledok dilatasyonu	857,50	5	5	5	4	5	4	90
175	803130	Perkütan koleksiyon/kist tedavisi	428,84	4	5	5	4	4	4	50
176	803140	Perkütan lenfosel tedavisi	714,67	4	5	5	4	5	4	50
177	803150	Perkütan nefrostomi	428,84	5	5	5	5	4	4	50
178	803160	Perkütan pankreatik kanal girişimleri	857,50	5	5	5	4	5	4	60
179	803170	Perkütan pnömotoraks tedavisi	428,84	5	5	5	5	4	4	40
180	803180	Perkütan psödokist tedavisi	714,67	4	5	5	4	4	4	50

Id	Code	Name	Point	Risk	Tech. Req.	Work. Req.	Urg.	Freq.	Alter.	Time
181	803190	Perkütan radyofrekans ablasyon tedavisi	845,40	5	5	5	4	4	4	90
182	803200	Perkütan renal kist ponksiyon ve tedavisi	428,84	4	5	5	4	4	4	45
183	803210	Perkütan safra kesesi drenajı	428,84	5	5	5	5	4	4	50
184	803220	Perkütan sistostomi	114,33	4	5	5	5	5	4	40
185	803230	Perkütan sistoüretografi	428,84	4	5	5	3	5	5	40
186	803240	Perkütan stenoz dilatasyonu	428,84	5	5	5	4	5	4	60
187	803250	Perkütan transhepatik kolanjiografi	841,79	4	5	5	4	4	4	40
188	803260	Perkütan üreteral stent konması	857,50	4	5	5	4	5	4	60
189	803270	Stent yerleştirilmesi	857,50	4	5	5	4	5	4	90
190	803280	Streotaktik meme işaretleme	221,59	4	5	4	4	4	5	40
191	803290	Ultrasonografi eşliğinde parasentez,torasentez	50,08	3	5	4	4	3	4	30
192	803300	Vertebroplasti	929,01	5	5	5	4	5	4	120
193		F-Ultrasonografik tetkikler								
194	803310	3-Boyutlu ultrasonografi	65,77	2	5	1	3	5	5	45
195	803320	Boyun US	24,45	2	3	1	3	3	3	15

Id	Code	Name	Point	Risk	Tech. Req.	Work. Req.	Urg.	Freq.	Alter.	Time
196	803330	Renal US, dinamik	41,48	2	3	1	3	5	4	25
197	803340	Eklem US (tek taraf)	12,98	2	3	1	3	4	3	15
198	803350	Endoskopik US	95,95	4	3	1	3	5	4	40
199	803360	Follikülometri (trans-abdominal fol-likülometri)	40,13	2	3	1	4	3	4	15
200	803370	Follikülometri (transvajinal fol-likülometri)	40,13	3	3	1	4	3	4	20
201	803380	Kontrastlı Doppler harmonik ultrasono-grafi (her bir bölge için)	64,42	2	3	1	3	5	3	20
202	803390	Hepatobilier US	17,20	2	3	1	3	3	3	15
203	803400	IVUS (intravasküler ultrasonografi)	107,25	5	5	1	4	5	4	40
204	803410	İntroperatif US	59,19	4	3	1	3	5	5	45
205	803420	Kalça eklemi US (tek taraf)	14,33	2	3	1	3	4	3	15
206	803430	Meme US (bilateral)	25,80	4	3	1	3	3	3	25
207	803440	Meme US (unilateral)	12,98	4	3	1	3	3	3	15
208	803450	Obstetrik US	25,80	5	3	1	3	3	5	30
209	803460	Orbita US (bilateral) (A veya B mod)	25,80	2	3	1	3	4	3	15
210	803470	Parotis bezi US	12,98	2	3	1	3	3	3	15
211	803480	Renal US	17,20	2	3	1	3	3	3	15
212	803490	Skrotal US	20,07	2	3	1	3	3	3	15
213	803500	Submandibuler bez US	12,98	2	3	1	3	3	3	15
214	803510	Tiroid US	24,45	2	3	1	3	3	3	15
215	803520	Toraks US	20,07	2	3	1	3	3	3	15
216	803530	Transkranial veya transfontanel US	20,07	2	3	1	3	3	3	15
217	803540	Transrektal US	32,88	3	3	1	3	3	4	20
218	803550	Transvajinal US	25,80	3	3	1	3	3	4	20
219	803560	Suprapubik pelvik US	25,80	2	3	1	3	3	3	15
220	803570	Abdomen US, tüm	40,13	2	3	1	4	3	3	25
221	803580	Üriner sistem US	25,80	2	3	1	3	3	3	15
222	803590	Abdomen US, üst	25,80	2	3	1	3	3	3	20
223	803600	Yüzeyel doku US	25,80	2	3	1	3	3	3	15
224	803601	Ultrason, diğer	20,07	2	3	1	3	3	3	15
225	803602	Ultrason, genel	14,33	1	3	1	1	1	1	15

Id	Code	Name	Point	Risk	Tech. Req.	Work. Req.	Urg.	Freq.	Alter.	Time
226		G-Renkli Doppler incelemeleri								
227	803610	3-boyutlu renkli Doppler ultrasonografi	64,42	2	5	1	3	5	5	30
228	803620	Abdominal aorta renkli Doppler US	35,75	2	3	1	3	3	4	20
229	803630	Abdominal renkli Doppler US	35,75	2	3	1	3	3	4	20
230	803640	Alt ekstremite perforan ven renkli Doppler US, tek taraflı	35,75	2	4	1	3	4	4	30
231	803650	Fötal biyometri ve biyofizik skorlama	43,00	2	3	1	3	3	4	30
232	803670	İntraoperatif renkli Doppler US	50,08	3	3	1	3	5	4	45
233	803680	Karotis renkli Doppler US (tek, bilateral)	35,75	2	3	1	3	3	4	20
234	803690	Kitle lezyonu renkli Doppler US	35,75	2	3	1	3	3	4	20
235	803700	Meme renkli Doppler US	35,75	2	3	1	3	3	4	25
236	803710	Obstetrik renkli Doppler US	41,48	5	3	1	5	4	5	30
237	803720	Orbita renkli Doppler US	41,48	2	3	1	3	4	4	20
238	803730	Pelvik renkli Doppler US	35,75	2	3	1	3	3	4	20
239	803740	Penil renkli Doppler US	41,48	5	3	1	3	4	4	30
240	803750	Portal ven renkli Doppler US	35,75	2	3	1	3	3	4	20

Id	Code	Name	Point	Risk	Tech. Req.	Work. Req.	Urg.	Freq.	Alter.	Time
241	803760	Renal renkli Doppler US (bilateral)	43,00	2	3	1	3	3	4	30
242	803770	Skrotal renkli Doppler US	35,75	2	3	1	5	3	4	20
243	803780	Alt ekstremite arteriel sistem RDUS, tek taraflı	35,75	2	3	1	3	3	4	25
244	803790	Alt ekstremite venöz sistem RDUS, tek taraflı	35,75	2	3	1	4	3	4	25
245	803800	Üst ekstremite arteriel sistem RDUS, tek taraflı	35,75	2	3	1	3	3	4	25
246	803810	Üst ekstremite venöz sistem RDUS, tek taraflı	35,75	2	3	1	4	3	4	25
247	803820	Tiroid bezi renkli Doppler US	35,75	2	3	1	3	3	4	20
248	803830	Transkranial veya transfontanel renkli Doppler	35,75	2	3	1	3	3	4	20
249	803840	Transrektal renkli Doppler	35,75	2	3	1	3	3	4	25
250	803850	Vertebral arter renkli Doppler US (tek, bilateral)	35,75	2	3	1	3	3	4	20
251	803860	Vezikoüreteral reflüks renkli Doppler US	35,75	2	3	1	3	4	4	30
252		H-Bilgisayarlı tomografiler								
253	803870	BT, 3 boyutlu görüntüleme	92,75	2	5	3	3	5	4	25
254	803880	BT, angiografi, tek anatomik bölge için	92,75	3	5	3	4	4	4	25
255	803890	BT, abdomen, alt	92,75	3	4	3	3	3	4	15

Id	Code	Name	Point	Risk	Tech. Req.	Work. Req.	Urg.	Freq.	Alter.	Time
256	803900	BT, beyin (aksiyel+koronal)	125,80	3	4	3	4	3	4	15
257	803910	BT, beyin	92,75	3	4	3	4	3	4	15
258	803920	BT, boyun	92,75	3	4	3	3	4	4	15
259	803930	BT, dental tomografi	92,75	2	4	3	3	3	4	15
260	803940	BT, extremite (20-50cm bölge)	92,75	3	4	3	3	3	4	15
261	803950	BT, hava veya opaklı sisternografi	92,75	4	4	3	3	3	4	30
262	803960	BT, hipofiz	92,75	3	4	3	3	3	4	15
263	803970	BT, kantitatif tomografi (kals.skor., BTBMD gibi)	92,75	2	4	3	3	3	4	25
264	803980	BT, larenks	92,75	3	4	3	3	4	4	15
265	803990	BT, maksillofasial tomografi, aksiyel	92,75	3	4	3	4	3	4	15
266	804000	BT, maksillofasial tomografi, koronal	92,75	3	4	3	4	3	4	15
267	804010	BT, nazofarinks	92,75	3	4	3	3	4	4	15
268	804020	BT, orbita	92,75	3	4	3	3	4	4	15
269	804030	BT, paranazal sinüs	92,75	3	4	3	3	3	4	15
270	804040	BT, radyoterapi planlaması için tomog.	72,85	3	4	3	3	3	4	15

Id	Code	Name	Point	Risk	Tech. Req.	Work. Req.	Urg.	Freq.	Alter.	Time
271	804050	BT, tempomandibular eklem	112,48	3	4	3	3	3	4	15
272	804060	BT, temporal kemik YRBT, tek düzlem	92,75	2	4	3	3	3	4	15
273	804070	BT, toraks	92,75	3	4	3	3	3	5	20
274	804080	BT, tomografi, diğer	92,75	3	4	3	3	3	4	15
275	804090	BT, üst abdomen	92,75	3	4	3	3	3	4	20
276	804100	BT, vertebra, servikal	92,75	3	4	3	3	3	4	15
277	804101	BT, vertebra torakal	92,75	3	4	3	3	3	4	15
278	804102	BT, vertebra lumbal	92,75	3	4	3	3	3	4	15
279	804110	BT eşliğinde girişimsel tetkik	119,06	5	4	5	3	5	5	45
280	804120	BT perfüzyon çalışmaları	92,75	3	5	3	3	4	4	45
281	804130	BT sanal endoskopi	119,06	3	5	3	3	5	4	45
282	804140	BT, dinamik, trifazik, bifazik inceleme	119,06	3	4	3	3	3	4	20
283	804150	BT, yüksek rezolusyonlu akciğer	92,75	2	4	3	3	3	5	15
284	804160	BT, yüksek rezolusyonlu akciğer, ekspratuar	92,75	2	4	3	3	4	5	15
285		I-Manyetik Rezonans Görüntüleme								
286	804170	MR, akciğer ve mediasten	109,61	2	4	3	3	5	3	25
287	804180	MR, abdomen, alt	109,61	2	4	3	3	4	3	25
288	804190	MR, beyin	109,61	2	4	3	3	3	4	25
289	804200	MR, BOS akım	109,61	2	4	3	3	5	5	40
290	804210	MR, boyun	109,61	2	4	3	3	3	4	25
291	804220	MR, diffuzyon	109,61	2	5	3	4	3	5	15
292	804230	MR, dinamik	109,61	2	5	3	3	3	4	25
293	804240	MR, Eklem tek	109,61	2	4	3	3	3	4	25
294	804250	MR, ekstremite tek taraflı	109,61	2	4	3	3	3	4	25
295	804260	MR, fonksiyonel	109,61	2	5	3	3	5	5	60
296	804270	MR, hipofiz	109,61	2	4	3	3	3	4	25
297	804280	MR, kardiak	109,61	3	5	3	3	4	4	45
298	804290	MR, kardiak fonksiyon	109,61	3	5	3	3	4	4	55
299	804300	MR, kardiak perfüzyon	109,61	3	5	3	3	4	4	55
300	804310	MR, kulak	109,61	2	4	3	3	3	4	25

Id	Code	Name	Point	Risk	Tech. Req.	Work. Req.	Urg.	Freq.	Alter.	Time
301	804320	MR, vertebra, lomber	109,61	2	4	3	3	3	4	25
302	804330	MR, meme	109,61	2	5	3	3	4	4	30
303	804340	MR Anjiyografi	109,61	2	5	3	3	4	3	30
304	804350	MR Kolanjiyografi	109,61	2	4	3	3	4	4	30
305	804360	MR Myelografi	109,61	2	4	3	3	5	4	30
306	804370	MR Spektroskopi (tek voksel tek eko)	103,04	2	5	3	3	5	5	40
307	804380	MR Spektroskopi (multivoksel tek eko)	109,61	2	5	3	3	5	5	40
308	804390	MR ürografi	109,61	2	5	3	3	5	4	30
309	804400	MR artrografi	109,61	4	5	5	3	5	4	45
310	804410	MR, diğer	109,61	2	4	3	3	3	4	25
311	804420	MR, Nazofarinks	109,61	2	4	3	3	3	3	25
312	804430	MR, Orbita	109,61	2	4	3	3	3	3	25
313	804440	MR, Perfüzyon	109,61	2	5	3	3	4	4	40
314	804450	MR, Vertebra, servikal	109,61	2	4	3	3	3	4	25
315	804460	MR, Temporo-mandibuler eklem (tek eklem)	109,61	2	4	3	3	3	4	25
316	804470	MR, Vertebra, torakal	109,61	2	4	3	3	3	4	25
317	804480	MR, Abdomen, üst	109,61	2	4	3	3	4	4	25
318	804490	MR, tüm vücut metastaz tarama, hareketli masa ile	109,61	2	5	3	3	5	4	45
319	804500	MR, Girişimsel	109,61	5	5	5	3	5	3	45
320	804510	MR, Yüz	109,61	2	4	3	3	5	3	25

APPENDIX E

ILP Model Implementation

```
public model InspectionAssignmentProblem solver lpsolve {
   final Set$<$Radiologist$>$ radiologists = new HashSet$<$Radiologist$>$();{
   radiologists.addAll(RadiologistUtil.generateSimplisticRadiologistSet());
   }

   final double totalSupply = sum{r.getWorkload() Radiologist r : radiologists};

   final Set$<$Inspection$>$ inspections = new HashSet$<$Inspection$>$();{
      inspections.addAll(InspectionUtil.generateSimplisticInspectionSet());
   }

   final int totalDemand = sum{i.getDemand() Inspection i : inspections};
   // Transportation cost from each factory to each customer
   // cost are random values and will change at each instantiation of the model.

   final double[Inspection][Radiologist] rating[Radiologist r :
      radiologists][Inspection i : inspections] =
         RatingUtil.calculateRating(i,r);

   final double[Inspection][Radiologist] experienceRate[Radiologist r :
      radiologists][Inspection i : inspections] =
         RatingUtil.calculateExperienceRate(i,r);

   final double[Inspection][Radiologist] responseTime[Radiologist r :
      radiologists][Inspection i : inspections] =
         RatingUtil.calculateResponseTime(i,r);

   final double[Inspection][Radiologist] workloadRate[Radiologist r :
      radiologists][Inspection i : inspections] =
         RatingUtil.calculateQuotaRate(i,r);

   final double[Inspection][Radiologist]  effort[radiologists][Inspection i :
      inspections] = i.getWorkloadMap().get("effort");

   final double[Inspection][Radiologist]
      storage[radiologists][Inspection i : inspections] =
         i.getTechnicalMap().get("storage");
```

```
final double[Inspection][Radiologist]  bandwidth[radiologists][Inspection i :
   inspections] = i.getTechnicalMap().get("bandwidth");

final var int[Inspection][Radiologist]
   quantity[radiologists][Inspection i : inspections] in 0 .. i.getDemand();

// Each inspection is assigned to one radiologist
constraints[Inspection] demand[inspections];
   constraints {
      forall(Inspection i : inspections) {
         demand[i] : sum{quantity[r][i]
            Radiologist r : radiologists} == i.getDemand();
         }
      }
// Each radiologist is assigned a certain workload
constraints[Radiologist] supply[radiologists];
   constraints {
      forall(Radiologist r : radiologists) {
         supply[r] : sum{effort[r][i]*quantity[r][i]
            Inspection i : inspections} <= r.getWorkload();
      }
   }

constraints[Inspection][Radiologist] storage_ri[radiologists][inspections];
   constraints {
      forall(Radiologist r : radiologists) {
         forall(Inspection i : inspections) {
            storage\_ri[r][i] : storage[r][i]*quantity[r][i] <=
               r.getReportingUnit().getStorage();
         }
      }
   }

constraints[Inspection][Radiologist] bandwidth_ri[radiologists][inspections];
   constraints {
      forall(Radiologist r : radiologists) {
         forall(Inspection i : inspections) {
            bandwidth_ri[r][i] : bandwidth[r][i]*quantity[r][i] <=
               r.getReportingUnit().getBandwidth();
         }
      }
   }

constraints[Inspection][Radiologist]
   experience_ri[radiologists][inspections];
   constraints {
      forall(Radiologist r : radiologists) {
         forall(Inspection i : inspections) {
```

```
            experience_ri[r][i] : experienceRate[r][i]*quantity[r][i] >= 0;
         }

   }

//Each inspection should be responded at a certain response time
constraints[Inspection] response[inspections];
   constraints {
      forall(Inspection i : inspections) {
         response[i] : sum{responseTime[r][i]*quantity[r][i]
         Radiologist r : radiologists} <= i.getRequiredResponseTime();
      }
   }

// Maximize objective function
maximize sum{
   rating[r][i]*quantity[r][i]
    Radiologist r : radiologists, Inspection i : inspections};
}
```

APPENDIX F

Curriculum Vitae

AYHAN OZAN YILMAZ

Guvenlik Cad. No: 66/10 Phone: +90 532 6986789

A. Ayranci, Ankara TURKEY email: ayhanozanyilmaz@gmail.com

F.1 Educational Background

2007 – 2015 Middle East Technical University (METU), ANKARA Informatics Institute, Health Informatics, PhD.

2004 – 2007 Middle East Technical University (METU), ANKARA Department of Electrical and Electronics Engineering, Biomedical Engineering, MSc.

2002 – 2006 Middle East Technical University (METU), ANKARA Department of Chemistry, Minor Degree

2000 – 2004 Middle East Technical University (METU), ANKARA Department of Electrical and Electronics Engineering, BS

1992 - 2000 Kadikoy Anatolian High School

F.2 Work Experience

06/2012 – Present Founder at Biyomod Ltd.

1. *PingaBeat* remote patient monitoring system funded by Tubitak. www.pingabeat.com
2. *eeApis* electrical impedance based sleep apnea detection and tracking system funded by Tubitak.
3. *PingaCase* medical case study archiving and sharing platform. pingacase.com
4. *ScoBox* collaborative e-learning interaction and sharing cloud platform
5. *Etudyo* e-learning content editing and aggregation platform

6. *Learnia* e-learning gamification engine, www.learnia.com

08/2009 – Present Co-founder at MVIS Ltd.

1. *AsmEveri* web based teleradiology system development.
2. *OlguSun* medical education and data sharing platform.

04/2006 – 07/2009 Software Engineer at Turk Telekom-Sebit.

1. Software Design and Development Team Captain in the development of TTNet Vitamin project.
2. Question Bank, Exam and Performance system design, development and deployment for TTNet Vitamin.
3. Backend design and development for iClass, a Europian Union WP6 project.
4. Web application development for exam and evaluation system of MEHSIM, a simulation and education project developed for Turkish Armed Forces.

06/2003 – 06/2007 METU Biomedical Research Project under supervision of Prof. Dr. Murat Eyuboglu.

1. Algorithms for MRI imaging and RF coil designs for MRI applications.
2. RF coil and magnet structure designs using Femlab, Matlab and HFSS.
3. RF coils designs to provide portable MRI as thesis study “RF Coil System Design For MRI Applications in Inhomogeneous Main Magnetic Field”.

09/2004 – 12/2005 METU-Siemens Corporation for ”Adaptive Learning Project”

1. Video Editing Tool development for editing SCORM integrated AVI, MPEG1, MPEG2 and overlaying various text, image and sound objects.
2. MPEG-4 Presenter Tool development.

F.3 Computer Skills

F.3.1 Programming Languages :

C/C++, C#, PICC, UML, Java, JSP, HTML, AJAX, MXML, SQL

F.3.2 Operating Systems:

Windows, Solaris, Linux

F.3.3 Design and Modeling:

Xilinx, MATLAB, FEMLAB, Quickfield

F.3.4 Testing Tools:

HP VEE, ORCAD, Electronics Workbench, HFSS, Rational Software Architect, Crystal Reports, JasperReports, SQL Developer, Oracle, PgAdmin, PostgreSQL, Eclipse, Flex, Visual Studio, Munin, Paros, HeatClick, JMeter, OpenSTA, Google Analytics

F.3.5 Other Tools :

Visual Source Safe, TortoiseSVN, SSH

F.3.6 Languages :

Turkish (Native Language), English (TOEFL: 290/300, 10/2006), German (Basic)

F.4 Honors and Awards

1. Awarded as ”The Best Poster of the Poster Session” at ”BIOMED2004, the 11^{th} International Conference on Biomedical Sciences and Technology” Hacettepe University, Ankara with the study ”An Approach to Geometrical Design of Permanent Magnets for Biomedical Applications” in September, 2004.
2. Awarded ”Special Jury Award” for Electrical-Electronics Department Senior Project Design Competition in June, 2004.
3. Honor as ”The Most Innovative and Robust Design” for Electrical-Electronics Department Senior Project Design Competition by Electrical and Electronics Engineering Department in June, 2004.
4. Demonstration of Individual paintings and drawings at METU Library Exhibition Hall in May, 2004.
5. Ranked 507^{th}in the National University Entrance Examination over approximately 1.5 Million in 2000.
6. Kadikoy Anatolian High School Best Student Award in 2000.
7. The Second Group Award in Kabatas Mathematics Group Competition.

8. Ranked 76th in the National Science High School Entrance Examination in 1997.
9. Honor in Istanbul Milli Egitim Theatre Festival and Istanbul Kuleli Theatre Festival in 1997.
10. Ranked the 2nd in Kadikoy Knowledge Competition, Istanbul in 1996.

F.5 Publications

1. An Infrastructure for Efficient Reporting Workflow in Grid Based Teleradiology Architectures Using Relation Based Semantic Matching and Integer Linear Programming, Proceedings of the 2014 Federated Conference on Computer Science and Information Systems, September 2014
2. Integration of Federated Medical Systems for Vendor Neutral Image Access in Teleradiology Applications, e-Health – For Continuity of Care 2014, European Federation for Medical Informatics and IOS Press, 2014
3. Homojen olmayan ana manyetik alanda manyetik rezonans goruntuleme icin RF sargisi tasarimi, Proc. of URSI-TURKIYE 2006 3rd National Congress, Ankara - TR, pp.207-9, 2006
4. RF Coil Design for MRI Applications in Inhomogeneous Main Magnetic Fields, World Congress 2006, Seoul-Korea, p.3084, August 2006.
5. An approach to geometrical design of permenant magnets for biomedical applications, 11th. International Biomedical Science and Technology Days, Ankara, Turkey, p.24, 2004.

F.6 Patents

1. ScoBox collaborative e-learning interaction and sharing system (Patent Pending)

F.7 Courses and Certificates

1. FedCSIS 2014 Certificate of Contribution, Warsaw Poland, September 2014
2. MIE 2014 Medical Infırmatics Europe 2014 Certificate of Contribution, Istanbul, August 2014
3. Technology to Market Accelerator, Intel Global Challenge at UC Berkeley, October 2013
4. Health Expo CNR Contribution Certificate, January 2013
5. Global File System and Cluster Setup Course and Certificate by Prosoft.
6. Postgresql course by Devrim Gunduz.
7. Learning Repostory Environment Workshop, Leuven.
8. iClass Contribution Certificate, Brussels.

F.8 Hobbies and Activities

Memberships : Ankara Nautical Club, METU Fine Arts Society, METU Couple Dance Society

Dancing : Argentina Tango and Salsa

Painting : Worked with Bahaddin Odabasi (Mimar Sinan University, Istanbul) in 1999 and studied for 2 years with Cezmi Orhan (Gazi University,Ankara) on drawing (2000 – 2002).

Theatre : Acting, decoration and writing plays. Wrote and directed a play (named S.O.S) for HABITAT Project, Istanbul, 1996 demonstrated at German Culture Association.

Music : Playing the guitar Studied the classic guitar with Yildiz Elmas (Marmara University, Istanbul, 1998-2000)

Sports and Traveling : Camping and trekking